2016

MEF2-regulated Gtl2-Dio3 noncoding RNAs in cardiac muscle and disease

BOSTON UNIVERSITY

GRADUATE SCHOOL OF ARTS AND SCIENCES

Dissertation

MEF2-REGULATED GTL2-DIO3 NONCODING RNAS IN

CARDIAC MUSCLE AND DISEASE

by

AMANDA LEAH RICE CLARK

B.A., Boston University, 2008

Submitted in partial fulfillment of the

requirements for the degree of

Doctor of Philosophy

2016

Approved by

First Reader   _____
                 Francisco J. Naya, Ph.D.
                 Associate Professor of Biology

Second Reader   _____
                 John Celenza, Ph.D.
                 Associate Professor of Biology

ACKNOWLEDGMENTS

me in a time of need. Also, sorry Jan, Martin, Hermann, and Jerome. I won't be able to access research articles for free anymore! Thank you to Joy Fletcher for taking me under your wing not once, but twice, at both jobs after college. Thank you for always being there for me and for talking about science and life. You're a true friend and I will always value our lunch dates. Thank you also to my non-science friends for your constant support. Kaitlin DeMartin, thank you for putting up with me throughout college and after, for being an amazing roommate and friend, and for always being free to grab a drink to chat. Julie Richard, oh Julz, thank you for being the best unfiltered friend the past 15 years and for always being there for me when I've needed you. Ida Soleimani, thank you for being a friend for the past 25+ years and for your support from across the country. Todd Nicholas, thank you for being such a great best friend to Mike. Also, thanks for marrying a science nerd (thanks to you too, Kat!) so I have someone to talk to when you and Mike bro out. To all of my other friends, thank you for your constant support and for always asking me how school was going even though most of you had no idea what I was doing every day.

Most importantly, I would like to thank my family. Your support has helped me get this far and I would not be the person I am without you. I am lucky to have so many family members to thank here. Of course a huge thank you to my husband, Mike. I can't thank you enough for being supportive when I told you I wanted to quit my job and apply to grad school. We've had quite the life journey these past 14 years but I'm glad I got to spend this journey with you. Dr. and Mr. it is! Thank you to my mom, Renee, for always believing I could do anything I wanted to do and for giving me the opportunity to pursue my dreams. To my dad, Tim, for always showing me how to do things and letting me learn how things

work. To my brother, Chris, for being not only the best big brother a girl could ask for but also for being a friend. You helped me become interested in science and always let me tag along to teach me new things. To my wonderful sister-in-law Tara, thank you for being part of this insane family and for being a sister and a friend to me. To my parents-in-law, Mike and Lu, thank you for being a great set II of parents and for trying to understand science for me for the past 14 years. To my brothers-in-law, Nick and Josh, thank you for easily accepting me as part of your family and to my other sister-in-law, Jess, thank you for always being there to talk to and to listen. Thank you to all my nephews, Noah, Jack, Evan, and Finn. I hope to be the cool aunt that can get you guys interested in science too. Thank you to my extended family as well. I would like to especially thank Jen and Nick and my "nieces" Robyn and Janie. Jen, thank you for being such a strong support for me throughout the years. Thanks for always being so excited about science, especially the science I have been working on. To my other extended family members, thank you all for all your love and support.

MEF2-REGULATED GTL2-DIO3 NONCODING RNAS IN

CARDIAC MUSCLE AND DISEASE

AMANDA LEAH RICE CLARK

Boston University Graduate School of Arts and Sciences, 2016

Major Professor: Francisco J. Naya, Associate Professor of Biology

ABSTRACT

The MEF2 transcription factor is a central regulator of skeletal and cardiac muscle development. Recently, we showed that MEF2A regulates skeletal muscle regeneration through direct regulation of the *Gtl2-Dio3* microRNA mega-cluster. In addition to their expression in skeletal muscle, temporal expression analysis of selected *Gtl2-Dio3* microRNAs revealed high enrichment in cardiac muscle. Therefore, I investigated the role of selected microRNAs from the *Gtl2-Dio3* noncoding RNA locus in the heart. First, I found that *Gtl2-Dio3* microRNAs are expressed at higher levels in perinatal hearts compared to adult, suggesting they function in cardiac maturation shortly after birth. I also demonstrated that these microRNAs are dependent on MEF2A in the perinatal heart and in neonatal cardiomyocytes. To determine the specific role in cardiac muscle, I overexpressed selected microRNA mimics in neonatal rat ventricular myocytes (NRVMs). My results showed that miR-410 and miR-495 stimulate cell cycle re-entry and proliferation of terminally differentiated NRVMs. Subsequent target prediction analyses revealed a number of candidate target genes known to function in the cell cycle and/or in cardiac muscle. One of these was Cited2, a cofactor required for proper cardiac development. Furthermore, I showed that Cited2 is a direct target of these microRNAs and that siRNA

knockdown of Cited2 in NRVMs resulted in robust cardiomyocyte proliferation. This phenotype was associated with reduced expression of *Cdkn1c/p57/Kip2*, a cell cycle inhibitor, and increased expression of *Vegfa*, a growth factor with proliferation-promoting effects.

Given the exciting possibility of manipulating the expression of these microRNAs to repair the damaged heart by stimulating cardiomyocyte proliferation, I then investigated whether they were regulated in cardiac disease and function in pathological signaling. Toward this end, I examined expression of microRNAs miR-410, miR-495, and miR-433, as well as the long noncoding RNA (lncRNA) *Gtl2* in various cardiomyopathies. Interestingly, the microRNAs and lncRNA were dynamically regulated in mouse models of cardiac disease including myocardial infarction and chronic angiotensin II stimulation. Furthermore, I showed for the first time that the *Gtl2* lncRNA and microRNAs are differentially regulated in myocardial infarction, indicating that the complex regulation of the *Gtl2-Dio3* noncoding RNA locus may be important for response to cardiac injury. Lastly, I showed that inhibiting select *Gtl2-Dio3* microRNAs in pathological signaling attenuated cardiomyocyte hypertrophy *in vitro*. Therefore, differential targeting of the *Gtl2-Dio3* noncoding RNAs could provide new therapeutic strategies to control the response of the heart to cardiac diseases with diverse etiologies.

TABLE OF CONTENTS

LIST OF FIGURES

LIST OF TABLES

LIST OF ABBREVIATIONS

AAV .... Adenoviral Associated Vector

ACE ....Angiotensin-Converting Enzyme

AML .... Acute Myeloid Leukemia

Amp .... Ampicillin

ANF ....Atrial Natriuretic Factor

Ang II .... Angiotensin II

AP-2 .... Activating Enhancer Binding Protein 2

APS .... Ammonium Persulfate

Asp .... Aspartic Acid

ATI ....Angiotensin II Type I

Axin2 ....Axis Inhibition Protein 2

β-gal ....β-galactosidase

bHLH ....Basic Helix-Loop-Helix

BMP ....Bone Morphogenic Protein

BNP .... Brain Natriuretic Peptide

BSA .... Bovine Serum Albumin

BU .... Boston University

°C ....Degrees Celsius

cAMP .... Cyclic Adenosine Monophosphate

CDKN1C ....Cyclin Dependent Kinase Inhibitor 1C/p57/Kip2

cDNA .... Copy DNA

xxi

CHAPTER ONE – INTRODUCTION

1.1   Introduction

This dissertation focuses on the role of the MEF2A-regulated *Gtl2-Dio3* microRNAs (miRNAs) in cardiac muscle. Mammalian cardiac muscle has a limited capacity for regeneration, making cardiac injury and disease the leading cause of death worldwide (Mozaffarian et al. 2015). Understanding cell cycle regulation in post-mitotic cardiomyocytes may lead to new therapeutic approaches to regenerate damaged cardiac tissue. The studies described herein highlight novel findings which characterize the MEF2A-regulated *Gtl2-Dio3* miRNAs as important regulators of cardiac muscle. First, I demonstrate that MEF2A regulates the *Gtl2-Dio3* miRNAs in cardiac muscle, in addition to in skeletal muscle as we previously demonstrated (Snyder et al. 2013). I show that these miRNAs are highly expressed in the perinatal heart compared to the adult heart, indicating a potential role for them during postnatal cardiac maturation. I show for the first time that overexpression of miR-410 and miR-495 robustly stimulates cardiomyocyte DNA synthesis and proliferation. I found that these miRNAs target Cited2, a transcriptional coactivator required for proper cardiac development. Consistent with miR-410 and miR-495 overexpression, siRNA knockdown of Cited2 in neonatal cardiomyocytes resulted in increased proliferation. This phenotype is associated with reduced expression of Cdkn1c/p57/Kip2, a cell cycle inhibitor, and increased expression of VEGFA, a growth factor with proliferation-promoting effects. Thus, miR-410 and miR-495 are among a growing number of miRNAs that have the ability to potently stimulate neonatal cardiomyocyte proliferation.

In addition, I examined the expression of the *Gtl2-Dio3* noncoding RNA locus in cardiomyopathy *in vivo*. I found that the *Gtl2-Dio3* miRNAs miR-410, miR-495, and miR-433 and the *Gtl2* lncRNA were dynamically regulated in multiple models of cardiomyopathy, including mouse models of cardiac disease such as myocardial infarction and angiotensin II stimulation. Additionally, I show that the miRNAs and lncRNA are differentially regulated in myocardial infarction, indicating that the regulation of the *Gtl2-Dio3* noncoding RNA locus may be important for response to cardiac injury. Lastly, I demonstrate that knocking down miR-410, miR-495, and miR-433 *in vitro* results in a decreased hypertrophic response in cardiomyocytes. The scientific findings from this work will contribute to a greater understanding of the role of miRNAs in cardiac muscle, the potential for cardiac regeneration, and the therapeutic potential to reduce the impact of cardiac disease and injury.

1.2   Striated Muscle

1.2.1   Mammalian Myogenesis

Myogenesis is the process of forming new muscle. The ectoderm, endoderm, and mesoderm germ layers form during the gastrulation stage of embryogenesis (Mok and Sweetman 2011). Striated muscle cells are derived from the mesoderm, which give rise to cardiac and skeletal muscle. (Pyle and Solaro 2004, Braun and Gautel 2011). Populations of cells from the lateral plate mesoderm, a discrete region within the mesoderm adjacent to the intermediate mesoderm, and neural crest cells are segregated to form the heart. Skeletal muscle forms from somites derived from the paraxial mesoderm, positioned next to the

neural tube (Buckingham et al. 2005, Gilbert 2006, van Weerd et al. 2011, Yokoyama and Asahara 2011).

1.2.2   Cardiac Muscle Differentiation

The heart is the first organ to form in mammals. The heart forms from two separate progenitor populations: the primary or first heart field (PHF/FHF) and the secondary heart field (SHF) (Harvey 2002, Black 2007). Cardiac development can be broken down into four main stages (Figure 1.1). Cardiac progenitor cells are first recognizable at mouse embryonic day 7.5 (E7.5) as a crescent-shaped epithelium, the cardiac crescent, shaped by signaling from bone morphogenic protein (BMP) and fibroblast growth factor 8 (FGF8). After the cardiac crescent has formed, several transcription factors involved in the cardiac program are activated including GATA zinc-finger family transcription factors 4, 5 and 6 (GATA4, -5 and -6), NK2 homeodomain transcription factor-related locus 5 (Nkx2-5), myocyte enhancer factor 2b and 2c (MEF2B and -C), heart and neural derivatives expressed transcripts 1 and 2 (HAND1 and -2), and T-box 5 and 20 (TBX5 and -20). Dysregulation of these cardiac transcription factors during embryogenesis results in congenital heart disease (Pierpont et al. 2007, Bruneau 2008). The cardiac cells migrate to the midline around E8.5 and elongate to form a linear tube. The linear heart tube undergoes looping morphogenesis and begins to balloon outward by E9.5. By E10.5, distinct left and right ventricles and atria are formed. After E11.5, the heart continues to mature throughout embryogenesis (Harvey 2002, Buckingham et al. 2005, Bruneau 2008).

1.3   Myocyte Enhancer Factor-2 Transcription Factors

1.3.1   Identification and Structure of MEF2 Factors

Myocyte enhancer factor 2 (MEF2) proteins are key regulators of diverse gene programs in skeletal and cardiac muscle. MEF2 proteins belong to the MADS-box family of transcription factors, a family named for the first four members identified: yeast mating-type selection factor <u>M</u>CM1, plant leaf identity homeodomain factors <u>A</u>gamous and <u>D</u>eficiens, and human <u>s</u>erum <u>r</u>esponse <u>f</u>actor (SRF) (Black and Olson 1998). MEF2 was first identified as a muscle-specific nuclear factor capable of binding a conserved A/T-rich consensus site in the muscle creatine kinase (MCK) promoter and was shown to be expressed prior to MCK in differentiated myotubes, making MEF2 an early marker for activation of the muscle differentiation program (Gossett et al. 1989). The conserved A/T-rich MEF2 binding site has since been found in the promoters of many muscle-specific genes (Black and Olson 1998). The MCK MEF2 binding site sequence was used in expression screening to identify subsequent family members (Pollock and Treisman 1991, Breitbart et al. 1993, Martin et al. 1993, Martin et al. 1994).

Invertebrates such as *Drosophila melanogaster*, *Caenorhabditis elegans* and sea urchins each possess one *Mef2* gene (Lilly et al. 1994, Black and Olson 1998, Gunthorpe et al. 1999, Dichoso et al. 2000). Yeast and *Xenopus laevis* both possess two MEF2 factors, Rlm1 and Smp1, and Xmef2a and Xmef2d, respectively (Chambers et al. 1992, Dodou and Treisman 1997). Vertebrates possess four *Mef2* genes, designated *Mef2a, -b, -c*, and *–d*, each found on different chromosomes (Black and Olson 1998). The vertebrate MEF2 proteins share approximately 50% amino acid identity overall and their amino acid identity

is 95% conserved in their MADS-box and MEF2 domains (Figure 1.2) (Black and Olson 1998, Potthoff and Olson 2007). Each MEF2 factor contains a highly conserved N-terminal domain region, which includes a MADS-box, a 57-amino acid motif, and a MEF2 domain, a 29-amino acid extension, that together are required for DNA binding and dimerization and facilitate cofactor interactions (Molkentin et al. 1996, Santelli and Richmond 2000, McKinsey et al. 2002, Wu et al. 2010). The MEF2 binding site is highly conserved. *Drosophila* D-MEF2 is capable of binding vertebrate MEF2 consensus sequences (Lilly et al. 1994). There is little homology in the MEF2 C-terminal domains, which include the transactivation domain and are subject to complex alternative splicing (Martin et al. 1994, Yu 1996, Black and Olson 1998, Iida et al. 1999, Zhu et al. 2005).

1.3.2   MEF2 Functions in Striated Muscle

In mammals, MEF2 factors exhibit extremely similar binding specificities and transactivation potential *in vitro*, suggesting that these factors act redundantly (Pollock and Treisman 1991, Yu et al. 1992, Breitbart et al. 1993, Lilly et al. 1995, Ornatsky and McDermott 1996). Recently, however, we have shown that each mammalian MEF2 factor regulates an overlapping but largely distinct set of genes in skeletal muscle (Estrella et al. 2015). Furthermore, murine knockout and overexpression models of each MEF2 isoform display different phenotypes, strongly suggesting unique roles for individual MEF2 factors *in vivo*.

Mef2a-null mice exhibit perinatal lethality due to severe cardiac cyto-architectural defects including dilation of the right ventricles and myofibrillar fragmentation in over 80% of mice between postnatal days 5 and 10 (P5-P10) (Figure 1.3). Microarray analysis

of RNA from hearts of 4-5 day old mice shows dysregulation of several structural proteins and stress-response genes. ANF and BNP, markers of cardiac hypertrophy, are also dysregulated (Naya et al. 2002). MEF2A regulates costamere gene expression in cardiomyocytes so this phenotype suggests that MEF2A plays a role in proper cardiac muscle differentiation (Ewen et al. 2011). Mutants that survive to adulthood exhibit mitochondrial deficiency and myofibrillar disorganization, but do not exhibit chamber dilation or cyto-architectural defects. These mice are subject to cardiac arrhythmias and sudden death (Naya et al. 2002).

In contrast to cardiac development, skeletal muscle develops normally in MEF2A knockout mice. However, the differentiation of skeletal muscle C2C12 cells is impaired by the loss of MEF2A *in vitro* and, upon injury, *Mef2a*-null mice exhibit defects in skeletal muscle with widespread necrosis and impaired myofiber formation, resulting in delayed skeletal muscle regeneration (Figure 1.4). Importantly, MEF2A regulates a miRNA mega-cluster, the *Gtl2-Dio3* locus, the downregulation of which disrupts WNT signaling, resulting in impaired regeneration. Furthermore, overexpression of a subset of these miRNAs rescued the differentiation defect in MEF2A-deficient myoblasts (Figure 1.5) (Snyder et al. 2013). The *Gtl2-Dio3* miRNA mega-cluster is described in detail in Chapter 1.5.4.

Mef2b-null mice are viable and display no obvious muscle defects, however detailed characterization of this knockout has not been published (Black and Olson 1998). *Mef2c* is the earliest MEF2 factor expressed in mouse embryonic development (Molkentin et al. 1996). *Mef2c*-null mice are embryonic lethal and display severe cardiac defects

including looping abnormalities (Lin et al. 1997, Lin et al. 1998, Potthoff and Olson 2007). Conditional knockout of *Mef2c* in the myocardium resulted in viable offspring, demonstrating that *Mef2c* is not required for the formation of the heart after cardiac looping morphogenesis (Vong et al. 2005). Together, these data indicate that *Mef2c* plays a critical role in early cardiac development but is not required after the heart has undergone looping morphogenesis, which may be due to the potential redundancy of MEF2 factors. *Mef2d*-null mice are viable but display a blunted cardiac stress response. Fetal gene activation is also blunted in response to pressure overload, indicating that MEF2D is required for fetal cardiac and stress response gene activation. Indeed, cardiac-specific overexpression of MEF2D is sufficient for inducing cardiac remodeling with upregulation of fetal cardiac genes (Kim et al. 2008). Together, these data indicate that MEF2D plays a role in cardiac remodeling in response to stress.

1.4. Cardiac Muscle Regeneration

1.4.1 Cardiac Regeneration in Lower Vertebrates

Cardiovascular disease is the leading cause of morbidity and mortality in the world (Mozaffarian et al. 2015). Improving cardiac function post-injury proves difficult because the underlying molecular mechanisms of cardiomyocyte differentiation and maturation are not well understood. Uncovering these mechanisms could unmask the regenerative potential of the adult mammalian heart.

Lower vertebrates are capable of cardiac regeneration. One of the first models of heart regeneration was described in newts (Oberpriller and Oberpriller 1974). Newt ventricles fully regenerate within three weeks post-amputation. Pre-existing

cardiomyocytes re-enter the cell cycle and proliferate, causing this regenerative ability (Flink 2002). Zebrafish are also able to undergo cardiac regeneration. Removal of 20% of the ventricle by surgical resection results in complete regeneration of the heart within 60 days post-injury (Poss 2007). Additionally, a hypoxia cardiac injury zebrafish model, which mimics ischemic injury in the mammalian heart, shows full regeneration with pre-existing cardiomyocyte cell cycle re-entry (Jopling et al. 2012, Parente et al. 2013). Furthermore, genetic fate-mapping studies show proliferation of pre-existing cardiomyocytes form the regenerated cardiac tissue (Jopling et al. 2010, Kikuchi et al. 2010).

1.4.2   Neonatal Mammalian Cardiomyocyte Proliferation

In mammals, there is potential for cardiac regeneration shortly after birth. Interestingly, the removal of up to 15% of the left ventricle by apical resection surgery via lateral thoracotomy of 1 day old (P1) mice resulted in completely regenerated hearts within 3 weeks. These mice showed no measurable fibrosis or cardiac dysfunction. Additionally, genetic fate-mapping in these mice confirmed the new cardiomyocytes were derived from proliferating pre-existing cardiomyocytes (Porrello et al. 2011). Furthermore, an ischemic injury mouse model shows a similar injury response. Ischemic myocardial infarction was induced by permanently ligating the left anterior descending (LAD) coronary artery of 1-day old mice. Within three weeks, 95% of the myocardium was viable in these mice compared to 25% viable three days after injury (Porrello et al. 2013).

By P5-P7 cardiomyocytes exit the cell cycle and are terminally differentiated (Li et al. 1996, Walsh et al. 2010). P7 mice failed to regenerate ventricles and, in addition,

developed significant fibrosis (Porrello et al. 2011). Taken together, these studies indicate that neonatal cardiomyocytes have the ability to regenerate, but this ability is lost shortly after birth.

1.4.3 Adult Mammalian Cardiomyocyte Proliferation

Until recently, the mammalian heart was thought of as a terminally differentiated organ, unable to undergo mitosis. While the adult mammalian heart has limited cardiomyogenesis and it is insufficient to restore cardiac function post-injury, there is continuous turnover of cardiomyocytes. By measuring carbon-14 from nuclear bomb tests in genomic DNA of human cardiomyocytes, one group reported that approximately 1% of cardiomyocytes undergo turnover at age 20 and by age 75 this number reduces to 0.45% (Bergmann et al. 2009, Bergmann et al. 2012).

Moreover, another study found the number of cardiomyocytes increases 3.4-fold from year 1 to year 20 in humans and concluded that adolescents may be able to regenerate myocardium. Furthermore, they found mitotic cardiomyocytes were detectable at the highest levels at 1 year, detectable 23% less between 10 and 20 years, and were detectable at low levels over 40 years (Mollova et al. 2013). These findings suggest the capacity for cardiomyocyte turnover is maintained throughout life and that manipulating the cell cycle activity of cardiomyocytes may have the potential to induce cardiac regeneration.

1.4.4 Cardiac Regeneration Therapies

1.4.4.1 Candidate Cells for Cardiac Regeneration

Cardiac regeneration research has focused on finding candidate cells for cardiac regeneration and inducing cardiac cells to proliferation. The first cells to be tested for

cardiac regeneration were skeletal myoblasts. Use of these cells in cardiac regeneration results in reduced fibrosis but has varying results because they form skeletal muscle fibers instead of cardiac muscle (Murry et al. 1996, Taylor et al. 1998). Bone marrow derived cells have also been used because they can transdifferentiate into skeletal muscle, heart, neuron, and endothelial cells. Additionally, adipose derived cells can replicate as undifferentiated cells and then differentiate into mesenchymal cell types (Doppler et al. 2013, Sanganalmath and Bolli 2013, Pfister et al. 2014). Furthermore, resident cardiac stem cells have been proposed as a viable method to regenerate cardiac muscle. There is a small, resident cell population that can differentiate into cardiomyocytes in the heart (Hierlihy et al. 2002). These cells account for 9% of the cells in the neonatal mouse heart and 1% of cells in the adult heart (Pfister et al. 2014). Lastly, inducing multipotent stem cells, including embryonic stem cells and induced pluripotent stem cells, into cardiomyocytes is currently being tested (Doppler et al. 2013, Sanganalmath and Bolli 2013, Pfister et al. 2014). To date, these methods have been minimally successful in regenerating the heart but are not efficient enough to induce cardiac regeneration in the adult heart.

1.4.4.2 Inducing Cardiomyocyte Proliferation

In order to reactivate the cell cycle, studies have focused on forcing cardiomyocyte proliferation by suppressing cell cycle inactivators or overexpressing cell cycle activators (Brooks et al. 1998, Ahuja et al. 2007). For example, overexpressing cyclin A2 enhances cardiac function post-injury (Woo et al. 2006). Additionally, transgenic mice overexpressing cyclin D2 exhibit higher rates of cardiomyocyte proliferation and display infarct regression in response to injury (Pasumarthi et al. 2005). Interestingly, a bHLH

transcription factor, myeloid ecotropic viral integration site 1 homolog (Meis1), was shown to regulate postnatal cardiomyocyte cell cycle arrest. Deleting Meis1 is sufficient to reactivate mitosis in the adult heart (Mahmoud et al. 2013). Additionally, overexpression of yes-associated protein (Yap), a transcription factor that promotes embryonic cardiomyocyte proliferation, in the adult heart stimulated cardiac regeneration (Xin et al. 2013). These findings provide evidence for the regenerative capacity of the adult mammalian heart and elucidating the underlying molecular mechanisms could uncover new therapeutic strategies to improve the quality of life after cardiac injury.

1.5 MicroRNAs

1.5.1 MicroRNAs and Gene Regulation

Non-coding RNAs (ncRNAs) are functional RNA molecules that are not translated into proteins. MicroRNAs (miRNAs) are a subset of small (~22 nucleotide) ncRNAs that inhibit translation or promote mRNA degradation to fine-tune gene expression. MiRNAs comprise one of the most abundant gene regulator molecules in multicellular organisms (Bartel 2009).

MiRNA biogenesis is summarized in Figure 1.6. MiRNAs are transcribed as 200 nucleotide long primary miRNAs (pri-miRNAs) which are processed into an approximately 70 nucleotide hairpin RNA or precursor miRNA (pre-miRNA) by the RNase III endonuclease Drosha and then exported into the cytoplasm by Exportin 5 (Expo5), a Ran-GTP-dependent nucleo/cytoplasmic cargo transporter. Once in the cytoplasm, pre-miRNAs are cleaved by Dicer into a double-stranded RNA duplex (miRNA:miRNA*) that is 21-25 nucleotides long. The mature miRNA is incorporated into

ribonucleoprotein RNA-induced silencing complex (RISC) for mRNA target recognition. (Lee et al. 2002, Lee et al. 2003, He and Hannon 2004, Bernardo et al. 2012). A single miRNA can target hundreds of mRNA sequences, demonstrating the complexity of miRNA function and regulation in biological processes.

1.5.2 MicroRNAs in Cardiac Disease

Dicer, the RNase III endonuclease responsible for miRNA processing, is required for proper embryogenesis. Global Dicer knockout mice are embryonic lethal (Bernstein et al. 2003). Dicer is also required for proper cardiac development and function. Targeted deletion of Dicer in the heart leads to progressive dilated cardiomyopathy and heart failure (Chen et al. 2008). The requirement of Dicer for proper heart function demonstrates the importance of miRNAs and their roles in normal cardiac function.

A number of miRNAs are firmly established, important modulators in cardiac development and stress remodeling pathways. For example, miR-1 and miR-133 regulate cardiomyocyte size and function. MiR-133 enhances myoblast proliferation and inhibits differentiation. Conversely, miR-1 acts as a repressor of cardiac growth and an activator of differentiation. (Chen et al. 2006, Liu et al. 2007, Zhao et al. 2007). These two miRNAs are downregulated in diseased human hearts and during cardiac hypertrophy (van Rooij et al. 2006). Additionally, miR-208 is exclusively cardiac tissue-specific and, although it is not required for cardiac development, it regulates cardiac stress-response genes for myocyte growth (van Rooij et al. 2007). MiR-208a knockout mice display reduced cardiac hypertrophy in response to stress. Moreover, inhibiting miR-208a suppresses cardiac

fibrosis and improves survival, indicating miR-208a is required for proper cardiac stress response (Callis et al. 2009).

Several miRNAs have been implicated in cardiac disease. MiR-21 is upregulated during cardiac hypertrophy and knocking down miR-21 using antagomiRs restores function in severely injured hearts. Interestingly, miR-21 knockout mice show no restorative function in severely injured hearts in response to stress, indicating that miR-21 may not be the only miRNA playing a role in this process (Thum et al. 2008). Moreover, miR-214 induces hypertrophy and *in vivo* silencing of miR-214 prevents hypertrophy (Yang et al. 2014).

1.5.3 MicroRNAs in Cardiac Proliferation

There is increasing evidence that miRNAs are also central regulators of mammalian cardiomyocyte proliferation. Deletion of the muscle-specific miR-1-2 resulted in cardiac defects associated with increased cardiomyocyte proliferation (Zhao et al. 2007). Knocking down members of the miR-15 family in neonatal mice is associated with an increase in mitotic cardiomyocytes and de-repression of checkpoint kinase 1, indicating there may be a role for this miRNA family in cardiac regeneration (Porrello et al. 2011, van Rooij and Olson 2012, van Rooij et al. 2012). Furthermore, direct involvement of miRNAs in cardiomyocyte proliferation was demonstrated in a high throughput screen which identified over 200 miRNAs capable of promoting proliferation in cultured primary cardiomyocytes (Eulalio et al. 2012).

Additional miRNAs have been shown to play a role in cardiomyocyte cell cycle regulation. miR-29a regulates cardiomyocyte cell cycle re-entry (Cao et al. 2013). miR-

195, a member of the miR-15 family, regulates cell cycle genes and its inhibition resulted in an increased number of cardiomyocytes (Porrello et al. 2011). The miR-17-92 cluster regulates cardiomyocyte proliferation through miR-19's modulation of phosphate and tensin homolog (PTEN) (Chen et al. 2013). Moreover, miR-302-367 was recently shown to promote cardiomyocyte proliferation through activation of the Hippo pathway (Tian et al. 2015). These findings make it clear that miRNAs regulate cardiomyocyte proliferation but do so by targeting a variety of pathways. Given their central roles in these cardiac pathways, identifying and investigating novel miRNAs in cardiomyocytes is essential to further our understanding of cardiac physiology and disease.

1.5.4 The *Gtl2-Dio3* microRNA Mega-Cluster

1.5.4.1 *Gtl2-Dio3* Identification, Structure, and Function

The *Gtl2-Dio3* miRNA mega-cluster, located on mouse chromosome 12 and human chromosome 14, represents the largest known mammalian miRNA cluster. This region is evolutionarily conserved in placental mammals beginning 100 million years ago and it appears to have originated from an ancestral repeat that was amplified over 250 times, leading to the cluster of miRNAs (Glazov et al. 2008). The *Gtl2-Dio3* region was initially discovered when performing a human-ovine comparative analysis of the 250-kb region encompassing the skeletal muscle hypertrophy callipyge (*clpg*) mutation mapped in the sheep genome (Charlier et al. 2001). Through this and subsequent analysis, it has been shown that the *Gtl2-Dio3* locus is an imprinted locus containing maternal and paternal imprinting and encodes both protein-coding and noncoding genes (Lin et al. 2003). This

locus contains areas of differential methylation and histone modification on paternally and maternally inherited alleles. An overview of the *Gtl2-Dio3* locus is depicted in Figure 1.7.

The paternally imprinted genes of this locus include the protein-coding genes Delta-like 1 (Dlk1) and Type 3-iodothyronine deiodinase (Dio3). Dlk1 gene encodes a transmembrane protein that belongs to the epidermal growth factor (EGF)-like homeotic protein family. It plays important roles in cell differentiation, skeletal muscle development and regeneration, and adipogenesis (Laborda 2000, Schmidt et al. 2000, Takada et al. 2000, da Rocha et al. 2008, Waddell et al. 2010, Andersen et al. 2013). Dio3 encodes an enzyme that degrades thyroid hormone to regulate the amount of thyroid hormone the embryo receives in order for proper tissue development (Tsai et al. 2002, Yevtodiyenko et al. 2002). The retrotransposon Rtl1 is also a paternally imprinted region and is required for normal embryonic tissue development (Seitz et al. 2003, da Rocha et al. 2008).

The maternally imprinted genes of this locus include the noncoding RNAs Gene trap locus 2 (Gtl2)/maternally expressed 3 (MEG3), C/D small nucleolar RNAs (snoRNAs), maternally expressed 8 (MEG8), and Mirg. Gtl2/MEG3 encodes a long noncoding RNA (lncRNA), the function of which remains poorly understood. This region is believed to be involved in physiological and pathological cellular processes and to possess tumor suppressor properties (Miyoshi et al. 2000, Schmidt et al. 2000). At least nine tandemly-repeated C/D snoRNAs are found in the Rian/MEG8 gene near Gtl2 (Cavaille et al. 2002). Rian/MEG8 also harbors a lncRNA (Benetatos et al. 2013). Lastly, Mirg noncoding RNA is expressed in the central nervous system and skeletal muscle during

embryogenesis but further studies determining the function and mechanism have yet to be completed (Seitz et al. 2003, Han et al. 2012).

The *Gtl2-Dio3* region is home to 54 miRNAs. The first miRNAs mapped to this locus were miR-136, -127, -154, and -134. These were the first miRNAs to show perfect complementarity to cellular mRNA in animals (Seitz et al. 2003). Subsequent research found an additional 40+ miRNAs clustered along this locus (Seitz et al. 2004).

The regulation of the *Gtl2-Dio3* locus is not yet fully understood. Interestingly, *Gtl2* knockout mutant mice show a parental origin-dependent lethality with maternally inherited knockouts being lethal while paternally inherited knockouts show no abnormalities (Takahashi et al. 2009, Zhou et al. 2010). Further studies demonstrated that *Gtl2* plays an important role in embryonic development and in regulating *Dlk1-Gtl2* imprinting. Deletion of the intergenic differentially methylated region (IG-DMR) upstream of *Gtl2* resulted in severe defects in striated muscle development and differentiation (Lin et al. 2007, Zhou et al. 2010). Additionally, studies suggest that some *Gtl2-Dio3* miRNAs are transcriptionally regulated as individual or smaller clusters (Song and Wang 2008, Fiore et al. 2009, Hagan et al. 2009). However, others suggest the entire *Gtl2-Dio3* locus is coordinately transcribed (Tierling et al. 2006, Zhou et al. 2010), so it remains to be determined if the *Gtl2-Dio3* miRNAs are transcribed individually or together as a single transcript.

1.5.4.2 *Gtl2-Dio3* microRNAs in Disease

Many roles for individual *Gtl2-Dio3* miRNAs have been described. The most prevalent role for *Gtl2-Dio3* miRNAs is found in cancer. *Gtl2-Dio3* miRNAs can be used

to diagnose multiple types of cancer including blood cancers such as acute myeloid leukemia (AML), esophageal squamous cell carcinoma (ESCC), colon, breast, and ovarian cancers (Bandres et al. 2006, Li et al. 2008, Zhang et al. 2010, Hwang-Verslues et al. 2011, Shih et al. 2011). These studies indicate the potential for miRNAs to serve as prognostic markers in cancer.

Gtl2-Dio3 miRNAs have also been implicated in central nervous system diseases. In human gliomas, miR-381 has been shown to interact with the glioma suppressor leucine-rich repeat-containing protein 4 (LRRC4) (Tang et al. 2011). MiR-495 inhibits proliferation of glioblastoma multiforme by targeting cyclin-dependent kinase 6 (Chen et al. 2013). Additionally, multiple *Gtl2-Dio3* miRNAs including miR-495, miR-543, miR-770, miR-379, miR-487, miR-889, miR-382, miR-136, and miR-411 are all downregulated in glioblastomas (Skalsky and Cullen 2011). *Gtl2-Dio3* miRNAs may be potential targets to improve and develop new therapies for patients with glioblastomas.

Furthermore, *Gtl2-Dio3* miRNAs have been implicated in cardiac disease. 29 miRNAs from the *Dlk1-Dio3* genomic imprinted region are upregulated following myocardial infarction, suggesting that the regenerative process is initiated following cardiac injury but is not completed (Janssen et al. 2013). The miRNAs from this region could be targets to alter the regenerative capacity of the injured myocardium. Additionally, 204 screened miRNA mimics, including 8 miRNAs from the *Gtl2-Dio3* locus, increased neonatal cardiomyocyte proliferation 2-fold or higher. Multiple downregulated transcripts could be potential targets of miRNAs that result in increased cardiomyocyte proliferation

(Eulalio et al. 2012). Taken together, these studies point to a potential role for *Gtl2-Dio3* miRNAs in cardiac proliferation and the regenerative capacity of cardiac muscle.

1.6   Cited2

1.6.1   Cited2 Acts as a Transcriptional Co-Activator

Cyclic adenosine monophosphate (cAMP)-response element binding protein (CREB)/p300-interacting transactivator with glutamic acid (Glu/E)/aspartic acid (Asp/D)-rich carboxy terminal domain 2 (CITED2) is a transcriptional co-activator also known as melanocyte-specific gene-related gene 1 (MRG1) and p35srj. It has been shown to interact with a number of transcription factors including transcription factor AP-2 (TFAP2) and hypoxia inducible factor 1 α (HIF1- α) (Yin et al. 2002, Braganca et al. 2003, Du and Yang 2012). Cited2 is required for TFAP2 to interact with p300 (Braganca et al. 2003). TFAP2 is required for cardiac outflow tract formation (Brewer et al. 2002). Additionally, TFAP2 mutations have also been linked to congenital heart disease activation (Lingaiah et al. 2011, Xiong et al. 2013). Whereas Cited2 functions to stimulate TFAP2 activity, it is a negative regulator of HIF1-α and HIF1-α is increased in *Cited2* knockout mice (Yin et al. 2002, Du and Yang 2012). Knocking out HIF1-α resulted in embryonic lethality due to neural tube defects and cardiovascular malformations (Iyer et al. 1998).

1.6.2   Cited2 in Cardiac Development

Cited2 is required for proper cardiac development. Cited2 is first expressed in pre-cardiac mesoderm and is detected homogenously throughout the heart in early stage embryos (Dunwoodie et al. 1998). Additionally, Cited2 has been implicated in playing a role in cardiomyocyte differentiation (Li et al. 2012). *Cited2* global knockout mice are

embryonic lethal due to cardiac defects in left-right patterning, septation, outflow tract, and aortic arch malformations (Bamforth et al. 2001, Bamforth et al. 2004, Weninger et al. 2005). Cardiomyocyte-specific *Cited2* knockout mice revealed a requirement specifically in cardiomyocytes with defects in normal myocardial thickening and ventricular septation (MacDonald et al. 2013). Furthermore, mutations in Cited2 are associated with congenital heart disease in humans and represent the most common congenital malformations in infants, pointing to an important role for this transcriptional co-activator in cardiac muscle (Sperling et al. 2005, Yang et al. 2010, Liu et al. 2014, Xu et al. 2014).

1.6.3 Cited2 and Proliferation

Regarding cell cycle control, Cited2 has been shown to play a role in regulating the cell cycle (Figure 1.8). Embryonic Stem (ES) cells can be maintained in an undifferentiated state when knocking down Cited2. Additionally, knocking out Cited2 specifically in cardiomyocytes resulted in a delay in cardiomyocyte differentiation (Li et al. 2012). Furthermore, Cited2 maintains quiescence of hematopoietic stem cells (HSCs) and knocking out Cited2 resulted in the loss of HSC quiescence (Du and Yang 2012). Cited2 positively regulates *p57* and negatively regulates *Vegfa* in HSCs (Du et al. 2012, Li et al. 2012).

1.6.3.1 CDKN1C/p57/Kip2

Cited2 positively regulates the expression of the negative cell cycle inhibitor cyclin-dependent kinase inhibitor 1C (CDKN1C)/p57/Kip2 in hematopoietic stem cells and *p57* levels are decreased in the Cited2 knockout mouse (Du et al. 2012, Du and Yang 2012). p57 is a cyclin dependent kinase inhibitor and its role in cell cycle arrest is well established.

p57 binds to G1 cyclin-CDK complexes, resulting in arrest of the cell cycle in G1 phase (Pateras et al. 2009). Inhibition of p57 results in increased cell cycle activity. EZH2, a histone methyltransferase, regulates p57 and leads to increased cell cycle activity (Yang et al. 2009, Guo et al. 2011). Additionally, TGFβ activity has been shown to induce degradation of p57 (Pateras et al. 2009). Furthermore, targeting p57 using shRNA-mediated suppression promotes adult human β cell replication (Avrahami et al. 2014). Together these data indicate that p57 inhibits cell cycle activity and that inhibition of p57 leads to increased cell cycle activity.

1.6.3.2 VEGF

Cited2 negatively regulates vascular endothelial growth factor A (*Vegfa*) by repressing the Vegfa promoter (Li et al. 2012). Mutations in CITED2 result in dysregulation of VEGF in humans (Li et al. 2012) and VEGF is upregulated in Cited2 null hearts (Yin et al. 2002). VEGF is an angiogenic growth factor that plays a role in angiogenesis and endothelial cell growth (Shibuya 2013). Additionally, VEGF has been shown to stimulate cell proliferation in a variety of tissue types including the brain (Sondell et al. 1999), kidney (Advani 2014), and lung (Brown et al. 2001), as well as in many cancers including leukemia, lymphomas, and malignant tumors (Delli Carpini et al. 2010, Kampen et al. 2013). Interestingly, delivery of VEGF to cardiac cells post-injury has been shown to improve cardiomyocyte proliferation and function and to reduce myocardial infarct size (Ferrarini et al. 2006, Vera Janavel et al. 2006, Tao et al. 2011, Awada et al. 2015). Together these data indicate VEGF has pro-proliferative capabilities in a variety of cell types.

1.7   Statement of Thesis Rationale

The goal of this study is to characterize the role of the MEF2A-regulated *Gtl2-Dio3* miRNAs in cardiac muscle. Previously, we showed that MEF2A directly regulates the *Gtl2-Dio3* miRNA mega-cluster in skeletal muscle. A subset of these miRNAs target Sfrp2 to modulate WNT signaling in skeletal muscle regeneration. Loss of these miRNAs results in impaired skeletal muscle regeneration (Snyder et al. 2013). Because the expression of *Gtl2-Dio3* miRNAs parallels MEF2A expression, and they are highly expressed in cardiac muscle as well as skeletal muscle, I was interested in elucidating the role of these miRNAs in cardiac muscle.

In the present study, I investigated the expression of selected miRNAs from the *Gtl2-Dio3* locus in the heart. I found that the *Gtl2-Dio3* miRNAs are expressed at higher levels in the perinatal heart compared to adult, suggesting they function in cardiac maturation shortly after birth. To determine their specific function in cardiac muscle, I overexpressed miRNA mimics miR-410 and miR-495 in neonatal rat ventricular myocytes (NRVMs) and found that overexpression of these miRs resulted in increased proliferation of terminally differentiated NRVMs. These miRNAs directly target Cited2, a transcriptional co-activator required for proper cardiac development. Accordingly, I detected a decrease in Cited2 upon overexpressing miR-410 and miR-495 in NRVMs. Furthermore, consistent with the result that loss of MEF2A causes a reduction in miR-410 and miR-495, I found that both Cited2 and p57 were upregulated, whereas Vegfa was significantly downregulated, in MEF2A-depleted NRVMs. Likewise, Cited2 and p57 were significantly upregulated in perinatal MEF2A knockout hearts. Collectively these studies

demonstrate a role for *Gtl2-Dio3* miRNAs in cardiomyocyte proliferation and may be key to unlocking the regenerative capacity of adult cardiac muscle.

Because these miRNAs are able to stimulate cardiomyocyte proliferation *in vitro*, I was also interested in examining their expression in heart disease *in vivo*. I found the *Gtl2-Dio3* miRNAs were upregulated in mouse models of cardiac stress including myocardial infarction and angiotensin-II treated mouse models as well as models of cardiac defects including the MEF2A adult knockout heart and two models of muscular dystrophy, the *mdx* dystrophin knockout mouse and the *DyW* laminin α2 knockout mouse. Interestingly, the *Gtl2-Dio3* miRNAs were also upregulated *in vitro* in hypertrophic NRVMs treated with phenylephrine and angiotensin II. Furthermore, knockdown of these miRNAs in NRVMs resulted in decreased hypertrophy. Further studies investigating this pathway and their role in hypertrophy *in vivo* in diseased or injured hearts may lead to other potential therapies to treat cardiac disease. Delivery of the *Gtl2-Dio3* miRNAs may be a potential therapeutic avenue to stimulate cardiomyocyte proliferation and reduce cardiac damage post-injury in the postnatal heart.

Stage:	Cardiac crescent	Linear heart tube	Looping heart	Chamber formation
Mouse: Human:	E7.5 Day 15	E8.5 Day 20	E9.5 Day 28	E10.5 Day 32
Milestones:	Cardiac differentiation Migration to midline	Heart tube formation Anterior-posterior and dorsal-ventral patterning First heartbeat	Looping to the right Early chamber formation	Chamber formation Cushion formation Outflow tract separation Early conduction system formation
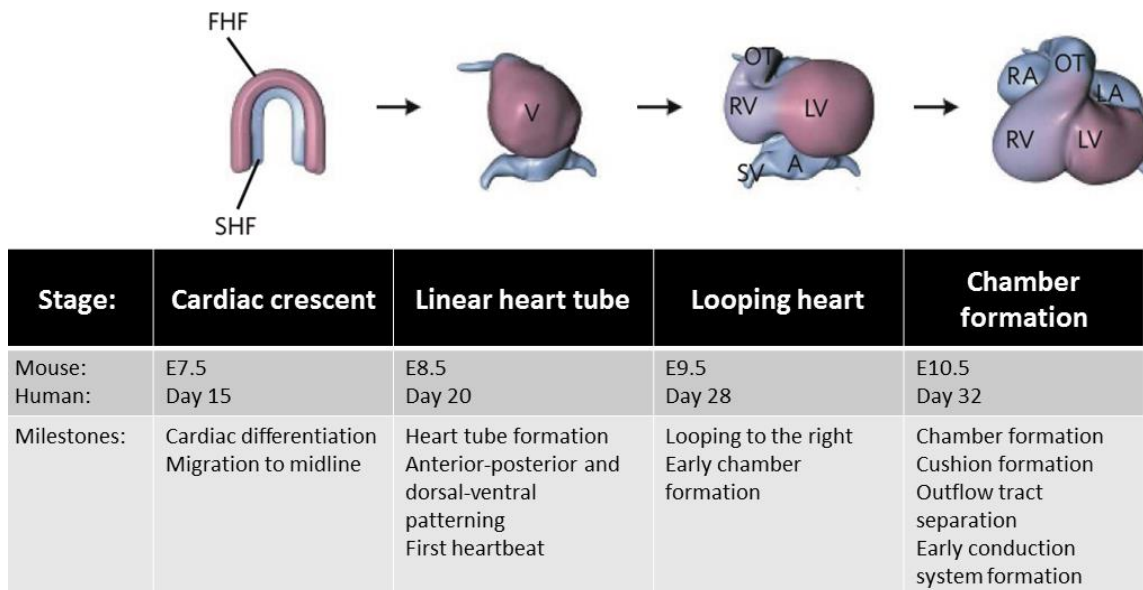
Figure 1.1 Early stages of mammalian heart development. At the earliest stages of heart formation (cardiac crescent), two pools of cardiac precursors exist. The first heart field (FHF) contributes to the left ventricle (LV), and the second heart field (SHF) contributes to the right ventricle (RV) and later to the outflow tract (OT), sinus venosus (SV), and left and right atria (LA and RA, respectively). V, ventricle (Adapted from (Bruneau 2008)).
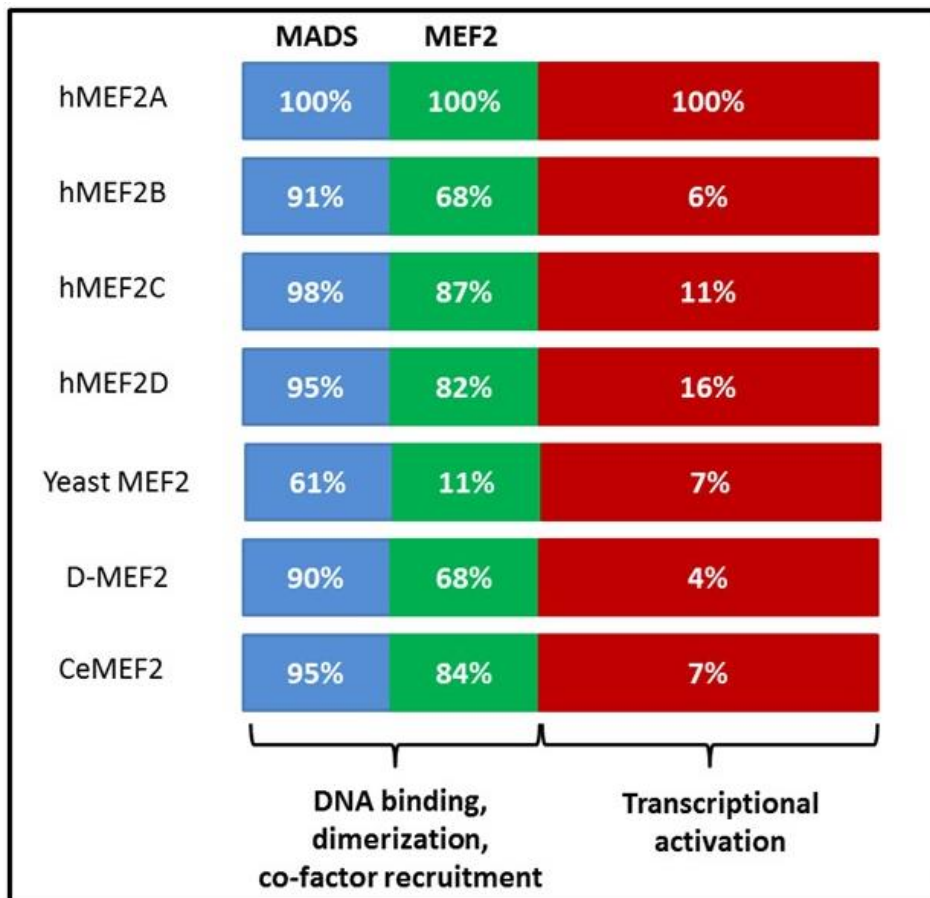
Figure 1.2 Sequence conservation of MEF2. The percentage of amino acid identity among the MADS, MEF2, and transcriptional activation domains of MEF2 proteins relative to human MEF2A. hMEF2, human; D-MEF2, *Drosophila*, CeMEF2, *C.elegans* (Adapted from (Potthoff and Olson 2007)).
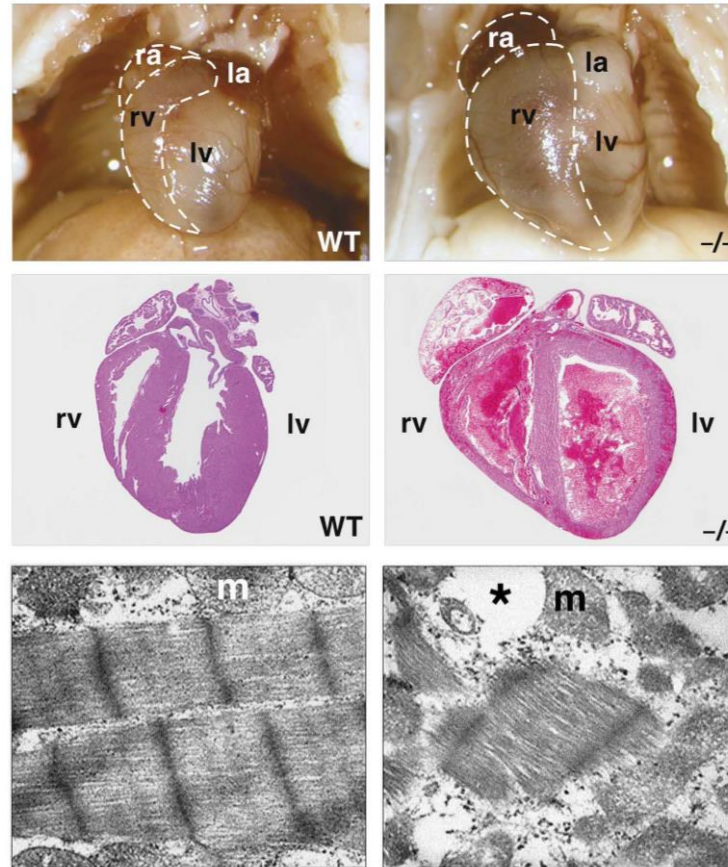
Figure 1.3 MEF2A knockout mice exhibit cardiac abnormalities. Evidence of cardiac dysfunction in MEF2A knockout mice. Gross (top panel) and histological sections (middle panel) of hearts from wild-type (left) and *Mef2a*$^{-/-}$ (right) neonatal P5 mice show right ventricular dilation in *Mef2a*$^{-/-}$ hearts. Transmission electron micrographs (bottom panel) of cardiac muscle from wild-type (left) and *Mef2a*$^{-/-}$ (right) show myofibrillar disorganization and fragmentation in *Mef2a*$^{-/-}$ hearts. Right atria (ra), left atria (la), right ventricle (rv), left ventricle (lv), mitochondria (m), vacuolization (*) (Adapted from (Naya et al. 2002)).
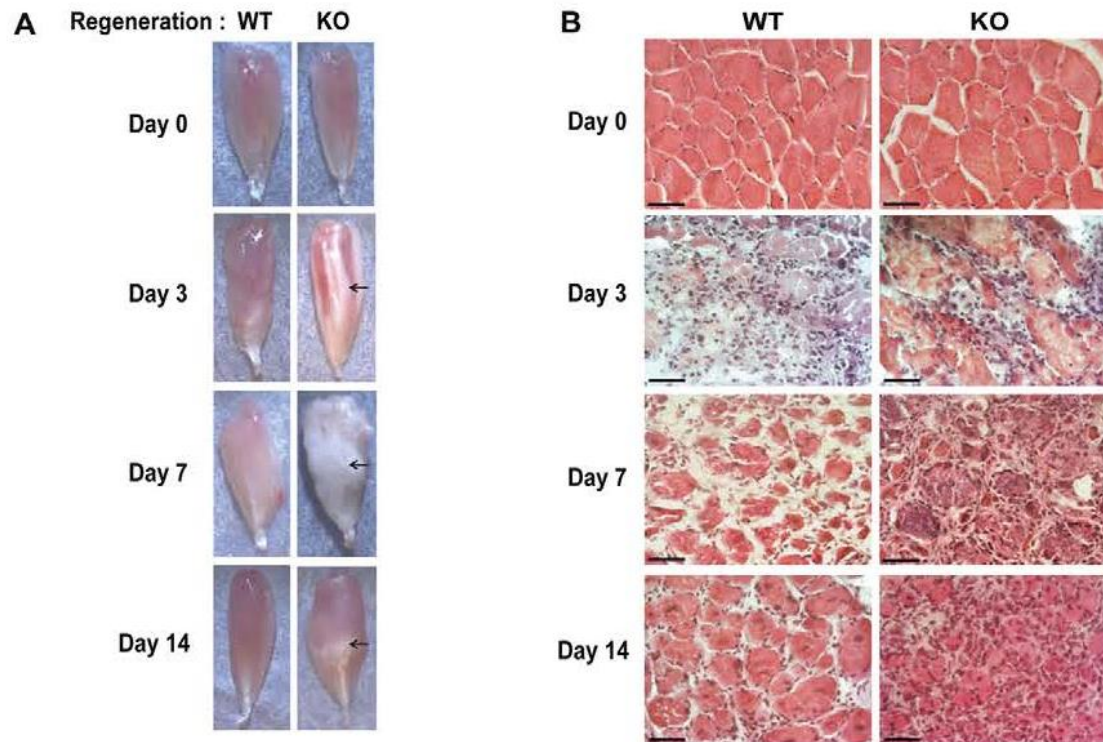
Figure 1.4 MEF2A knockout mice exhibit delayed skeletal muscle regeneration post-injury. A) Images of whole muscle and B) hematoxylin and eosin staining of tibialis anterior muscle from adult wild-type (WT) and *Mef2a$^{-/-}$* (KO) mice post-cardiotoxin induced injury show KO mice exhibit impaired regenerative myogenesis. Arrows indicate areas of necrosis. Scale bars are 50 µm (Snyder et al. 2013).
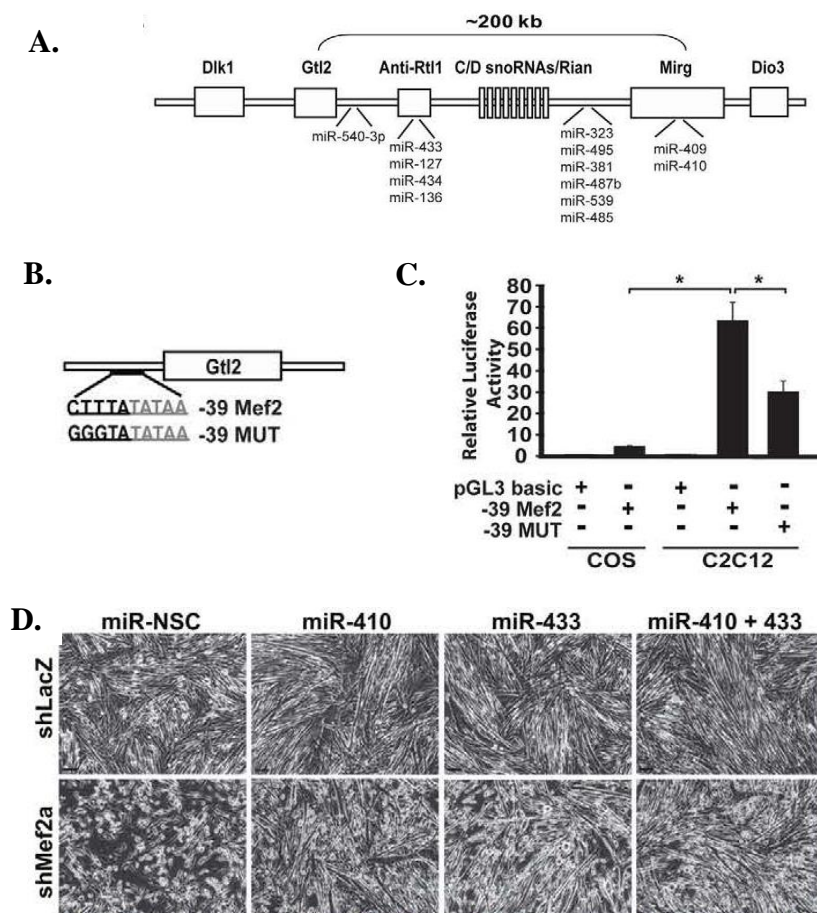
Figure 1.5 MEF2A regulates the *Gtl2-Dio3* microRNA mega-cluster to modulate WNT signaling in skeletal muscle regeneration. A) Depiction of the *Gtl2-Dio3* miRNA mega-cluster locus on mouse chromosome 12. Relative positions of the top downregulated miRNAs in *Mef2a^{-/-}* mice are shown. B) The -39 MEF2 site upstream of *Gtl2* is shown with the overlapping TATA box (gray). A luciferase reporter was generated containing the WT MEF2 site (-39 MEF2) and a mutant MEF2 site (-39 MUT). C) Luciferase analysis of the *Gtl2* promoter showing muscle-specific activation of the reporter. D) Phase contrast images of C2C12 DIFF3 cells transduced with sh*lacZ* or sh*Mef2a*, and transfected with 40nM miR-NSC, miR-410, or miR-433 mimics demonstrate rescue of myogenic differentiation (Adapted from (Snyder et al. 2013)).
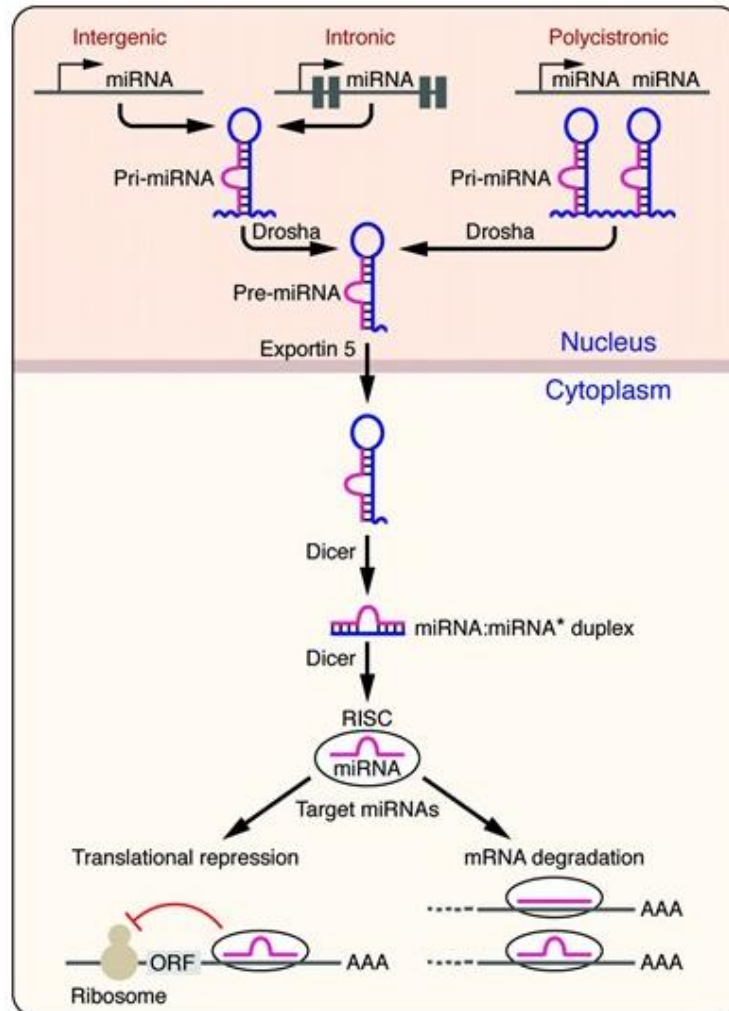
Figure 1.6 microRNA biogenesis. Nascent primary-miRNAs (pri-miRNAs) are processed by Drosha into precursor-miRNAs (pre-miRNAs). Pre-miRNAs are transported into the cytoplasm by Exportin 5 and are cleaved by Dicer into a miRNA:miRNA* duplex. The mature miRNA is incorporated into the RNA-Induced Silencing Complex (RISC) for mRNA targeting (Adapted from (van Rooij 2011)).
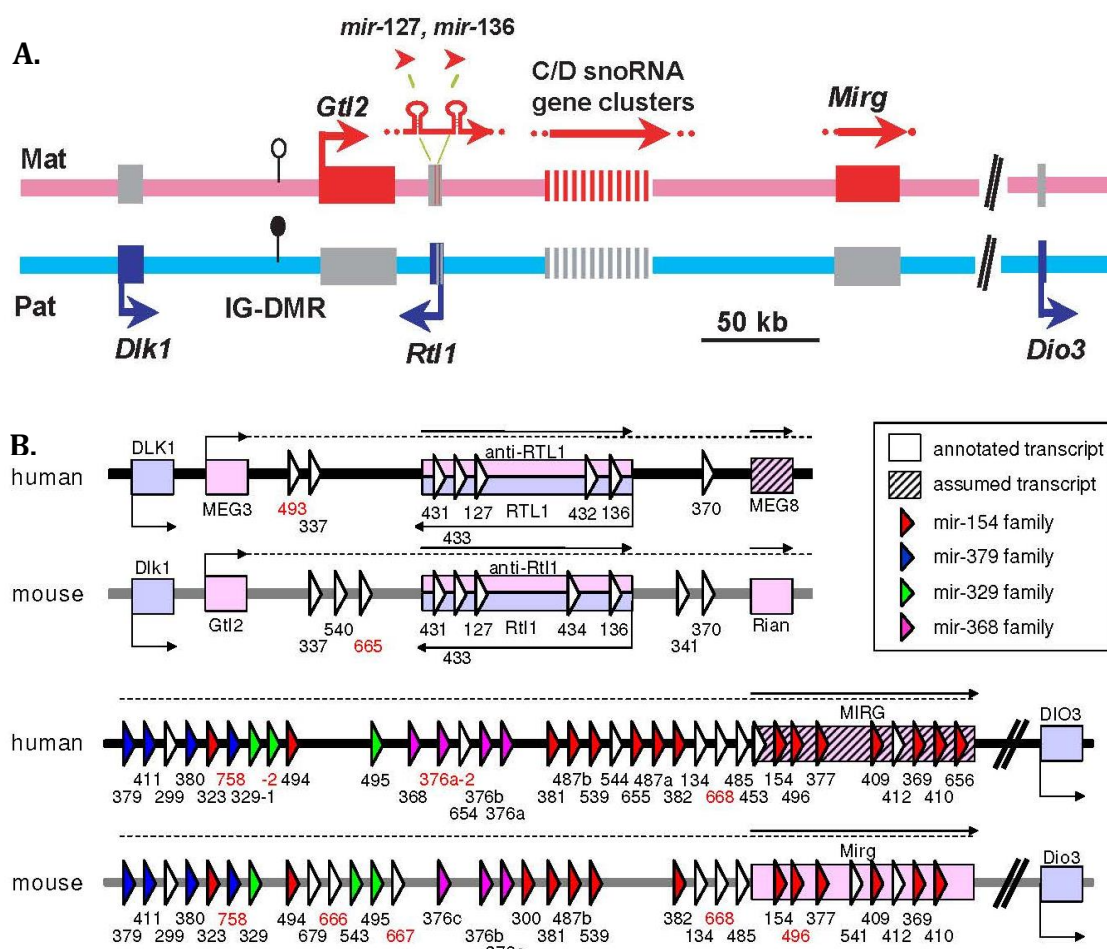
Figure 1.7 The *Gtl2-Dio3* microRNA mega-cluster. A) Schematic representation of the 1-Mb imprinted cluster on mouse chromosome 12. Maternally imprinted genes (top) include Gtl2/MEG3, Rian C/D snoRNAs, and Mirg. Paternally imprinted genes (bottom) include Dlk1, Rtl1, and Dio3 (adapted from (Lin et al. 2003)). B) Schematic representation of the location of many of the miRNAs in the locus. Paternal (blue), maternal (pink). (Adapted from (Kircher et al. 2008)).
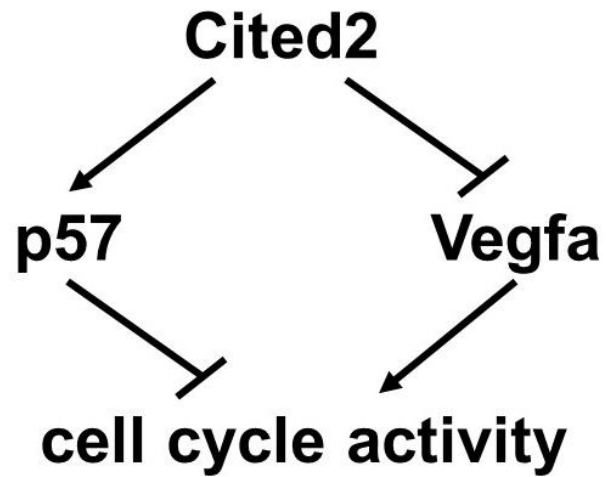
Figure 1.8 Cited2 regulates cell proliferation. Cited2 is a positive regulator of p57 and a negative regulator of Vegfa. Knockdown of Cited2 results in decreased p57 and increased cell cycle activity. Knockdown of Cited2 results in increased Vegfa and increased cell cycle activity.

CHAPTER TWO – MATERIALS AND METHODS

2.1   Cell Culture

2.1.1   Cell Lines

COS1 and A293 cell lines were maintained in Dulbecco's Modified Eagle Medium (DMEM, Invitrogen) supplemented with 10% fetal bovine serum (FBS, Atlanta Biologicals) and 1% Penicillin/Streptomycin/L-Glutamine (Invitrogen), referred to as growth medium. Cells were maintained in a 37°C humidified incubator with 5% CO_2. At subconfluency, adherent cells were passaged by washing with 1X phosphate-buffered saline (PBS, Invitrogen), application of 2mL Trypsin-EDTA (Invitrogen) for 3 minutes, and resuspending cells in 8mL growth medium. Cells were passaged at a 1:10 or 1:20 dilution for maintenance of cell lines.

2.1.2   Neonatal Rat Ventricular Myocytes (NRVM) Isolation

NRVMs were isolated from mixed sex 1-2 day old Sprague-Dawley rat pups (Charles River Laboratories). Typically, hearts were isolated from 9-11 neonatal rats. Rats were sacrificed using cervical dislocation for the harvesting of hearts. Hearts were removed and placed in chilled, sterile 1X Hanks' Balanced Salt Solution (HBSS, Invitrogen) on ice until all the hearts were isolated. Once all the hearts were harvested, they were brought into the sterile tissue culture hood for dissection. The 1X HBSS was removed and hearts were placed into a clean 6cm tissue culture dish containing 5mL of fresh 1X HBSS. Ventricles were dissected from the atria and vessels and placed into a new 6cm dish containing 5mL fresh 1X HBSS. Ventricles were then dissected into 3-4 equal sized pieces and washed 3 times with 1X HBSS. After the final wash, ventricles were placed into 25mL of a 1mg/mL

solution of Trypsin EDTA/1X HBSS (Invitrogen) overnight at 4°C. The next day, 10mL

of pre-warmed 10% FBS growth medium was added and allowed to shake at 37°C in a

shaking incubator at 100 RPM for 3 minutes. The trypsin/medium solution was removed

and 10mL of pre-warmed 10mg/mL collagenase II (Worthington Biochemical) was added.

Hearts were incubated in the collagenase II solution for 6 minutes at 37°C while shaking

at 100 RPM. The supernatant containing individual cardiomyocytes was removed and put

into a tube on ice. This step was repeated 7 times until only very small (~1mm) ventricle

pieces remained. Once all cardiomyocytes were isolated, a total of two tubes containing

40mL of cardiomyocytes/collagenase solution were centrifuged at 4000 RPM for 4 minutes

to pellet the cells. The supernatant was removed and the cells were resuspended with 20mL

of 10% FBS growth medium. The resuspended cells were centrifuged at 4000 RPM for 4

minutes. The supernatant was removed and 10mL of fresh 10% FBS growth medium was

added to resuspend the cells. The 20mL total of cardiomyocytes/growth medium were

plated onto a 10cm tissue culture plate and incubated for 1 hour at 37°C in the tissue culture

incubator to allow the cardiac fibroblasts to adhere first. After 1 hour, the solution was

placed onto a new 10cm plate and incubated for another hour at 37°C, to reduce the number

of cardiac fibroblasts in the final NRVM cultures. Cells were counted using a

hemocytometer and plated at a density of $4x10^6$ cells/10cm^2, $1x10^6$ cells/6cm^2, or $3x10^5$

cells/well of 6-well gelatinized plates. After 12-20 hours in culture, the medium was

removed and replaced with fresh 10% FBS growth medium. The next day, the medium was

removed and replaced with 0.5X Nutridoma DMEM with no antibiotics (Roche), a low

serum medium, and changed every day thereafter. For hypertrophy experiments, NRVMs

were treated with 20 µM phenylephrine (Sigma) or 50 µM angiotensin II (Sigma) for 48 hours.

2.2   Mouse Husbandry

2.2.1   Mouse Strains

Mouse strains derived from a mixed background of 192Sv and C57B6 (Jackson Laboratories) included wild type (WT) and MEF2A knockout (KO) mice (Naya et al. 2002). The *mdx* mouse strain is derived from a C57BL/10ScSn background (Jackson Laboratories). The MEF2A/*mdx* mouse was generated by crossing the MEF2A knockout mouse to the *mdx* mouse for multiple generations. Tissue samples from the myocardial infarction and angiotensin II mouse models were obtained from the Walsh Laboratory at the Whitaker Cardiovascular Institute, Boston University School of Medicine. Ligating the left coronary artery is a surgical technique that mimics myocardial infarction and leads to heart failure. Left anterior descending coronary artery (LAD) ligation was performed on these mice as previously described (Shibata et al. 2007, Araki et al. 2012). Angiotensin II is a hypertensive agonist drug that promotes myocardial damage (Kim and Iwao 2000). Angiotensin II promotes hypertrophy by activating the Angiotensin II type I (ATI) receptor, which stimulates multiple signal transduction pathways (Gray et al. 1998). Angiotensin II was administered via subcutaneous osmotic mini-pumps for 14 days (Shibata et al. 2004). Tissue samples from the *DyW* laminin-α2 knockout mouse model were obtained from the Girgenrath Laboratory at Sargent College, Boston University.

2.2.2 Genotyping

Genomic DNA was isolated from mouse tail samples taken from mice at postnatal day 20, weaning age. Tail samples were digested in 200µL tail lysis buffer (10mM Tris-HCl pH 8.5, 25mM EDTA pH 8.0, 1% SDS, 100mM NaCl, 0.2mg/mL Proteinase K (NEB) at 55°C overnight. 200µL of phenol:chloroform (1:1) was added to the tail solutions and mixed by vortexing. Samples were centrifuged at 13,000 RPM for 1 minute. The top aqueous layer was placed into a new microcentrifuge tube. 1mL cold 100% ethanol was added to each sample and centrifuged for 5 minutes. DNA pellets were washed with 200µL cold 70% ethanol, centrifuged for 1 minute, and allowed to air dry before resuspending in 200uL sterile water. Genomic DNA was then used in genotyping PCRs set up in 25uL final volume: 1uL genomic DNA, 2.5µL 10X Thermopol Buffer (NEB), 2uL 2.5mM dNTPs (NEB), 1uL 25µM primer mix (1:2:1 ratio of 100µM forward primer: Baxter dH$_2$O: 100µM reverse primer), 0.5-1.0µL Taq polymerase (NEB), and Baxter water. The thermocycler program for the PCR reactions was as follows: 94°C for 4 minutes, 94°C for 30 seconds, 60°C for 30 seconds, 72°C for 30 seconds. Steps 2-4 were repeated 29 times for a total of 30 cycles and a final extension was performed at 72°C for 10 minutes. Samples were held at 4°C until removed from the thermocycler. PCR products were electrophoresed on a 0.8% agarose gel containing ethidium bromide in a 1X TAE buffer at 120V for 20-30 minutes. Gels were imaged under UV light. Primer sets used for these reactions are listed in Table 2.1. M2A and Neo: Mice with only a MEF2A band were considered wild type, mice with only a Neo band were considered MEF2A knockouts, and mice with both a MEF2A and Neo band were considered heterozygous for the MEF2A knockout allele.

2.2.3 Tissue Dissection

Mice of mixed sexes were sacrificed by cervical dislocation. Hearts were harvested at perinatal time points (P3-P5) and adult (6-8 weeks) from wild type (N=5) and MEF2A knockout (N=5). Muscle was harvested for total protein, RNA isolation, or histology. For histology, muscle was placed in optimal temperature embedding compound (OCT), snap-frozen in dry-ice-cooled isopentane and stored at -80°C. Transverse muscle sections (10uM) created with a Leica CM 1850 cryostat microtome at -80°C were then immunostained with protein-specific antibodies or stained with hematoxylin & eosin (H&E) for visualization of basic muscle morphology.

2.3   Recombinant DNA Techniques

2.3.1   Preparation of DH5α Cells

The DH5α strain of *Escherichia coli* (*E. coli*) cells were made chemically competent for introduction of recombinant DNA for these studies using the following protocol. DH5α cells were streaked onto Luria Broth (LB) agar plates (10g/L casein peptone, 5g/L yeast extract, 5g/L NaCl, 15g/L agar) and incubated overnight at 37°C. A single colony was picked and used to inoculate a 3mL LB liquid culture (10g/L casein peptone, 5g/L yeast extract, 5g/L NaCl) and grown 18-24 hours in a shaking incubator at 37°C. The 3mL culture was then used to inoculate a 200mL LB culture and grown to early log phase, shaking at 37°C for an additional 3 hours. Cells were pelleted by centrifugation at 4000 RPM for 5 minutes at 4°C. Pelleted cells were resuspended in 20mL pre-chilled 10nM NaCl, then 80mL additional chilled 100mM $CaCl_2$ was added for a final volume of 100mL. Cells were incubated on ice for 30-60 minutes then centrifuged at 4000 RPM for

5 minutes at 4°C. The pellet was resuspended in 17mL filter-sterilized, pre-chilled 100mM CaCl$_2$ with 3mL 100% glycerol. Resuspended DH5α *E. coli* were aliquoted in 100μL volumes into 1.7mL microcentrifuge tubes, snap frozen using liquid nitrogen, and stored at -80°C.

2.3.2 Cloning

For routine cloning, restriction endonuclease reactions were used to isolate DNA fragments of interest and to prepare vector DNA for subcloning. Generally, 1μL of DNA was digested for 1 hour at 37°C using appropriate restriction endonucleases and buffer (NEB). Following digestion, 6X loading dye (0.7% xylene cyanol, 0.5% bromophenol blue, and 60% glycerol in deionized water (dH$_2$O)) to a final concentration of 1X was added and samples were electrophoresed on a 0.8% agarose gel (BioExpress) containing ethidium bromide in 1X TAE buffer (40mM Tris, 50mM sodium acetate, 1mM EDTA pH 8.0) at 120V for 20-30 minutes. DNA digestion reactions were visualized and photographed under ultraviolet (UV) light. Appropriate DNA fragments were excised from the gel and purified on QIAquick columns using the QIAquick Gel Extraction Kit (Qiagen), according to the manufacturer's instructions. Briefly, 600μL of buffer QG was added to the excised gel slices and incubated at 55°C for 10 minutes to dissolve the gel. 200μL of isopropanol was added and the solution was then added to a QIAquick column to bind the DNA and centrifuged at 14,000 RPM for 1 minute at room temperature. The flow-through was discarded and the sample was centrifuged again until the total volume had passed through the column. 750μL of Buffer PE was added to wash the column and the sample was centrifuged at 14,000 RPM for 1 minute at room temperature. Flow-through was

discarded and the column was centrifuged again at 14,000 RPM for 1 minute at room temperature to remove any remaining buffer. The QIAquick column was placed into a new 1.7mL microcentrifuge tube and the DNA was eluted by adding 30μL of Buffer EB and centrifuged at 14,000 RPM for 1 minute at room temperature. The purified DNA in the elution buffer was then used for ligation reactions. Generally, ligations were performed using a 5:1 ratio of restriction enzyme-digested insert DNA to vector DNA: 15μL (~250ng) insert DNA, 1μL (~50ng) vector DNA, 2μL 10X T4 DNA ligase buffer, and 1μL T4 DNA ligase (NEB) in a 25μL total volume with dH_2O. Ligations were incubated in a thermocycler for 4 hours at 16°C, prior to use in DH5α *E. coli* transformation reactions.

2.3.3   Transformation of Competent DH5α Cells

Frozen aliquots of chemically competent DH5α *E. coli* cells were thawed on ice. For transformation of ligation reactions, 50μL of cells were pre-incubated with half the ligation reaction (~100ng of DNA) for 10 minutes on ice. For other transformations, 10μL of cells were pre-incubated with 1μg plasmid DNA (1-2μL) for 10 minutes on ice. Competent cells were then "heat-shocked" in a 42°C water bath for 30 seconds to permeabilize the cell membranes and facilitate introduction of plasmid DNA into the cells. Fresh LB (250μL for cloning ligations) was added to transformed bacteria and cells were incubated on ice for 10 minutes, then allowed to recover for 1 hour in a 37°C shaking incubator. Transformed bacteria were plated on LB agar plates containing the appropriate antibiotic (Amp 100μg/mL, Kan 50ug/mL) to select for clones with the transformed plasmid. Plates were incubated overnight at 37°C. Single colonies were picked to inoculate

3mL LB liquid cultures with antibiotic. Liquid cultures were then used for DNA isolation and preparation (section 2.3.4).

2.3.4 DNA Preparation

2.3.4.1 Mini-Prep DNA Preparations

For small-scale crude DNA preparation, mini-preparation was used. A single colony of bacteria was selected from an LB agar plate and placed into 3mL of LB broth containing appropriate antibiotics. The selected colony was grown overnight in a 37°C shaking incubator. The next day, 1.5mL of the 3mL overnight culture was centrifuged at 13,000 RPM for 1 minute at room temperature. The pellet was resuspended in 100µL of Solution #1 (50mM glucose, 10mM EDTA pH 8.0, 25mM Tris) and then lysed in 200µL of Solution #2 (0.2M NaOH, 1% SDS). Cell lysis was stopped by adding 150µL of Solution #3 (3M potassium acetate, 11.5% glacial acetic acid). 400µL of phenol:chloroform (1:1) was added and the sample was mixed by vortexing. The upper aqueous layer containing nucleic acids was transferred to a new tube. DNA was precipitated by adding 800µL cold 100% ethanol and samples were centrifuged at 13,000 RPM for 10 minutes at 4°C. DNA pellets were washed with 200µL 70% ethanol, centrifuged at 13,000 RPM for 1 minute, inverted and allowed to dry. Dried pellets were resuspended in 20µL Baxter water with 0.1mg/mL RNase and incubated at 37°C for 15 minutes.

2.3.4.2 MIDI-Prep DNA Preparations

For large scale DNA preparation, MIDI-preparation was used. 100µL of cultured DH5α cells in LB liquid was incubated with 100mL of LB broth containing the appropriate concentration of antibiotic in a shaking 37°C incubator overnight. Cells were pelleted by

centrifugation at 7,000 RPM for 5 minutes at 4°C. DNA isolation was performed using NucleoBond Plasmid Purification MIDI Prep System (BD Biosciences), according to the manufacturer's instructions. Briefly, the bacteria was resuspended in 4mL buffer S1, lysed in 4mL buffer S2, and neutralized in 4mL buffer S3. The NucleoBond column was equilibrated with 2.5mL buffer N2 and the solution was passed through a folded filter onto the column. The column was washed three times with 10mL buffer N3 and the DNA was eluted with 5mL buffer N5. 3.5mL isopropanol was added to the eluted buffer and the solution was centrifuged at 9,000 RPM for 30 minutes at 4°C. The DNA pellet was washed with 2mL 70% ethanol, centrifuged at 9,000 RPM for 5 minutes at 4°C, allowed to dry, and resuspended in 200μL dH$_2$O and stored at -20°C.

2.3.4.3 DNA Sequencing

DNA sequencing was performed by sending 10μL of 100ng/μL purified plasmid DNA and 10μL of 3μM primers to MWG Operon.

2.4   Transfection Techniques

2.4.1   General Plasmid Transfection

General transfections of expression vectors in mammalian cell lines were performed through lipid-mediated plasma delivery for all experiments. Three types of lipid-mediated transfection reagents were used for plasmid transfections: FuGENE (Roche), Polyethylenimine (PEI, Polysciences, Inc.), and Trans-iT (Mirus Bio, LLC). Generally, cells were seeded on cell culture plates 24 hours prior to transfection so they would be 40-70% confluent at the time of transfection. FuGENE was used at a 3:1 ratio (μL FuGENE:μg plasmid DNA) in COS1 cells, PEI was used at a ratio of 6:1 for all cell

lines, and Trans-iT was used at a 1.5:1 ratio in COS1 cells. For all transfections, the transfection reagent was pre-warmed to room temperature and added to pre-warmed serum free DMEM (100μL sfDMEM per 1μg DNA) in a sterile Eppendorf tube and incubated at room temperature for 5 minutes. DNA to be transfected was added to the transfection reagent/sfDMEM mixture and incubated at room temperature for 15 minutes. Complexed DNA and transfection reagent in sfDMEM was then added dropwise to cells and incubated in a 37°C incubator for 36-48 hours before harvesting.

2.4.2   microRNA Mimic and microRNA Inhibitor (Anti-miR) Transfections

For miRNA mimic and inhibitor (anti-miR) (Dharmacon) transfections, lipid-mediated transfections were performed using Lipofectamine 2000 transfection reagent (Invitrogen). For miRNA mimic transfections in NRVMs, the transfection reagent/DNA mixture was prepared directly in each well or tissue culture plate by adding 500μL OptiMEM medium (Invitrogen), 4μL Lipofectamine 2000, 10μM miRNA mimic (5μL for 6-well plate and 12.5μL for 6cm plate) for a final concentration of 25nM. The transfection reagent/DNA mixture was incubated at room temperature for 20 minutes. NRVMs were resuspended in antibiotic-free medium (DMEM with 10% FBS) and $3x10^5$ cells in 1.5mL total volume were plated per well of a 6-well plate containing the transfection mixture (2mL total final volume) or $2x10^6$ cells in 4.5mL total volume were plated on a 6cm plate containing the transfection mixture (5mL total final volume). Wells were mixed by swirling and incubated at 37°C. 24 hours later, medium was switched to 0.5% Nutridoma (low serum medium). 36 hours post-transfection, RNA and/or protein was harvested (see section 2.6.1 and 2.7.1).

For luciferase assays in COS1 cells and NRVMs, cells were reverse transfected at the time of plating. The transfection reagent/DNA mixture was prepared directly in each well of a 24-well cell culture plate by adding 100μL OptiMEM medium (Invitrogen), 1μL Lipofectamine 2000, 20ng pMIR-REPORT-3'UTR-Cited2, 200ng pMIR-REPORT-βgal (transfection control), and 7.5μL 10μM miRNA mimics (for a final concentration of 150nM). The transfection reagent/DNA mixture was incubated at room temperature for 20 minutes. COS1 cells were resuspended in antibiotic-free medium (DMEM with 10% FBS) and 40,000 cells in 400μL total volume were plated per well containing the transfection mixture (500μL total final volume). Wells were mixed by swirling and incubated at 37°C for 24-36 hours prior to harvesting the cells for luciferase assays.

For MEF2A knockdown rescue experiments in NRVMs, NRVMs were seeded in antibiotic-free DMEM at a density of 300,000 cells per well on 6-well plates. 24 hours later, cells were transduced with sh*lacZ* or sh*Mef2a* adenovirus at MOI 25. Cells were incubated for 24 hours at 37°C. Medium was then changed to 0.5X Nutridoma and transfected with miRNA mimics as follows: 500μL OptiMEM, 5μL 10μM miR mimic (25nM final concentration), and 4μL RNAiMAX were combined and incubated at room temperature for 30 minutes. For miR-410/495 combined transfections, 2.5μL of each 10μM miRNA mimic was added for a combined final concentration of 25nM. The transfection mixture was added dropwise to each well. All mimics were obtained from Dharmacon.

2.5   Cell-Based Assays

2.5.1   Luciferase Assays

Luciferase assays were performed 24-36 hours post-transfection using Luciferase Assay Reagent (LAR, Promega), and results were normalized using a β-galactosidase assay (section 2.5.2).

Cells were harvested for luciferase assays by washing with 1X PBS and lysing in 1X passive lysis buffer (Promega) by shaking for 15 minutes at room temperature. To measure luciferase activity in cells, 5μL of each cell lysate was placed into an Eppendorf tube. 30μL of LAR was added and 10 second measurements of the light absorbance was measured for firefly luciferase activity. To measure luciferase activity of the TOPflash plasmid in NRVMs, cell lysates were prepared in tubes as described above. Firefly luciferase activity was measured by adding 30μL LARII to each tube containing cell lysate, and performing 10 second measurements of the light absorbance in each tube. Following the first reading, 30μL of 1X Stop and Glo reagent (Promega) was added and Renilla luciferase measurements were taken. Firefly luciferase relative light unit (RLU) values were then normalized to Renilla RLU values and fold change in activity over reporter was calculated for each sample.

For 3'UTR luciferase experiments in COS1 cells and NRVMs analyzing the effects of miRNA mimics on 3'UTR of *Cited2*, cells were reverse transfected at the time of plating. The transfection reagent/DNA mixture was prepared directly in each well of a 24-well cell culture plate to be transfected by adding 100μL OptiMEM (commercial serum-free medium, Invitrogen), 20ng pMIR-REPORT-3'UTR-CITED2, 200ng pMIR-

REPORT-β-galactosidase (transfection control), 7.5μL of 10μM miRNA mimics (for a final concentration of 150nM), and 1μL RNAiMAX transfection reagent (Invitrogen). For miR-410/495 combined transfections, 3.25μL of each 10uM miRNA mimic were combined for a final concentration of 150nM. The transfection mixture was incubated for 30 minutes at room temperature. Cells were resuspended in antibiotic-free medium (DMEM with 10% FBS only) and 40,000 cells in 400uL volumes were plated per well on top of the reaction mixture for 500μL total volume per well. Wells were incubated 36-48 hours at 37°C and cells were harvested for luciferase assays.

2.5.2   β-galactosidase Assays

β-galactosidase (β-gal) assays were performed in 96-well plates to determine the transfection efficiency of each cell lysate sample. To measure β-gal activity, 15μL of cell lysates were added to 1.7mL microcentrifuge tubes and incubated with a sample reaction mixture containing 15μL 10X Z-buffer (100mM NaH_2PO_4, 10mM KCl, 1mM $MgSO_4$), 16.5μL 8mg/mL ONPG, 0.2μL β-mercaptoethanol, and 103.5μL dH_2O. The mixture was incubated at 37°C in a water bath until a slight yellow color appeared. To stop the reaction, 250μL of 1M Na_2CO_3 was added to each sample. The light absorbance of each well was measured at 415nm on a microplate reader (Model 550, Bio-Rad). β-gal readings were then used to normalize firefly luciferase readings using LAR.

2.6   RNA Techniques

2.6.1   RNA Isolation (Cell Culture)

NRVM cells harvested for RNA were cultured according to 2.1.2. Cells were rinsed with 1X PBS and RNA was isolated using TRIzol Reagent (Invitrogen). The volume of

TRIzol Reagent was dependent on the surface area of the culturing dish (350μL for 6-well plate, 500μL for 6cm plate, and 1mL for 10cm plate). Cells harvested in TRIzol Reagent were then processed according to the manufacturer's instructions. Briefly, 200μL of chloroform was added for every 1mL of TRIzol used. The mixture was mixed by vortexing for 30 seconds and was then centrifuged for 10 minutes at 13,000 RPM at 4°C. The upper phase containing the RNA was added to a new microcentrifuge tube containing an equal volume of 100% isopropanol and remained at room temperature for 10 minutes. RNA was precipitated by centrifugation at 13,000 RPM at 4°C for 10 minutes. The RNA pellet was washed with 1mL 70% ethanol for every 1mL TRIzol used and pellets were allowed to air dry. RNA pellets were resuspended in 15-40μL of Baxter water and stored at -80°C.

2.6.2 RNA Isolation (Animal Tissue)

Whole hearts were harvested and homogenized in 1-2mL TRIzol using the Polytron PT 10-35 homogenizer (Kinematics) for 30 seconds. Homogenate was placed in two microcentrifuge tubes and 200μL chloroform was added for every 1.0mL TRIzol. Samples were vortexed for 30 seconds and incubated at room temperature for 2-3 minutes. Samples were then centrifuged at 11.4K at 4°C for 10 minutes. The top phase was separated into a new tube and 500μL isopropanol was added and mixed. Samples were incubated at -20°C for 1 hour and then spun at 4°C at 11.4K for 30 minutes. Supernatant was removed and 1.0mL 70% ethanol was added to the pellet. The sample was then centrifuged for 5 minutes at 4°C. Pellets were then allowed to dry for 5-15 minutes and resuspended in 40μL of RNA-only water. The concentration of the RNA was taken using a nanodrop. Samples were stored at -80°C until use.

2.6.3   Reverse Transcription

The concentration of extracted RNA (described in 2.6.1 and 2.6.2) was measured by spectrophotometry using a nanodrop. cDNA was generated from 2μg of RNA, which was reverse transcribed using M-MLV Reverse Transcription Reagents (Promega). Reverse transcription reactions were set up containing 2μg of RNA in 9.3μL total volume dH$_2$O, 3μL 2.5mM dNTPs (NEB), and 3.35μL 15.4μM random hexamers (Promega). The solution was incubated at 65°C for 5 minutes, then on ice for 5 minutes. To each sample 0.5μL of RNasin (Promega), 0.5μL M-MLV Reverse Transcriptase (Promega), and 3μL 5X M-MLV RT Buffer (Promega) was added and the entire reaction was incubated at 37°C for 1 hour. Synthesized cDNA was stored at -20°C.

2.6.4   Polymerase Chain Reaction (PCR)

Polymerase chain reaction was performed for genotyping analyses (2.2.2), amplification of DNA fragments for cloning (2.3.2), and for gene expression analysis by semi-quantitative methods (2.6.6). To amplify DNA fragments from genomic or copy DNA (cDNA), the general protocol was as follows: 100ng-1μg DNA template, 2.5μL Thermo-Polymerase Buffer (NEB), 2μL 2.5mM dNTPs (NEB), 1μL 25μM gene specific primers, 0.5μL Taq polymerase (NEB), and 18.5μL dH$_2$O. Each sample was mixed gently, centrifuged briefly, and subjected to a PCR program on a bench-top thermocycler (MJ Research). A typical PCR program was as follows: denature for 4 minutes at 94°C, followed by 23-30 cycles of 94°C for 30 seconds, 56-60°C for 30 seconds (temperature varies with primer T_m), and 68°C for 30 seconds, followed by a final extension for 10

minutes at 68°C. Samples were held at 4°C until removed from the thermocycler when they were then stored at -20°C.

2.6.5   Site-Directed Mutagenesis

Site-directed mutagenesis was performed using overlap extension PCR for the generation of expression plasmids containing mutated cDNA sequences. Two PCR products were generated from the cDNA template. One reaction used a primer mix of a forward universal primer and a reverse mutagenic primer and the other reaction used a reverse universal primer and a forward mutagenic primer. Both mutagenic primers hybridized to the same sequence and induced guanine mutations but were oppositely oriented to amplify different halves of the desired cDNA fragment. Each PCR reaction was as follows: 1μg template DNA, 2.5μL 10X Thermopol Buffer (NEB), 2μL 2.5mM dNTPs (NEB), and Baxter water to a final volume of 25μL. The PCR reactions were run on thermocycler programs. PCR products from these reactions were electrophoresed on a 0.8% agarose gel containing ethidium bromide in 1X TAE buffer at 120V for 30 minutes. Gels were imaged under UV light and the appropriate size bands corresponding to the mutated cDNA fragment amplified were excised and gel extracted using the QIAquick Gel Extraction Kit as described previously. The extracted fragments were then used as template DNA sequences for subsequent overlap extension PCR. The reaction was as follows: 1μL fragment #1, 1μL fragment #2, 2.5μL 10X Thermopol Buffer (NEB), 2μL 2.5mM dNTPs (NEB), 1μL 25μM universal primer mix (1:2:1 ratio of 100μM forward universal primer:Baxter water:100μM reverse universal primer), 0.5-1.0μL Taq polymerase (NEB), and Baxter water to a final volume of 25μL. The thermocycler PCR program was run as

before and the appropriate size band was extracted using the QIAquick Gel Extraction Kit (NEB). The extracted fragment was digested with restriction endonucleases (NEB) prior to ligation into a destination vector. Mutations in cDNA sequences were confirmed after midiprep column purification through DNA sequencing (MGW Operon).

2.6.6 Semi-Quantitative RT-PCR

Semi-quantitative RT-PCR was performed in 25µL reaction volumes. Briefly, 1µL cDNA, 2.5µL 10X Thermopol buffer (NEB), 2µL 2.5mM dNTPs (NEB), 1µL primer mix (1:2:1 ratio of 100µM forward primer: Baxter dH_2O: 100µM reverse primer), 0.25µL of Taq polymerase (NEB), and 18.25uL dH_2O samples were subjected to a PCR program using a thermocycler with the general format: 94°C for 4 minutes, 94°C for 30 seconds, 53-60°C for 30 seconds (temperature varies with T_m), and 72°C for 30 seconds. Steps 2-4 were repeated 18-30 times and a final extension was performed at 72°C for 10 minutes. Samples were held at 4°C until removed from the thermocycler. Samples were then run on 0.8% agarose gels with ethidium bromide to visualize PCR product bands. GAPDH or 18S rRNA PCR products were used as controls.

2.6.7 Quantitative RT-PCR

2.6.7.1 mRNA Expression Analysis

qRT-PCR was performed using Power SYBR Green Master Mix (Invitrogen) using the ABI Prism 7900HT Sequence Detection System (Applied Biosystems). Each sample was run in triplicate on a 384-well plate (Applied Biosystems). For one reverse-transcribed cDNA and one primer set the protocol was as follows: 1µL cDNA, 15µL Power SYBR Green Master Mix, 6µL primer mix (5µL 100µM forward primer + 5µL 100µM reverse

primer + 190μL dH$_2$O), 8uL dH$_2$O. 8.5μL of each sample reaction was plated per well in triplicate. Plates were briefly centrifuged and subjected to thermocycling with the following amplification program: 50°C for 2 minutes, 95°C for 10 minutes, 95°C for 15 seconds, 60°C for 1 minute; steps 3-4 were repeated 39 times for a total of 40 cycles. Data was analyzed using SDS 2.2.4 software (Ambion) and C$_T$ values were compared between gene specific primers and controls. The C$_T$ value for each gene were averaged and subtracted from the average internal control (GAPDH, 18S rRNA or 5S rRNA) C$_T$ value to determine the gene ΔC$_T$ value. The ΔΔC$_T$ was calculated by subtracting the ΔC$_T$ of the condition from the ΔC$_T$ of the control sample set. Fold changes between samples were calculated using the formula FC=2$^{-ΔΔCT}$. Differences in relative gene expression were analyzed for significance using a Student's T-Test. A p-value of ≤0.05 was considered statistically significant.

Primers for qRT-PCR were designed or obtained from the Primer Bank Website (http://pga.mgh.harvard.edu/primerbank). Sequences can be found in Table 2.1.

2.6.7.2 Stem-Loop RT-PCR for microRNA Expression Analysis

Stem-loop qRT-PCR was performed for detection of mature miRNAs as described by Chen *et al.* (Chen et al. 2005). Stem-loop specific primers for 5S ribosomal RNAs and mature miRNAs (miR-410, miR-495, and miR-433) were used to reverse-transcribe pooled cardiac muscle or NRVMs using the TaqMan miRNA Reverse Transcriptase Kit (Applied Biosystems) according to the manufacturer's instructions. Stem-loop primers can be found in Table 2.1. Briefly, the reaction was as follows: 0.15μL 100mM dNTPs, 1.5μL 10X reverse transcription buffer, 0.19μL RNasin, 0.75μL 1uM stem-loop specific primer, 500ng

RNA, 1μL (50U) Multiscribe reverse transcriptase, and nuclease-free dH_2O to a final volume of 15μL. Reverse transcription reactions were performed on a thermocycler with the following program: 16°C for 30 minutes, 42°C for 30 minutes, 85°C for 5 minutes, cooled to 4°C and immediately stored at -20°C.

MiRNAs and 5S rRNA sequences were amplified by qRT-PCR using a forward-specific primer and a universal reverse primer with the following reaction: 2μL miRNA-specific cDNA, 15μL Power SYBR Green Master Mix, 0.5μL 20uM miRNA-specific forward primer, 0.5μL 20uM universal reverse primer, 12μL dH_2O. qRT-PCR was described as above (2.6.7.1) in triplicate in a 384-well plate on the 7900HT Sequence Detection System using a modified thermocycling program: 50°C for 2 minutes, 95°C for 2 minutes, 95°C for 15 seconds, 60°C for 1 minute; steps 3-4 were repeated 39 times for a total of 40 cycles. C_T values and fold change analysis were determined as described in 2.6.7.1.

2.7   Protein Techniques

2.7.1   Protein Isolation (Cell Culture)

For cultured cells, protein was isolated by first washing the cells with 1X PBS twice. Cells were scraped into 500μL 1X PBS using a Cell Lifter (Corning). Cells were centrifuged for 1 minute at 13,000 RPM at 4°C. The cell pellet was resuspended in 200μL cold ELB Buffer (50mM HEPES, 250mM NaCl, 5mM EDTA, 0.1% NP40, 1mM DTT, 1mM PMSF, 1X Protease Inhibitors (Roche), dH2O) and dounce homogenized. Homogenized cells were incubated on ice for 10 minutes and centrifuged at 13,000 RPM

for 10 minutes at 4°C. Supernatant containing protein was transferred to a new Eppendorf tube and stored at -80°C until use.

2.7.2 Protein Isolation (Animal Tissue)

For mouse tissue samples, protein was harvested by homogenizing tissue in 1-2mL ELB Buffer (without 0.1% NP40) using the Polytron PT 10-35 homogenizer (Kinematics) for 30 seconds. Homogenized cells were centrifuged at 13,000 RPM for 10 minutes at 4°C. Protein extraction then followed the same steps as cell culture protein isolation, with the supernatant containing protein being saved in a new Eppendorf tube and stored at -80°C until use.

2.7.3 Bradford Assay

To determine protein concentrations of cell extracts, Bradford Assays were performed. Dilution stocks of bovine serum albumin (BSA) we made as standards for protein concentrations of 0.2μg, 0.5μg, 1.0μg, 2.5μg, 5μg, and 10μg. BSA standards and protein samples were aliquoted in 10μL volumes into individual wells of a 96-well plate. 200μL 1X Bio-Rad Protein Assay Dye Reagent (Bio-Rad Laboratories) was added and absorbance was measured at 595nm on a microplate reader (Model 550, Bio-Rad) using Microplate Manager III software. The standard curve plot was created in Excel using the BSA standard dilutions. A best-fit linear trend line was assigned to the plot and the concentrations of the protein samples were extrapolated using the equation of the best-fit linear trend line, $y=mx+b$, where y=absorbance value, m=slope of the line, b=y-intercept, and x=unknown concentrations of the protein samples.

2.7.4   Western Blotting

Protein extracts (COS1, NRVM, or cardiac muscle) were electrophoresed using SDS-PAGE according to the following protocol. 10-20μg protein extract was added to SDS-loading buffer (1.52% Tris base [w/v], 20% glycerol, 2% SDS [w/v], 0.1% bromophenol blue [w/v], 2% β-mercaptoethanol) to a 40μL final volume and were denatured at 95°C for 5 minutes. Protein samples were loaded onto a 10% polyacrylamide gel made up of a lower separating gel (1.7mL 30% acrylamide/0.8% bis-acrylamide, 1.3mL separation buffer (375mM Tris-HCl pH 8.8, 0.1% SDS [w/v]), 50uL 10% APS, 2μL TEMED, 1.9mL dH2O) and an upper stacking gel (0.5mL 30% acrylamide/0.8% bis-acrylamide, 0.75mL stacking buffer (125mM Tris-HCl pH 6.8, 0.1% SDS [w/v]), 25μL 10% APS, 3μL TEMED, 2.1mL dH2O) and electrophoresed in 1X SDS Running Buffer (25mM Tris-HCl, 190mM glycine, 0.1% SDS [w/v]) at 190V for 1 hour. After electrophoresis, the gel was washed for 10 minutes in 1X Transfer Buffer (20% methanol, 20mM Tris, 150mM glycine) and proteins were transferred to an Immuno-blot PDVF membrane (Bio-Rad) at 200mAmps for 1 hour at 4°C or at 50mAmps overnight at 4°C. After transfer, the membrane was blocked in blotto solution (5% non-fat dry milk [w/v], 30mL 1X TBS) for 1 hour at room temperature or overnight at 4°C. Blocked membranes were then incubated with primary antibody for 1 hour at room temperature or overnight at 4°C. The membrane was then washed three times with 1X TBS/0.1% Tween for 5 minutes at room temperature and incubated with the appropriate HRP-conjugated secondary antibody for 30 minutes at room temperature. The membrane was then washed three times with 1X TBS/0.1% Tween for 5 minutes at room temperature. 300μL of a 1:1 solution of

Western Lightning Chemiluminescent Reagent (Perkin-Elmer) was added to the membrane for 1 minute at room temperature. Target protein-antibody complexes were visualized by exposing the reactive membranes to Blue Basic Autorad X-Ray Film (ISC BioExpress).

2.8   Histology and Immunofluorescence

2.8.1   Immunohistochemistry

For NRVM experiments, NRVMs were seeded on 0.1% gelatin-coated coverslips in 6-well plates at a density of 500,000 cells per coverslip/dish. For miRNA mimic overexpression experiments, mimics were reverse transcribed on the day of seeding. For MEF2A knockdown experiments, the following day NRVMs were transduced with adenoviruses.

For immunofluorescence analyses, cells were fixed on coverslips with 4% paraformaldehyde at room temperature for 20 minutes. Cells were then blocked in 3% BSA for 1 hour at room temperature. Cells were then incubated with primary antibody diluted in 200uL primary antibody dilution buffer (200μL 10X PBS, 1.8mL dH2O, 0.02g BSA, 6μL TritonX-100) for 1 hour at room temperature protected from light or overnight at 4°C. Primary antibodies included: anti-α-actinin (1:200; Sigma), anti-Ki67 (1:500; Sigma). Primary antibody was removed and cells were washed 3X for 10 minutes in 1X PBS. Secondary antibody was then applied for 1 hour at room temperature. Secondary antibodies included: anti-mouse Alexa Fluor 488, anti-rabbit Alexa Fluor 488, anti-rabbit Alexa Fluor 555 (Invitrogen). Excess secondary antibody was washed from cells as before and mounted in Vectashield mounting medium with DAPI (Vector Labs) on clean slides. Fluorescent

images were taken using an Olympus DSU Spinning Disk Confocal microscope or Olympus FV10i confocal imaging system.

2.8.2 EdU Assay

EdU assays were performed on NRVMs overexpressed with miRNA mimics using the Click-iT EdU Alexa Fluor 555 Imaging Kit (Molecular Probes). Cells were allowed to recover for 24 hours post-mimic reverse transfection. Medium was changed to 0.5X Nutridoma and 28 hours later EdU was added for a final concentration of 10uM per well. Cells were incubated for 20 hours with EdU. After incubation, medium was removed and cells were fixed in 4% paraformaldehyde for 15 minutes at room temperature. Fixative was removed and cells were washed twice with 3% BSA in PBS. 1mL TritonX-100 in PBS was added to each well and incubated at room temperature for 20 minutes. Permeabilization buffer was removed and cells were washed twice in 3% BSA in PBS. 500uL of Click-iT reaction cocktail was added to each coverslip (430μL 1X Click-iT reaction buffer, 20μL $CuSO_4$, 1.2μL Alexa Fluor azide, 50μL reaction buffer additive). Plates were rocked gently to insure the reaction cocktail was distributed evenly over the coverslips. Plates were incubated at room temperature for 30 minutes protected from light. Reaction cocktail was removed and wells were washed with 1mL 3% BSA in PBS. Primary antibody staining was then performed as previously described.

2.9   Statistical Analysis

All numerical quantification is represented as the mean ± the standard error of the mean (S.E.M.) of at least three independently performed experiments. Statistically significant differences between two sets of data were determined using the student's paired

t-test. Statistically significant differences between three or more sets of data were determined using analysis of variance (ANOVA). P-values of ≤ 0.05 were considered to be statistically significant.

Table 2.1 Oligonucleotide Table. Oligonucleotide primer sequences used in all PCRs are shown. Underlined sequences refer to mutations incorporated into the primers.

qRT-PCR:		
Oligo	**Direction**	**Sequence (5' to 3')**
Gapdh	Forward	TGGCAAAGTGGAGATTGTTGCC
	Reverse	AAGATGGTGATGGGCTTCCCG
Sfrp2	Forward	CCCCTGTCTGTCTCGACGA
	Reverse	CTTCACACACCTTGGGAGCTT
Axin2	Forward	TGACTCTCCTTCCAGATCCCA
	Reverse	TGCCCACACTAGGCTGACA
Cited2	Forward	TGGGCGAGCACATACACTAC
	Reverse	GGGTGATGGTTGAAATACTGGT
Nr3c1	Forward	TCTCAGGCAGATTCCAAGCA
	Reverse	TGGACAGTGAAACGGCTTTG
Errfi1	Forward	GCACAATGTCAACAGCAGGA
	Reverse	TCCAGAGATGGGTCCTCAGA
Ppp1cb	Forward	GAGTGTGCTAGCATCAACCG
	Reverse	GTCAAACTCGCCGCAGTAAT
Smad7	Forward	AGCATCTTCTGTCCCTGCTT
	Reverse	CTCCTCGAATTCTGTGCACG
Rere	Forward	TCATGTACTTGAGGGCAGCA
	Reverse	CACTTCTCGATCAGCTTGG
Stat3	Forward	TCAGTGAGAGCAGCAAGGAA
	Reverse	TTTCCGAATGCCTCCTCCTT
Gad1	Forward	ATGTGTGCAGGCTACCTCTT
	Reverse	TCGGAGGCTTTGTGGTATGT
Bim	Forward	TCGTCCACCCAATGTCTGACTC
	Reverse	CTCCTGTCTTGCGATTCTGTCTGT
Cdkn1c/p57	Forward	GACTGAGAGCAAGCGAACAG
	Reverse	CAGCGAGAAAGAAGGGAACG
Vegfa	Forward	TTCCTGTAGACACACCCACC
	Reverse	TCCTCCCAACTCAAGTCCAC
Gtl2	Forward	TGGAATAGGCCAACATCGTCA
	Reverse	AGGCTCTGTGTCCATGTGTCC
Nppa	Forward	ACCTGCTAGACCACCTGGAGGAG
	Reverse	CCTTGGCTGTTATCTTCGGTACCGG
Nppb	Forward	ATCTCCAGAAGGTGCTGCCCAG
	Reverse	CGCGGTCTTCCTAAAACAACCTCAG

qRT-PCR microRNAs:		
Oligo	**Direction**	**Sequence (5' to 3')**
5S rRNA stem loop	Forward	GTTGGCTCTGGTGCAGGGTCCGAGGTATT-CGCACCAGAGCCAACAAAGCC
miR-410 stem loop	Forward	GTTGGCTCTGGTGCAGGGTCCGAGGTATT-CGCACCAGAGCCAACACAGGC
miR-495 stem loop	Forward	GTTGGCTCTGGTGCAGGGTCCGAGGTATT-CGCACCAGAGCCAACAAGAAG
miR-433 stem loop	Forward	GTTGGCTCTGGTGCAGGGTCCGAGGTATT-CGCACCAGAGCCAACACACCG
5S rRNA	Forward	GAATACCGGGTGCTGTAGGC
miR-410	Forward	CCGCCAATATAACACAGATGGCC
miR-495	Forward	GCCAAACAAACATGGTGCACTT
miR-433	Forward	ATCATGATGGGCTCCTCGGT
Universal	Reverse	GTGCAGGGTCCGAGGT

Cloning:		
Oligo	**Direction**	**Sequence (5' to 3')**
Cited2 3'UTR	Forward	AATTACTAGTCAGATCCTGAAAGG-GTTGAG
	Reverse	AATTACGCGTGCTTTCAACACAGT-AGTATC
Cited2 miR410 MUT	Forward	TGTGCTAATAG<u>GGGGGGG</u>CAGTAC-ATGA
	Reverse	TCATGTACTG<u>CCCCCCC</u>CTATTAGC-ACA
Cited2 miR495 MUT	Forward	TCTTTTTTGT<u>GGGGGGGG</u>TTTACTC-CTT
	Reverse	AAGGAGTAAA<u>CCCCCCCC</u>ACAAAA-AAGA

Genotyping:		
Oligo	**Direction**	**Sequence (5' to 3')**
Mef2a	Forward	GCTAGCCAACATTTCACCTTTGAGATCT
	Reverse	CAACGATATCCGAGTTCGTCCTGCTTTC
Neo	Forward	TTGGCTACCCGTGATATTGCTGAAGAGC
Mdx	Forward	GCGCGAAACTCATCAAATATGCGTGTTA-GTGT
	Reverse WT	GATACGCTGCTTTAATGCCTTTAGTCACT-CAGATAGTTGAAGCCATTTG
	Reverse mdx	CGGCCTGTCACTCAGATAGTTGAAGCCA-TTTTA

CHAPTER THREE – MICRORNAS IN THE MEF2-REGULATED GTL2-DIO3 NONCODING RNA LOCUS PROMOTE CARDIOMYOCYTE PROLIFERATION BY TARGETING THE TRANSCRIPTIONAL COACTIVATOR CITED2

3.1   Introduction

MEF2A is known to be an important transcription factor for cardiomyogenesis in mice. Approximately 80% of MEF2A knockout mice die perinatally due to right ventricular dilation and myofibrillar fragmentation (Naya et al. 2002). We recently showed that although skeletal muscle develops normally in these mice, there is a delay in skeletal muscle regeneration. MEF2A mediates the *Gtl2-Dio3* miRNA cluster in skeletal muscle. Members of this cluster, specifically miRNA-410 and miRNA-433, target Sfrp2, an inhibitor of Wnt signaling. Downregulation of this cluster in MEF2A knockout mice results in impaired Wnt signaling, leading to impaired regeneration (Snyder et al. 2013).

To determine if this miRNA cluster plays a role in cardiac muscle, I first examined the expression of the *Gtl2* promoter in cardiomyocytes. I showed that the *Gtl2* promoter is active in cardiomyocytes via a reporter assay, and this activity is lost when MEF2A is knocked down *in vitro*. Additionally, the expression of the *Gtl2-Dio3* miRNAs *in vivo* was significantly higher in perinatal wild type mice compared to adult. Furthermore, knockdown of MEF2A *in vitro* and loss of MEF2A *in vivo* results in the downregulation of the *Gtl2-Dio3* miRNAs.

To investigate the specific role of the MEF2A-regulated *Gtl2-Dio3* miRNAs in cardiac muscle, I initially overexpressed miR-410 and miR-495 using miRNA mimics in

NRVMs and observed a dramatic increase in cardiomyocyte proliferation. Target prediction analysis of miR-410 and miR-495 found that they commonly target and repress Cited2, a transcriptional coactivator. Significantly, its inhibition also triggered cardiomyocyte proliferation. Proliferation induced by miRNA overexpression or Cited2 knockdown was associated with reduced expression of the cell cycle inhibitor Cdkn1c/p57/Kip2 and elevated VEGFA. These studies reveal a novel miRNA-transcriptional coactivator pathway in the control of cardiomyocyte proliferation.

3.2 miRNA-410 and miRNA-495 are Expressed in the Heart and Downregulated in MEF2A-Deficient Cardiomyocytes

We previously reported that expression of the MEF2-regulated *Gtl2-Dio3* miRNAs is enriched in the brain, skeletal muscle, and heart (Snyder et al. 2013). Given their expression in the heart and the established role of MEF2 in cardiac development and disease, I aimed to investigate the MEF2-*Gtl2-Dio3* miRNA pathway in this tissue. I chose to focus on a subset of *Gtl2-Dio3* miRNAs that we have shown to modulate the activity of the WNT signaling pathway (Snyder et al. 2013). Initially, I examined the cardiac expression of two of these *Gtl2-Dio3* miRNAs, miR-410 and miR-495, in perinatal and adult hearts to determine if there was a temporal expression pattern for the *Gtl2-Dio3* miRNAs. Our prior studies have revealed low but detectable expression levels of several *Gtl2-Dio3* miRNAs in the adult mouse heart. As shown in Figure 3.1, miR-410 and miR-495 are expressed in both the perinatal and adult heart, but their expression was significantly higher in perinatal hearts, suggesting a role in perinatal cardiac function.

Moreover, the temporal expression pattern of these *Gtl2-Dio3* miRNAs is consistent with MEF2 transcriptional activity in the postnatal heart (Naya et al. 1999).

Given the above result, I then examined miR-410 and miR-495 expression in perinatal MEF2A knockout hearts. The majority of MEF2A knockout mice die in the perinatal period with severe structural abnormalities in cardiomyocytes (Naya et al. 2002). I found that miR-410 and miR-495 are significantly downregulated in perinatal MEF2A knockout hearts (Figure 3.2). To determine whether miR-410 and miR-495 are specifically downregulated in cardiac muscle and are dependent on MEF2A, I examined their expression in NRVMs in which I had depleted MEF2A using shRNA adenovirus (Ewen et al. 2011). shRNA-mediated knockdown of MEF2A in NRVMs resulted in a significant decrease in miR-410 and miR-495 expression (Figure 3.3).

To determine whether transcription of this locus is dependent on MEF2, I analyzed the activity of the *Gtl2* promoter in NRVMs. Previously, we demonstrated that the proximal promoter region of the *Gtl2-Dio3* locus is directly regulated by MEF2 in skeletal muscle and required for proper expression of miRNAs encoded by this locus (Snyder et al. 2013). Similar to our results in C2C12 skeletal myoblasts, the wild type *Gtl2* promoter was active in NRVMs. A mutation in the MEF2 binding site in the *Gtl2* promoter significantly reduced its activity, demonstrating that transcription of the *Gtl2-Dio3* locus is dependent on endogenous MEF2 in cardiomyocytes (Figure 3.4). Moreover, activity of the *Gtl2* promoter was significantly reduced in MEF2A-deficient NRVMs (Figure 3.5). Together, these results indicate that the *Gtl2-Dio3* noncoding RNA locus is dependent on MEF2, particularly MEF2A, activity in perinatal cardiac muscle.

Based on the established role of MEF2 in regulating the muscle cytoarchitecture, I was interested in determining whether expression of sarcomere genes is dependent on these *Gtl2-Dio3* miRNAs (Estrella and Naya 2014). As expected, acute knockdown of MEF2A in NRVMs resulted in significant downregulation of sarcomere genes (Figure 3.6). Using hairpin inhibitors (anti-miRs), I knocked down miR-410 and miR-495 in NRVMs. Similar to MEF2A depletion, knockdown of miR-495, but not miR-410, caused a significant reduction in sarcomere gene expression (Figure 3.7). Although sarcomere genes were downregulated, transient knockdown of either miR-410 or miR-495 or a combination of the two did not cause an overt morphological phenotype. Finally, to determine whether these miRNAs are involved in the structural and cell death phenotype in MEF2A-deficient NRVMs (Ewen et al. 2011), I overexpressed miR-410 and miR-495 in MEF2A-depleted NRVMs. As shown in Figure 3.8, overexpression of these miRNAs resulted in a modest but significant upregulation of sarcomere gene expression compared to MEF2A-depleted NRVMs alone. Furthermore, upregulation of BIM expression, a pro-apoptotic gene, was significantly reduced compared to MEF2A-depleted NRVMs alone. Taken together, these results strongly suggest that the *Gtl2-Dio3* noncoding RNAs function downstream of MEF2A and play a role in cardiomyocyte differentiation and/or maturation.

3.3 Overexpression of *Gtl2*-Dio3 miRNA-410 and miRNA-495 Promotes Cardiomyocyte Proliferation

Given the expression of miR-410 and miR-495 in NRVMs and perinatal hearts and the effect of miR-495 knockdown on sarcomere genes, I asked whether overexpression of these miRNAs alters cardiomyocyte maturation and growth. Toward this end, I

overexpressed miR-410 and miR-495 in NRVMs using miRNA mimic oligonucleotides. Upon overexpression of these miR-410 or miR-495 mimics, I noticed an abundance of cardiomyocytes compared to the control mimic (Figure 3.9). The apparent increase in cardiomyocyte number suggested an effect on proliferation. To determine whether these miRNAs were inducing cell cycle activity in cardiomyocytes, I performed Ki67 immunostaining on NRVMs in which I overexpressed miR-410 or miR-495 mimics. Quantification of Ki67$^+$ NRVMs revealed a significant 3-fold increase in Ki67 immunofluorescence upon addition of miR-410 or miR-495 mimics (Figure 3.10).

In a complementary set of experiments, I asked whether increased cell cycle activity was associated with increased DNA synthesis. I performed an EdU incorporation assay and found that overexpression of miR-410 or miR-495 caused a noticeable increase in EdU immunofluorescence in NRVMs. Quantification revealed a 2.5-fold increase in EdU$^+$ NRVMs upon addition of miR-410 or miR-495 (Figure 3.11). Furthermore, as an independent means of verifying the increase in DNA synthesis, I examined the expression of proliferating cell nuclear antigen (PCNA), an essential cofactor in DNA replication. Western blot analysis revealed a 2.0-fold or greater increase in PCNA upon overexpression of miR-410 or miR-495 (Figure 3.12). Taken together, these results indicate a role for miR-410 and miR-495 in promoting neonatal cardiomyocyte proliferation.

3.4   WNT Activity is Not Dysregulated in NRVMs Depleted of MEF2A or Overexpressing miRNA-410 and miRNA-495

We previously showed that in skeletal muscle both of these MEF2-regulated miRNAs were predicted to target *Sfrp2*, an inhibitor in the wingless (WNT) signaling

pathway, and subsequently showed that miR-410 directly repressed *Sfrp2* expression. We also demonstrated impaired WNT signaling in MEF2A-deficient skeletal muscle. Loss of MEF2A, and therefore a reduction in expression of these miRNAs, results in an increase in Sfrp2, resulting in attenuated WNT signaling, causing in a delay in skeletal muscle regeneration (Snyder et al. 2013). Therefore, I was interested in determining whether MEF2A and miR-410 and miR-495 modulate WNT signaling in cardiomyocytes and whether the WNT pathway is involved in proliferation induced by these miRNAs. Initially, to determine whether WNT signaling was also affected in MEF2A-deficient cardiomyocytes, I examined expression of *Sfrp2* and *Axin2*, a WNT responsive target gene. I found no significant dysregulation of these WNT signaling components in MEF2A-depleted NRVMs (Figure 3.13). Moreover, I found no significant difference in TOPflash activity, a WNT-sensitive luciferase reporter, in MEF2A-depleted NRVMs (Figure 3.14). Subsequently, I asked whether WNT signaling is perturbed upon overexpression of miR-410 or miR-495. Overexpression of miR-410 or miR-495 significantly repressed *Sfrp2* expression (Figure 3.15A), but did not affect the expression of *Axin2* (Figure 3.15B). Additionally, I found no increase in TOPflash activity when overexpressing miR-410, miR-495, or a combination of both miR-410 and miR-495 (Figure 3.16). These results indicate that while *Sfrp2* expression is downregulated by these *Gtl2-Dio3* miRNAs in cardiomyocytes, unlike in skeletal muscle, reduction of *Sfrp2* expression is not sufficient to attenuate WNT activity in neonatal cardiomyocytes. Taken together, these results suggest that WNT signaling is not a major pathway through which miR-410 and miR-495 stimulate proliferation in neonatal cardiomyocytes.

3.5   Identification and Validation of Predicted Target Genes of miRNA-410 and miRNA-495

To determine the pathway potentially targeted by these miRNAs, I subjected miR-410 and miR-495 sequences to messenger RNA (mRNA) target prediction algorithms (miRANDA, TargetScan, miRDB). Because miRANDA generated thousands of predicted targets, I only analyzed targets with a miRNA support vector regression (mirSVR) score of -1.00 or higher. The mirSVR score is algorithm that indicates the likelihood of the predicted target being a good target based on secondary structure and binding site accessibility and a cutoff of -1.00 indicates the top 7% of targets (Betel et al. 2010). This resulted in 746 and 1,388 predicted targets for miR-410 and miR-495, respectively (Figure 3.17). Then I compared these predicted targets across all three prediction algorithms and this comparative analysis resulted in a total of 64 and 148 overlapping predicted targets for miR-410 and miR-495, respectively (Figure 3.17). Because this was still a relatively large number of potential targets for each miRNA, I further narrowed down this list by looking for genes that were in common in the miR-410 and miR-495 target prediction sets and involved in either cell proliferation or cardiac muscle. Using this approach, I identified and selected ten genes that fulfilled these criteria (Table 3.1) (Edelhoff et al. 1993, Wick et al. 1995, Fiorentino et al. 2000, Tsai et al. 2000, Bamforth et al. 2001, Takakura et al. 2001, Waerner et al. 2001, Yoshida et al. 2002, Bamforth et al. 2004, Kobayashi et al. 2005, Otte et al. 2010, Hashimoto et al. 2013, Feng et al. 2015). To validate these predictions, I examined expression of eight of these candidate target genes in NRVMs overexpressing miR-410 or miR-495. As shown in Figure 3.18, the majority of the eight predicted common

targets were significantly downregulated in NRVMs overexpressing either miR-410 or miR-495.

3.6 miRNA-410 and miRNA-495 Directly Target the 3'UTR of *Cited2*

Of the validated candidate target genes, I chose to focus on Cited2. Cited2 interacts with the CBP/p300 coactivator and its deficiency in mice results in cardiac septal defects and other cardiac morphological abnormalities (Bamforth et al. 2001, Bamforth et al. 2004, MacDonald et al. 2013). To determine whether miR-410 and miR-495 could directly repress Cited2, I examined their seed sequences and the target sequence in Cited2. The seed sequences of miR-410 and miR-495 and their target sequences in Cited2 are conserved between human, mouse, and rat (Figure 3.19). I cloned the 3'UTR of Cited2 into the pMIR-REPORT vector (Ambion) and used this construct in transient transfection assays to examine the ability of these miRNAs to repress this reporter. Co-transfection of the pMIR-REPORT-3'UTR-CITED2 with either miR-410 or miR-495 mimics resulted in significant inhibition of the reporter (Figure 3.20). Mutation of the binding site for miRNA-410 or miRNA-495 in Cited2 reduced the ability of these miRNAs to repress the reporter, resulting in no significant difference between the wild type (WT) and miRNA-410 mutant or miRNA-495 mutant (MUT) reporters, respectively (Figure 3.20). These results demonstrate that miRNA-410 and miRNA-495 are capable of directly inhibiting Cited2 in cardiomyocytes.

3.7   Dysregulated Expression of p57 and Vegfa is Associated with miRNA-Induced Neonatal Cardiomyocyte Proliferation

To better understand the mechanism by which miR-410 and miR-495 promote cardiomyocyte proliferation, I reasoned that target genes of Cited2 would be misregulated in this process. Specifically, I searched for Cited2 target genes that have been linked to cellular proliferation. *Cdkn1c/p57/Kip2,* a cell cycle inhibitor, has been shown to be positively regulated by Cited2 in hematopoietic stem cells (Du et al. 2012, Du and Yang 2012). On the basis of the reduction in *Cited2* expression, we would expect downregulation of *Cdkn1c/p57/Kip2* expression in NRVMs overexpressing miR-410 or miR-495 mimics. To test this hypothesis, I examined expression of *Cdkn1c/p57/Kip2* in NRVMs overexpressing miR-410 or miR-495 mimics and, as expected, observed a significant downregulation (Figure 3.21A). To reinforce these observations, I then examined the expression of an established Cited2 target gene negatively regulated by this coactivator. Previous studies have shown that the *Vegf* promoter is repressed by Cited2 (Li et al. 2012). In addition, delivery of VEGF to the injured heart has been shown to induce cardiomyocyte proliferation (Ferrarini et al. 2006, Tao et al. 2011). As shown in Figure 3.21B, overexpression of both miR-410 and miR-495 resulted in a significant increase in *Vegfa*.

3.8   miRNA-410, miRNA-495, and Cited2 Function in the Same Pathway to Promote Neonatal Cardiomyocyte Proliferation

To confirm that knockdown of *Cited2* is capable of promoting cardiomyocyte proliferation, I inhibited Cited2 in NRVMs. NRVMs transfected with siCited2 resulted in a significant increase in EdU incorporation, similar to levels observed in miR-410 and miR-

495 overexpression experiments (Figure 3.22). Additionally, transfection of siCited2 resulted in a modest but significant decrease in *p57* and increase in *Vegfa* levels, similar to the effect observed upon miR-410 and miR-495 overexpression (Figure 3.23).

To demonstrate that miR-410 and miR-495 function in the same genetic pathway as Cited2 and that this gene is a relevant physiological target in cardiomyocytes, I co-silenced miR-410 and miR-495 along with Cited2. As shown in Figure 3.24, this combinatorial knockdown prevented NRVMs from proliferating. This result demonstrates that loss of Cited2 is likely responsible for the miR-410- and miR-495-induced cardiomyocyte proliferation.

3.9 Dysregulated Expression of *p57* and *Vegfa* in MEF2A-Deficient Cardiomyocytes

Because the *Gtl2-Dio3* miRNAs function downstream of MEF2A in cardiomyocytes, I asked whether the genes dysregulated in miR-410 and miR-495 overexpression were also affected in MEF2A deficiency. Consistent with my results that loss of MEF2A causes a reduction in miR-410 and miR-495, I found that both *Cited2* and *p57* were upregulated, whereas *Vegfa* was significantly downregulated in MEF2A-depleted NRVMs (Figure 3.25A). In a similar fashion, *Cited2* and *p57* were significantly upregulated in perinatal MEF2A knockout hearts (Figure 3.25B). The above gene expression pattern is contrary to that observed in miR-410- and miR-495-induced cardiomyocyte proliferation but entirely consistent with the downregulation of these miRNAs in MEF2A deficiency. Collectively, these data strongly support the notion that

the MEF2-*Gtl2-Dio3* noncoding RNA pathway regulates proper neonatal cardiomyocyte growth and survival.

3.10   Discussion

Molecularly defining the mechanisms by which differentiated cardiomyocytes can be induced to proliferate remains an important endeavor given the possibilities of translating this knowledge to stimulate repair of damaged cardiac tissue. In this chapter, I demonstrate that miR-410 and miR-495, miRNAs transcribed from the *Gtl2-Dio3* noncoding RNA locus, effectively promote proliferation in neonatal cardiomyocytes. My results also show that expression of miR-410 and miR-495 and regulation of the *Gtl2* promoter in cardiomyocytes are dependent on the MEF2A transcription factor. Previously, we reported that miR-410 and miR-495 belong to a subset of miRNAs in the *Gtl2-Dio3* locus that modulate WNT signaling in skeletal muscle differentiation and regeneration (Snyder et al. 2013). By contrast, these miRNAs and MEF2A do not significantly modulate WNT activity in cardiomyocytes. Instead, miR-410 and miR-495 regulate the expression of the transcriptional coactivator Cited2, whose downregulation induces cardiomyocyte proliferation.

Recently, miRNAs have emerged as key regulators of cardiomyocyte proliferation (Xin et al. 2013, Zacchigna and Giacca 2014). These small regulatory RNAs have been shown to modulate proliferation in either a positive or negative manner, indicating that cardiomyocytes employ these molecules to tightly control the cell cycle. Indeed, a high throughput overexpression screen revealed that miR-199a and miR-590 stimulated proliferation of post-mitotic, neonatal and adult cardiomyocytes (Eulalio et al. 2012).

Interestingly, this study listed miR-495 among a cohort of miRNAs capable of stimulating cardiomyocyte proliferation. However, this miRNA was not molecularly characterized, and the mechanism by which it promotes proliferation was not investigated.

MiRNAs encoded by the *Gtl2-Dio3* noncoding RNA locus have been linked to cancer, tumor formation, and central nervous system diseases (Bandres et al. 2006, Li et al. 2008, Chen et al. 2009, Zhang et al. 2010, Hwang-Verslues et al. 2011, Shih et al. 2011, Skalsky and Cullen 2011, Tang et al. 2011). Regarding the individual function of miR-410 and miR-495, the vast majority of reports have linked both of these miRNAs to oncogenic pathways. Some studies have suggested a tumor suppressor role for these miRNAs (Chen et al. 2012, Chu et al. 2014, Wang et al. 2014), whereas others have indicated a pro-proliferative effect on tumor growth. Along these lines, miR-410 was shown to be upregulated in liver cancer and enhanced tumor cell growth (Wang et al. 2014). MiR-495 has been shown to stimulate proliferation of human umbilical vein endothelial cells (Liu et al. 2015). Taken together, these findings provide strong evidence that miR-410 and miR-495 have the ability to regulate cell cycle activity and that this function has been conserved in cardiomyocytes.

It is intriguing that Cited2 emerged as a top predicted target for both miR-410 and miR-495 since this transcriptional coactivator has been linked to important developmental processes in the heart. *Cited2* global knockout mice are embryonic lethal because of defects in left-right patterning, ventricular septation, outflow tract and aortic arch malformation (Bamforth et al. 2001, Bamforth et al. 2004). Cardiomyocyte-specific *Cited2* knockout mice revealed a requirement specifically in cardiomyocytes with defects in normal

myocardial thickening and ventricular septation (MacDonald et al. 2013). Furthermore, mutations in *Cited2* are associated with congenital heart disease in humans, pointing to an important role for this transcriptional coactivator in cardiac muscle (Sperling et al. 2005, Xu et al. 2014).

Cited2 interacts with a number of transcription factors including TFAP2 and HIF1-α (Yin et al. 2002, Braganca et al. 2003). Interestingly, TFAP2 mutations have also been linked to congenital heart disease (Zhao et al. 2001, Mani et al. 2005). Cited2 has also been shown to regulate the expression of the cell cycle inhibitor p57 in hematopoietic stem cells and *p57* levels are decreased in the *Cited2* knockout mouse (Bamforth et al. 2001, Bamforth et al. 2004). Furthermore, TFAP2 overexpression results in increased *p57* expression (Jonckheere et al. 2009). Consistent with the above findings, I showed that loss of Cited2 resulted in a decrease in *p57* expression, leading to increased cell cycle activity and cardiomyocyte proliferation.

Whereas Cited2 functions to stimulate TFAP2 activity, it is a negative regulator of HIF1-α (Yin et al. 2002). Indeed, HIF1-α is increased in *Cited2* knockout mice, resulting in the increase in HIF1-α-responsive genes, such as VEGF (Du et al. 2012). I show that increased cardiomyocyte proliferation is associated with increased expression of *Vegfa*. Curiously, delivery of VEGF to cardiac cells post-injury has been shown to improve cardiomyocyte proliferation and function and to reduce myocardial infarct size (Ferrarini et al. 2006, Vera Janavel et al. 2006, Tao et al. 2011, Awada et al. 2015). Interestingly, a recent study reported that miR-410 directly targets human VEGF in osteosarcoma cells (Zhao et al. 2015). These observations suggest that the proliferation phenotype in miR-410

overexpressing NRVMs may be due to a direct effect of this miR on *Vegfa* expression. Because *Vegfa* expression was upregulated upon miR-410 and miR-495 overexpression, it is unlikely that miR-410 is directly repressing *Vegfa* in this context and reinforces the notion that *Vegfa* is primarily regulated through Cited2 activity in cardiomyocytes. Therefore, the fine-tuning of Cited2 activity by miR-410 and miR-495 appears to be important for proper perinatal cardiomyocyte maturation and proliferation.

This chapter clearly demonstrates a role for the *Gtl2-Dio3* miRNAs in cardiomyocyte proliferation and the potential of these regulatory RNAs to induce regeneration of diseased cardiac muscle *in vivo*. Delivery of the *Gtl2-Dio3* miRNAs may be a potential therapeutic target to stimulate cardiomyocyte proliferation and reduce cardiac damage post-injury in the postnatal heart.
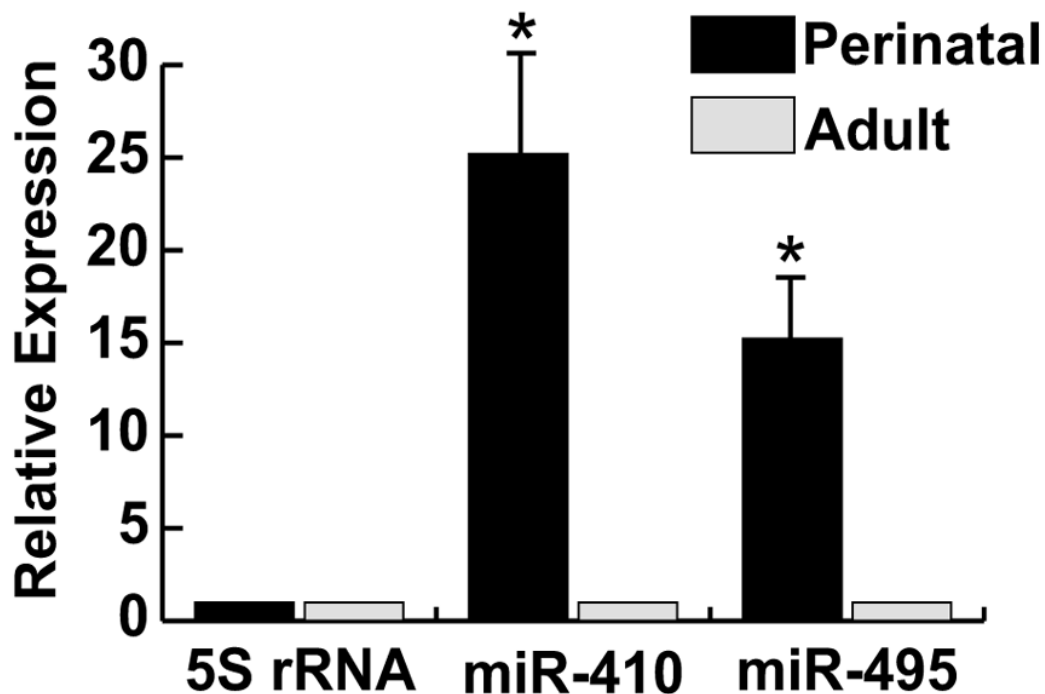
Figure 3.1 *Gtl2-Dio3* microRNA expression in wild-type cardiac muscle. Quantitative

RT-PCR analysis of miR-410 and miR-495 in perinatal and adult wild-type cardiac muscle

shows miRNAs are highly expressed in the perinatal heart compared to 5S rRNA control.

miRNA expression values in adult tissue was normalized to one. Relative expression of

miRNAs represents the fold change in expression in the perinatal time period compared to

the adult. Error bars represent S.E.M. n≥3. *, *p*<0.05.
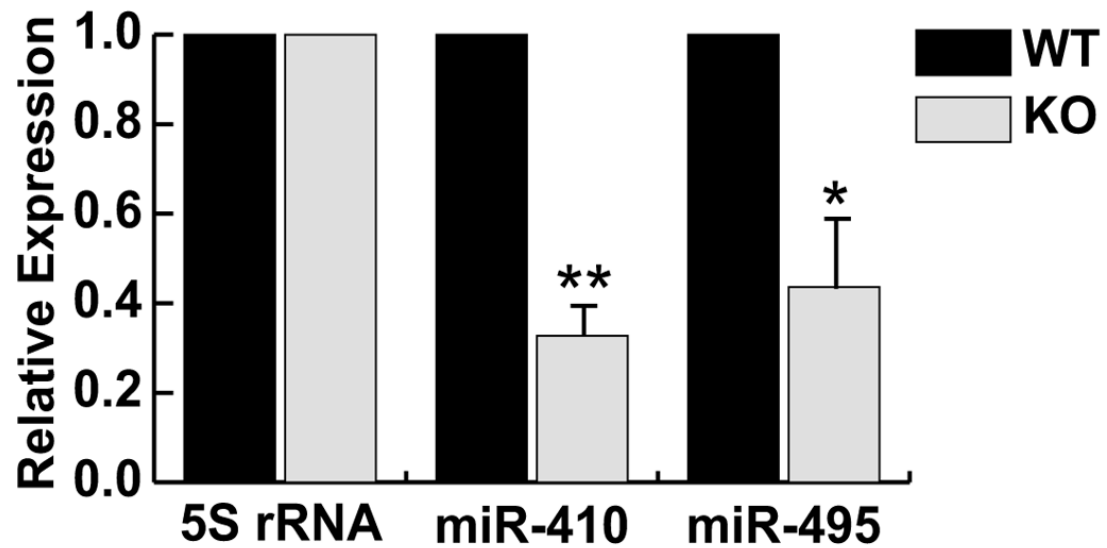
Figure 3.2 *Gtl2-Dio3* **microRNA expression in MEF2A knockout perinatal cardiac muscle.** Quantitative RT-PCR analysis of miR-410 and miR-495 in perinatal wild-type (WT) and MEF2A knockout (KO) cardiac muscle shows decreased miRNA expression in MEF2A KO mice compared to 5S rRNA control. miRNA expression values in WT tissue was normalized to one. Relative expression of miRNAs represents the fold change in expression in KO tissue compared to WT tissue. Error bars represent S.E.M. n≥3. *, $p<0.05$; **, $p<0.01$.
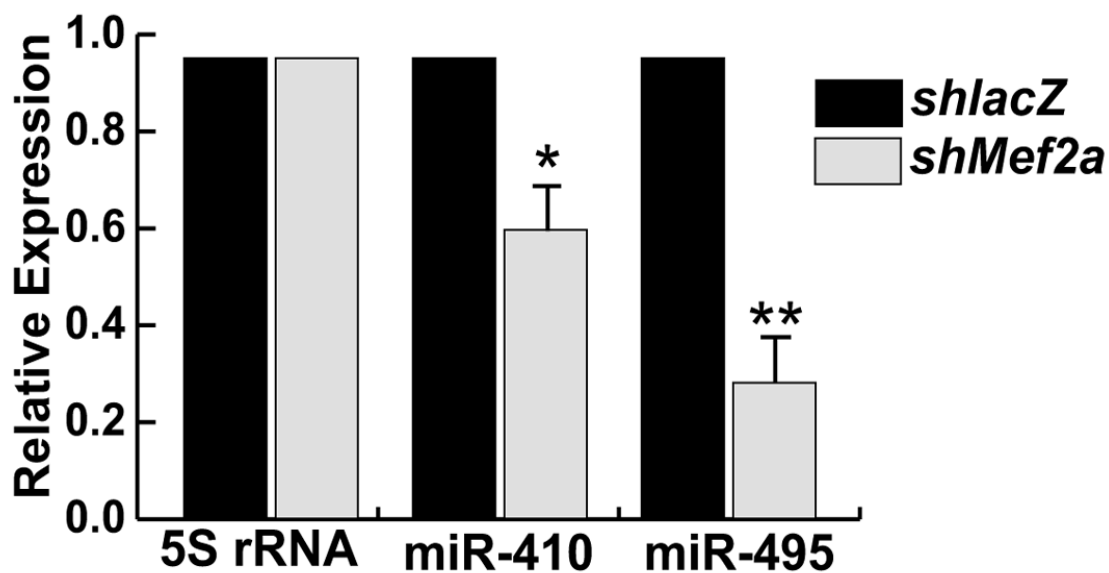
Figure 3.3 *Gtl2-Dio3* microRNA expression in MEF2A-deficient NRVMs. Quantitative RT-PCR analysis of miR-410 and miR-495 in control (sh*lacZ*) and MEF2A-deficient (sh*Mef2a*) NRVMs shows decreased miRNA expression in MEF2A-deficient cardiomyocytes compared to 5S rRNA control. miRNA expression values in sh*lacZ* NRVMs was normalized to one. Relative expression of miRNAs represents the fold change in expression in sh*Mef2a* NRVMs compared to sh*lacZ* NRVMs. Error bars represent S.E.M. n≥3. *, $p<0.05$; **, $p<0.01$.
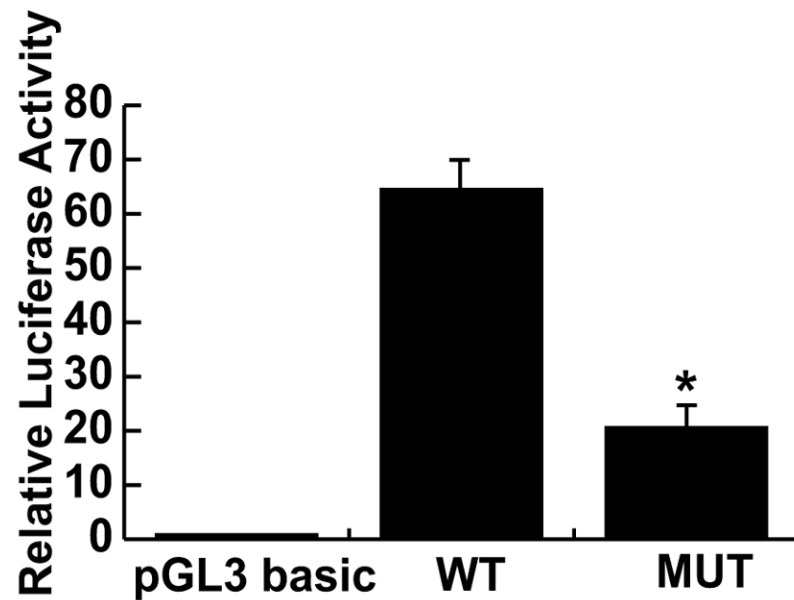
Figure 3.4 MEF2 regulates transcription of the *Gtl2-Dio3* microRNAs in cardiac muscle. Luciferase assay analysis of pGL3 basic MEF2 site activation by MEF2A was performed by transient transfection in NRVMs. WT MEF2 site activation (WT) versus empty vector (pGL3 basic) showed increased activity of the *Gtl2* promoter reporter. Mutation of the MEF2 site (MUT) significantly decreased luciferase activity relative to the wild type site. Error bars represent S.E.M. n≥3. *, *p<0.05*.
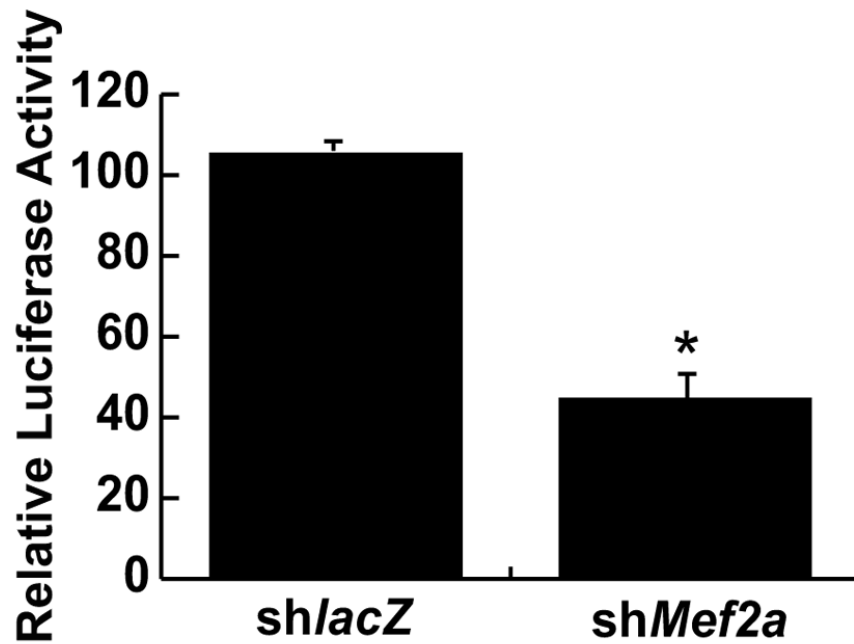
Figure 3.5 MEF2A directly regulates transcription of the *Gtl2-Dio3* microRNAs in cardiac muscle. WT MEF2 site activation in control sh*lacZ* versus sh*Mef2a* transduced NRVMs. MEF2A-deficient NRVMs show a significant decrease in luciferase reporter activity relative to the sh*lacZ* control. Error bars represent S.E.M. n≥3. *, $p<0.05$.
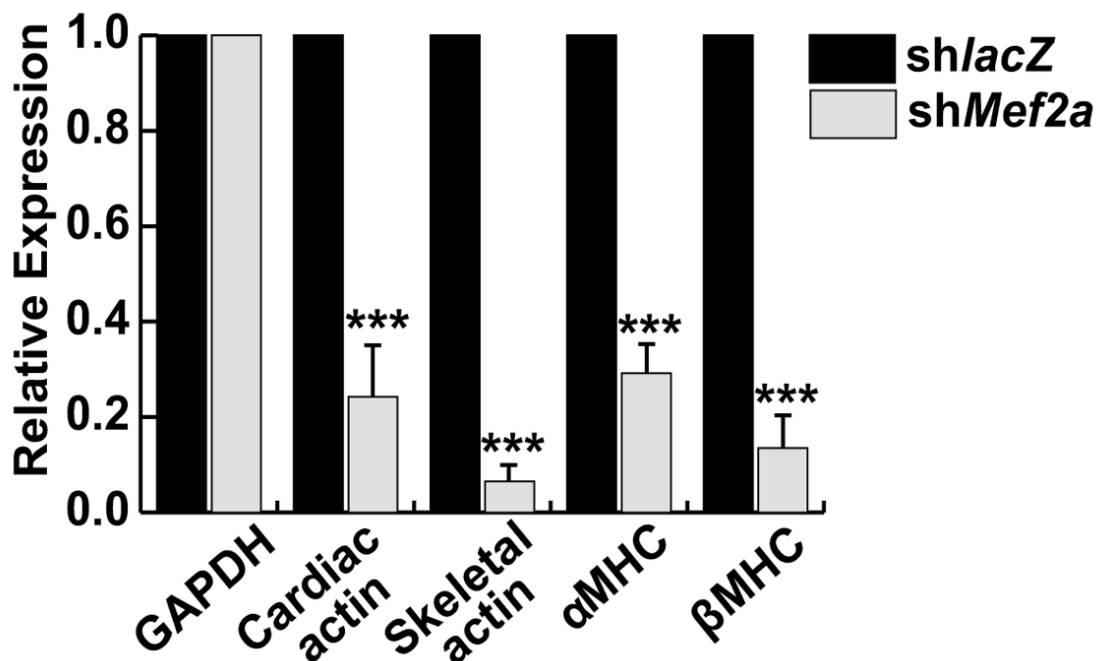
Figure 3.6 Sarcomere gene expression is downregulated in MEF2A-depleted NRVMs.
Quantitative RT-PCR analysis of cardiac sarcomere genes in control (sh*lacZ*) and MEF2A knockdown (sh*Mef2a*) NRVMs compared to GAPDH. Gene expression values in sh*lacZ* NRVMs were normalized to one. Relative expression represents the fold change in expression in sh*Mef2a* NRVMs compared to sh*lacZ* NRVMs. Error bars represent S.E.M. n≥3. ***, *p<0.001*.
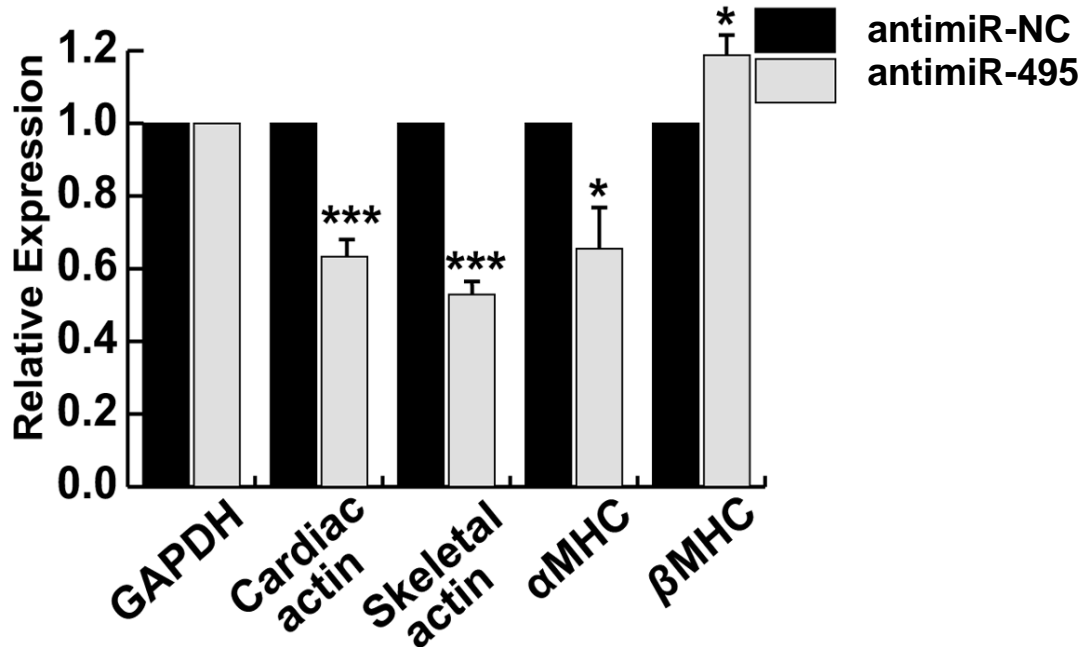
Figure 3.7 Sarcomere gene expression is downregulated in miRNA-495 knockdown NRVMs. Quantitative RT-PCR analysis of cardiac sarcomere genes in control (antimiR-NC) and miR-495 knockdown (antimiR-495) NRVMs compared to GAPDH. Gene expression values in miR-NC knockdown NRVMs were normalized to one. Relative expression represents the fold change in expression in antimiR-495 knockdown NRVMs compared to antimiR-NC knockdown NRVMs Error bars represent S.E.M. n≥3. *, $p<0.05$; ***, $p<0.001$.
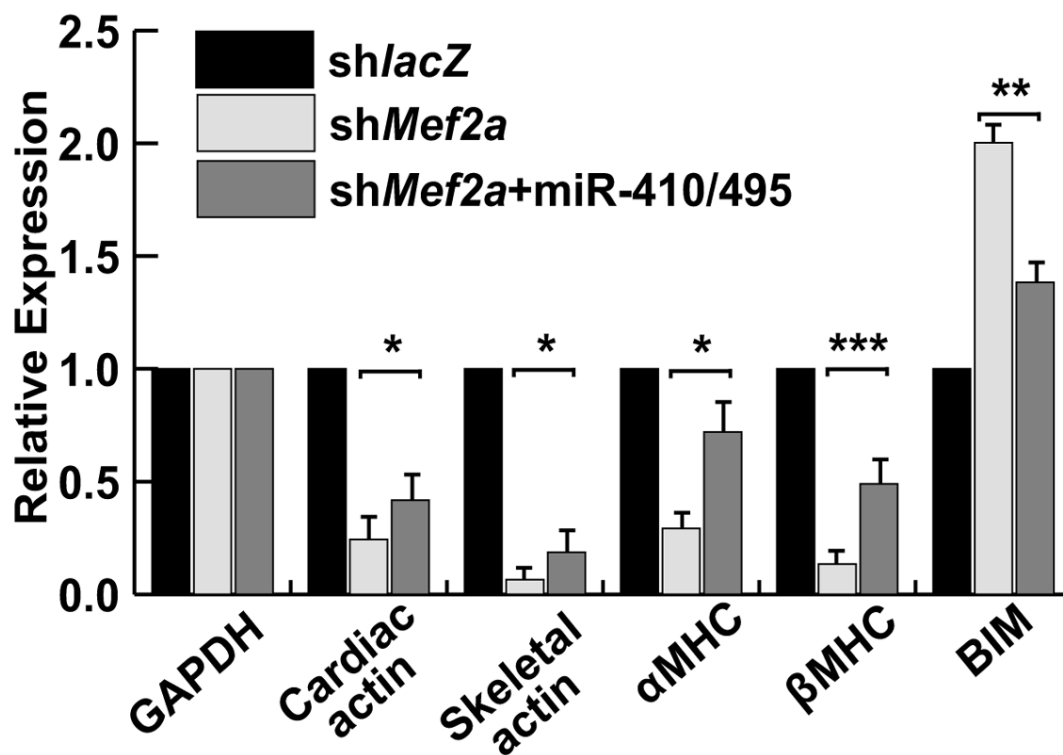
Figure 3.8 Overexpression of miRNA-410 and miRNA-495 partially rescues the MEF2A-deficient downregulation of sarcomere genes and upregulation of apoptotic gene BIM. Overexpression of miR-410 and miR-495 in MEF2A-depleted NRVMs upregulates sarcomere gene expression and reduces BIM expression compared to GAPDH. Gene expression values in sh*lacZ* NRVMs were normalized to one. Relative expression represents the fold change in expression in sh*Mef2a* and sh*Mef2a*+miR-410/495 NRVMs compared to sh*lacZ* NRVMs Error bars represent S.E.M. n≥3. *, $p<0.05$; **, $p<0.01$; ***, $p<0.001$.
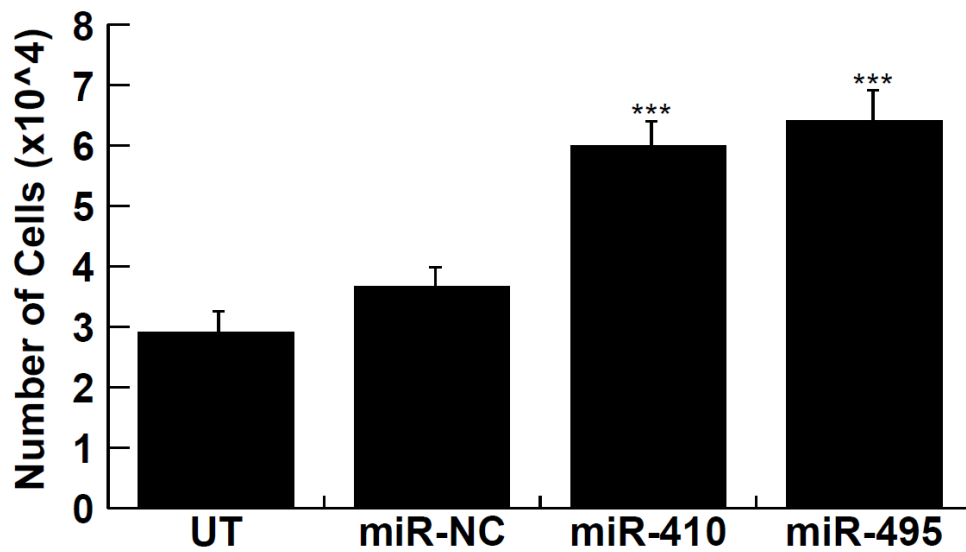
Figure 3.9 Overexpression of miRNA-410 and miRNA-495 results in increased cell number. Cell number upon overexpression of miR-NC, miR-410, or miR-495 compared to untransfected control NRVMs shows a 1.64-fold increase in cells upon overexpression of miR-410 and a 1.75-fold increase in cells upon overexpression of miR-495. Error bars represent S.E.M. n≥3. ***, $p<0.001$.
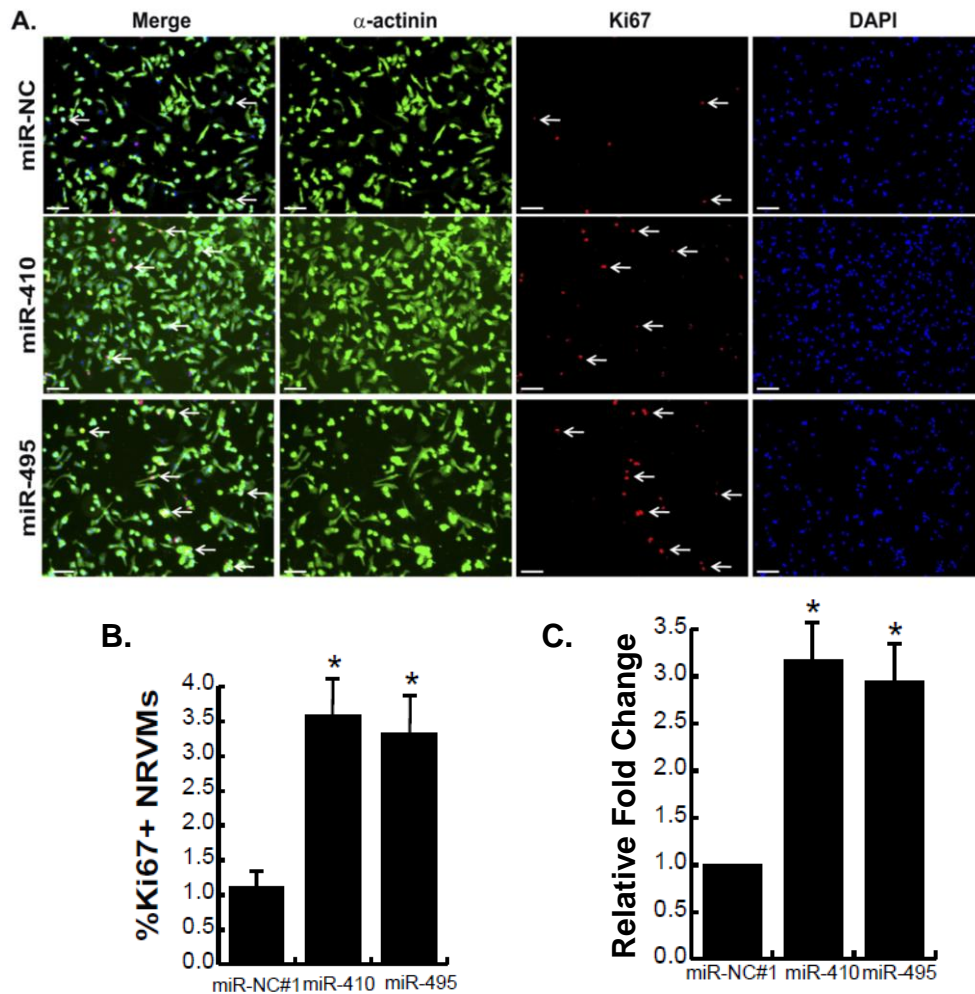
Figure 3.10 Overexpression of miRNA-410 or miRNA-495 results in increased Ki67 immunostaining in NRVMs. A) Representative images of Ki67 immunostaining. miR-NC#1 (top), miR-410 (middle), miR-495 (bottom). α-actinin staining in green, Ki67 staining in red, DAPI staining in blue. B) Quantification of Ki67^{+} NRVMs. C) Relative fold change of Ki67^{+} NRVMs in miR-410 and miR-495 overexpression compared to miR-NC#1. Arrows indicate Ki67^{+} NRVMs. For each miR mimic overexpression, a total of 1500 cardiomyocytes were counted. Scale bars are 20 μm. Error bars represent S.E.M. n≥3. *, $p<0.05$; **, $p<0.01$.
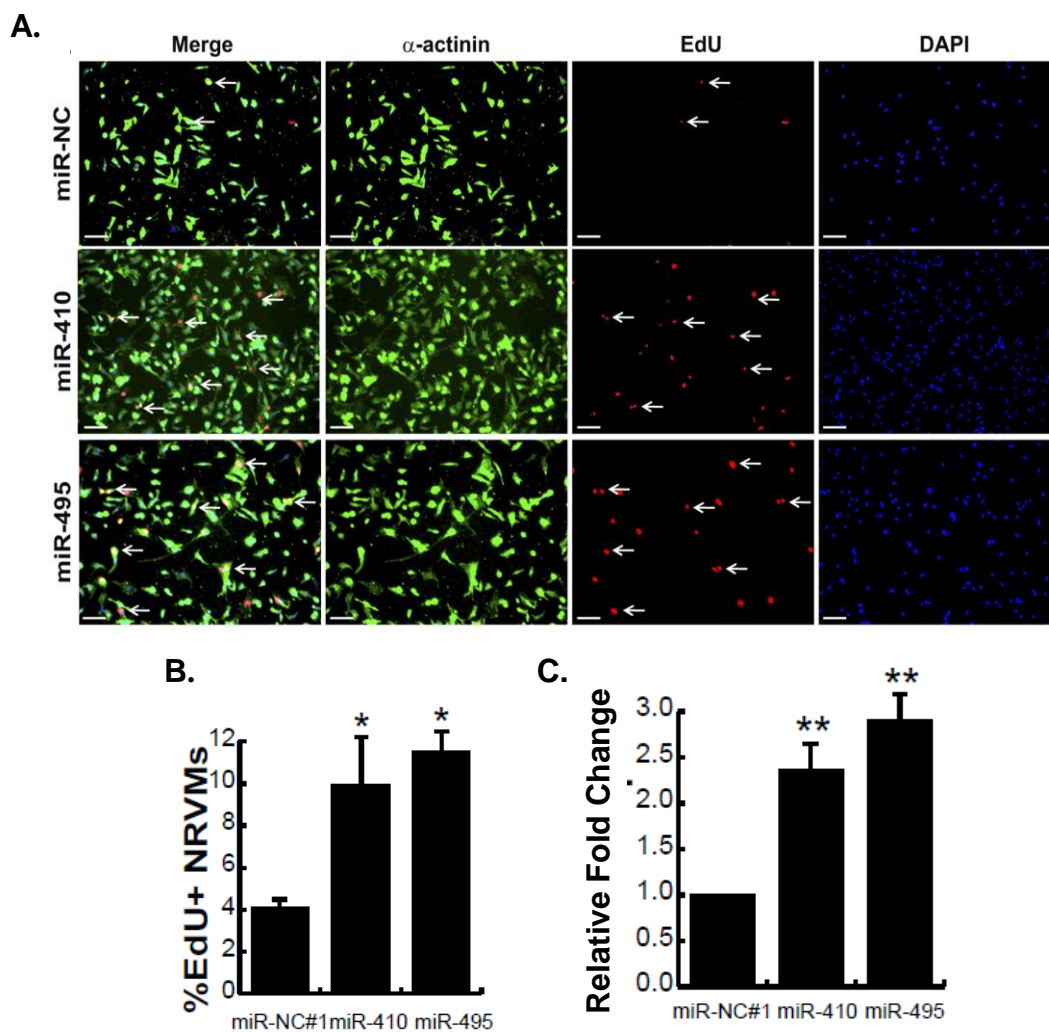
Figure 3.11 Overexpression of miRNA-410 or miRNA-495 results in increased EdU incorporation in NRVMs. A) Representative images of EdU assay. miR-NC#1 (top), miR-410 (middle), miR-495 (bottom). α-actinin staining in green, EdU staining in red, DAPI staining in blue. B) Quantification of EdU$^+$ NRVMs. C) Relative fold change of EdU$^+$ NRVMs in miR-410 and miR-495 overexpression compared to miR-NC#1. Arrows indicate EdU$^+$ NRVMs. For each miR mimic overexpression, a total of 1500 cardiomyocytes were counted. Scale bars are 20 μm. Error bars represent S.E.M. n≥3. *, $p<0.05$; **, $p<0.01$.
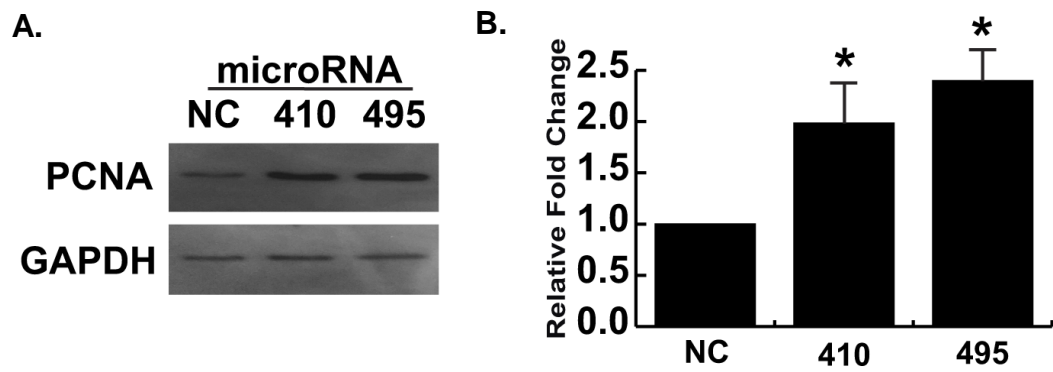
Figure 3.12 Overexpression of miRNA-410 or miRNA-495 results in increased PCNA.

A) Representative western blot analysis of proliferating cell nuclear antigen (PCNA) in NRVMs overexpressed with miR-NC#1, miR-410, and miR-495. B) Densitometry of PCNA western blot. Error bars represent S.E.M. n≥3. *, $p<0.05$.
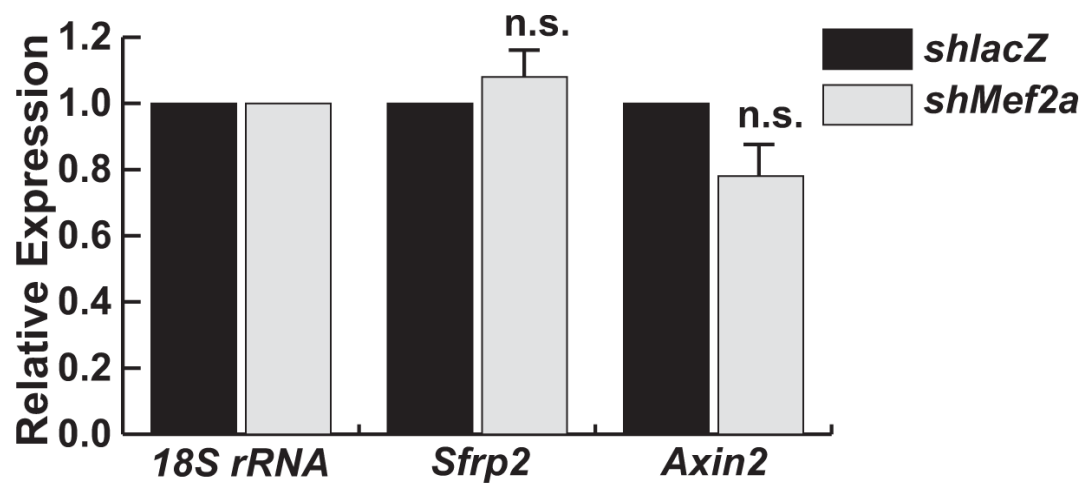
Figure 3.13 WNT signaling pathway members are not affected in MEF2A-deficient cardiomyocytes. Quantitative RT-PCR of WNT signaling members Sfrp2 and Axin2 show no significant change in MEF2A-deficient cardiomyocytes. Gene expression values in sh*lacZ* NRVMs were normalized to one. Relative expression represents the fold change in expression in sh*Mef2a* NRVMs compared to sh*lacZ* NRVMs. Error bars represent S.E.M. n≥3. n.s. not significant.
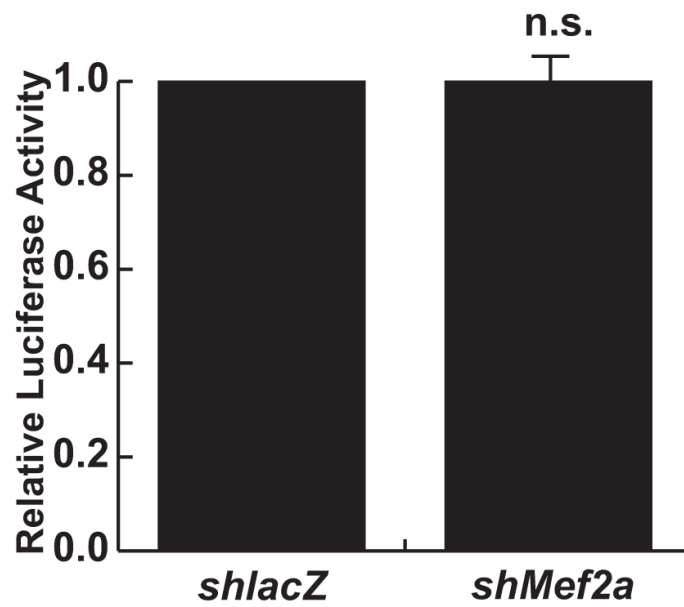
Figure 3.14 TOPflash reporter indicates no dysregulation of WNT signaling in MEF2A-deficient NRVMs. TOPflash luciferase reporter activity shows no significant difference in activity when knocking down MEF2A (sh*Mef2a*) relative to sh*lacZ* control. Error bars represent S.E.M. n≥3. n.s. not significant.
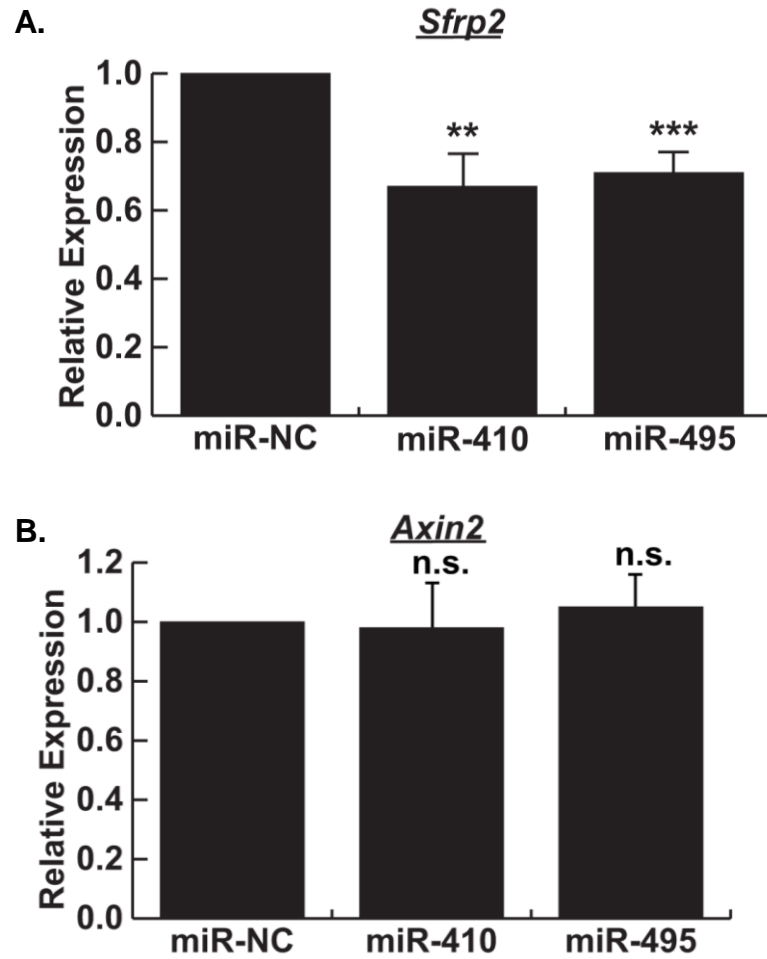
Figure 3.15 Overexpression of miRNA-410 or miRNA-495 does not alter WNT signaling in cardiomyocytes. A) Quantitative RT-PCR of *Sfrp2* upon overexpression of miR-410 and miR-495 relative to miR-NC. B) Quantitative RT-PCR of *Axin2* upon overexpression of miR-410 and miR-495 relative to miR-NC. Gene expression values in miR-NC NRVMs were normalized to one. Relative expression represents the fold change in expression in miR-410 NRVMs and miR-495 NRVMs compared to miR-NC NRVMs. Error bars represent S.E.M. $n \geq 3$. n.s. not significant; **, $p < 0.01$; ***, $p < 0.001$.
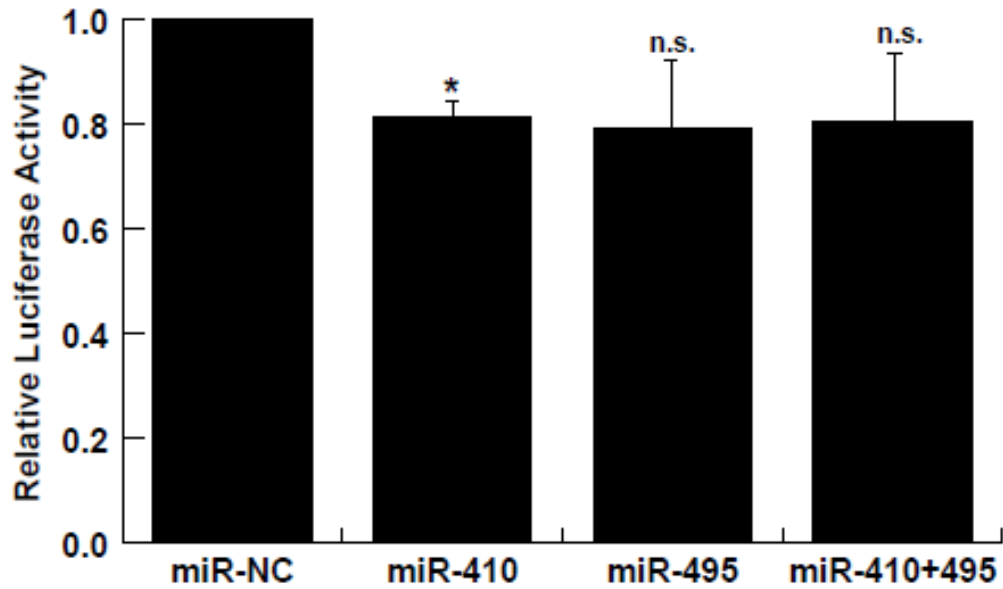
Figure 3.16 TOPflash reporter indicates no upregulation of WNT signaling in miRNA overexpression NRVMs. TOPflash luciferase reporter activity when overexpressing miR-410, miR-495, and miR-410+miR-495 in NRVMs relative to miR-NC. Error bars represent S.E.M. n$\geq$3. n.s. not significant; *, $p<0.05$. (A. Clark, unpublished data)
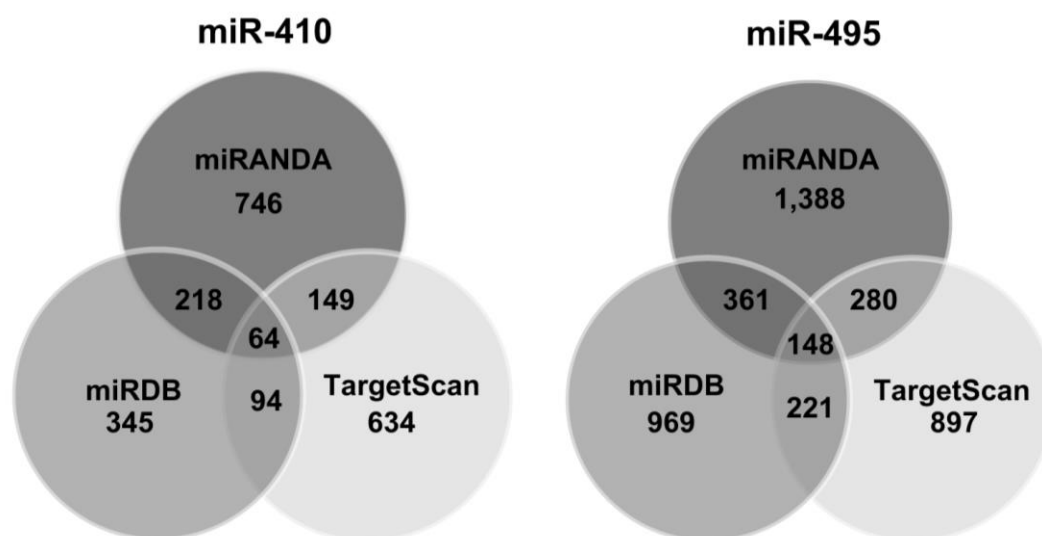
Figure 3.17 Predicted Targets of miRNA-410 and miRNA-495. Venn diagrams showing

the predicted targets for miR-410 and miR-495 based on target prediction algorithms

(miRANDA, miRDB, TargetScan).
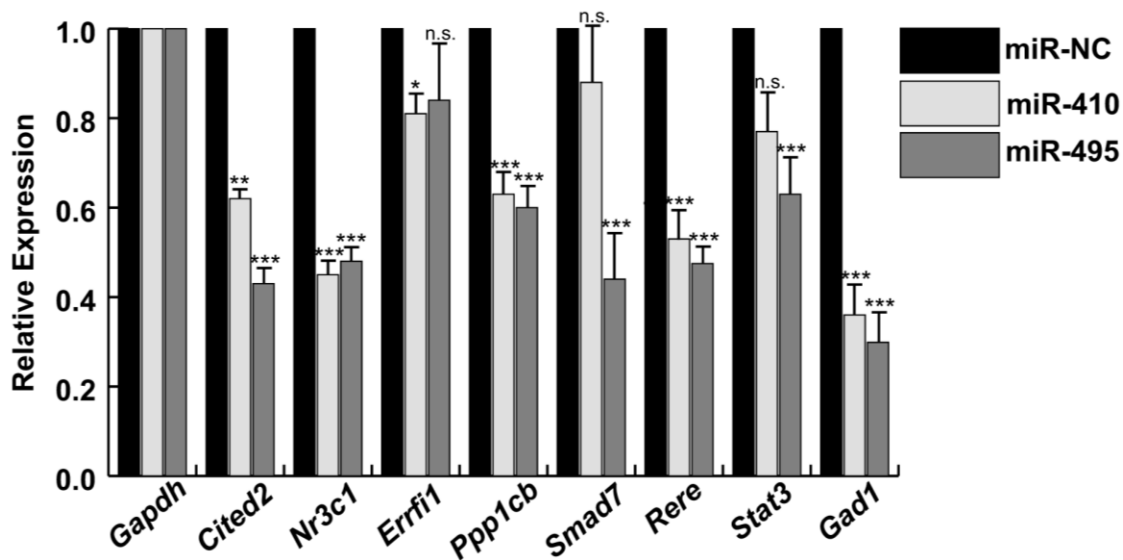
Figure 3.18 Validation of Predicted Targets of miRNA-410 and miRNA-495.
Quantitative RT-PCR of eight of the top 10 predicted targets for miR-410 and miR-495 in NRVMs transfected with miR-410 or miR-495 mimics relative to GAPDH. Gene expression values in miR-NC NRVMs were normalized to one. Relative expression represents the fold change in gene expression in miR-410 NRVMs and miR-495 NRVMs compared to miR-NC NRVMs. Error bars represent S.E.M. n≥3. n.s. = not significant; *, $p<0.05$; **, $p<0.01$; ***, $p<0.001$.

miR-410 alignment:

3'- U G U C C G G U A G A C A **C A A U A U A A** -5' hsa-miR-410
                          | | | | | | | |
5'- C A C T G T G C T A A T A **G T T A T A T T** -3' human Cited2

3'- U G U C C G G U A G A C A **C A A U A U A A** -5' mmu-miR-410
                          | | | | | | | |
5'- C A C T G T G C T A A T A **G T T A T A T T** -3' mouse Cited2

3'- U G U C C G G U A G A C A **C A A U A U A A** -5' rno-miR-410
                          | | | | | | | |
5'- C A C T G T G C T A A T A **G T T A T A T T** -3' rat Cited2

miR-495 alignment:

3'- C U U C A C G U G G U A **C A A A C A A A** -5' hsa-miR-495
                        | | | | | | | |
5'- G T C T T T T T C G T T **G T T T G T T T** -3' human Cited2

3'- C U U C A C G U G G U A **C A A A C A A A** -5' mmu-miR-495
                        | | | | | | | |
5'- G T C T T T T T C G T T **G T T T G T T T** -3' mouse Cited2

3'- C U U C A C G U G G U A **C A A A C A A A** -5' rno-miR-495
                        | | | | | | | |
5'- G T C T T T T T C G T T **G T T T G T T T** -3' rat Cited2
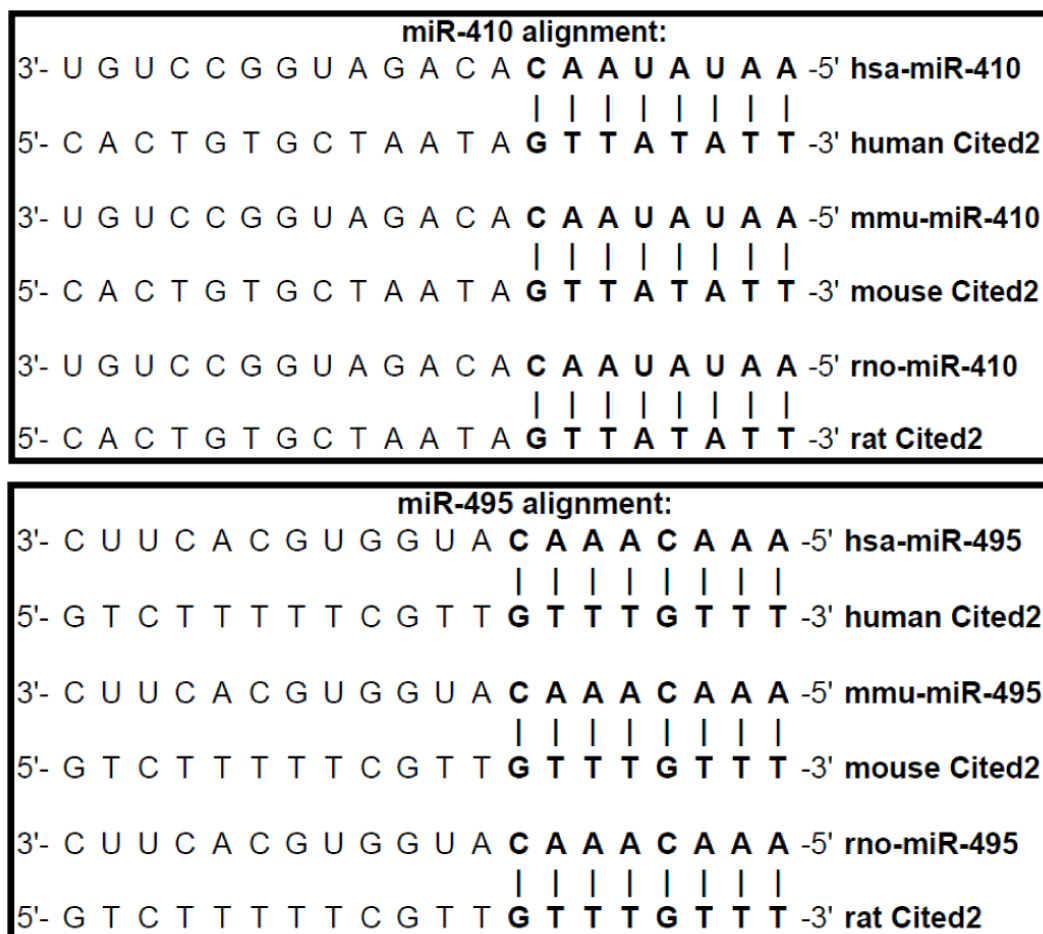
Figure 3.19 miRNA-410 and miRNA-495 target sequences are evolutionarily conserved. Sequence alignments of miR-410 and miR-495 seed sequences and predicted 3'UTR *Cited2* target sites show 100% conservation between human, mouse, and rat. hsa, H*omo sapiens;* mmu, *Mus musculus;* rno, *Rattus norvegicus.*
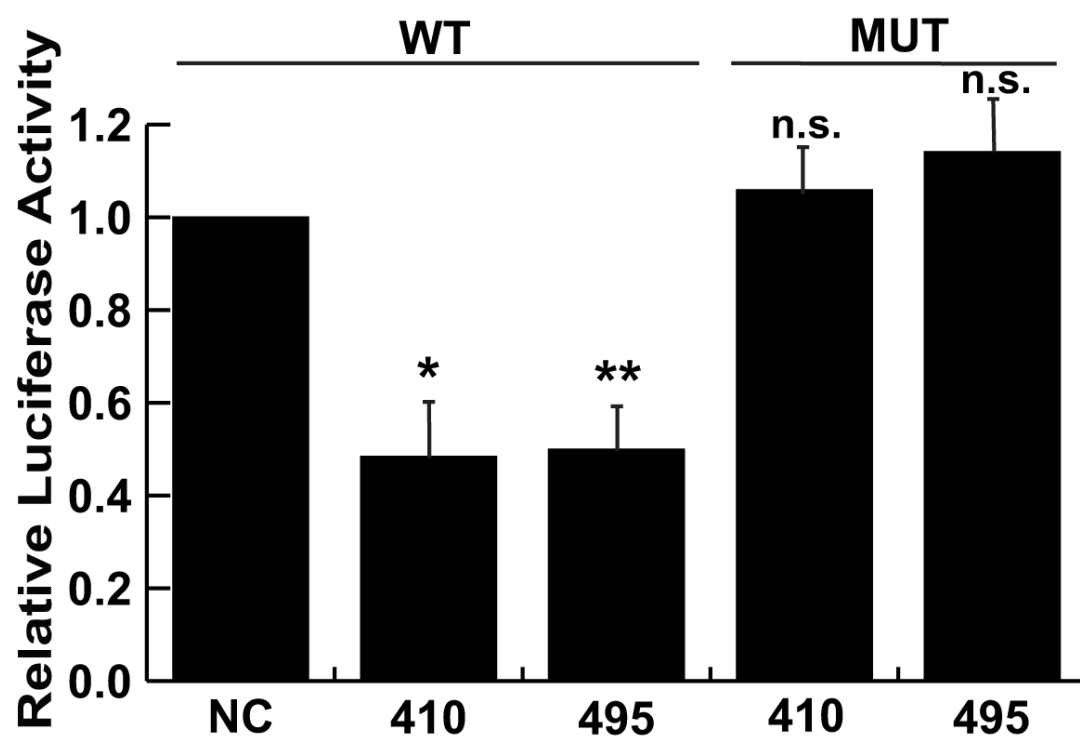
Figure 3.20 miRNA-410 and miRNA-495 directly target *Cited2*. Luciferase analysis of

pMIR-REPORT-3'UTR-*Cited2* (WT) co-transfected with miR-410 and miR-495 mimics

(150nM, Dharmacon) in NRVMs cells compared with a non-specific control (miR-NC#1).

Luciferase analysis of miR-410 seed sequence mutant and miR-495 seed sequence mutant

(MUT) co-transfected with miR-410 and miR-495 mimics (150nM, Dharmacon) in

NRVMs compared with a non-specific control (miR-NC#1). Error bars represent S.E.M.

n≥3. *, $p<0.05$; **, $p<0.01$; ***, $p<0.001$.
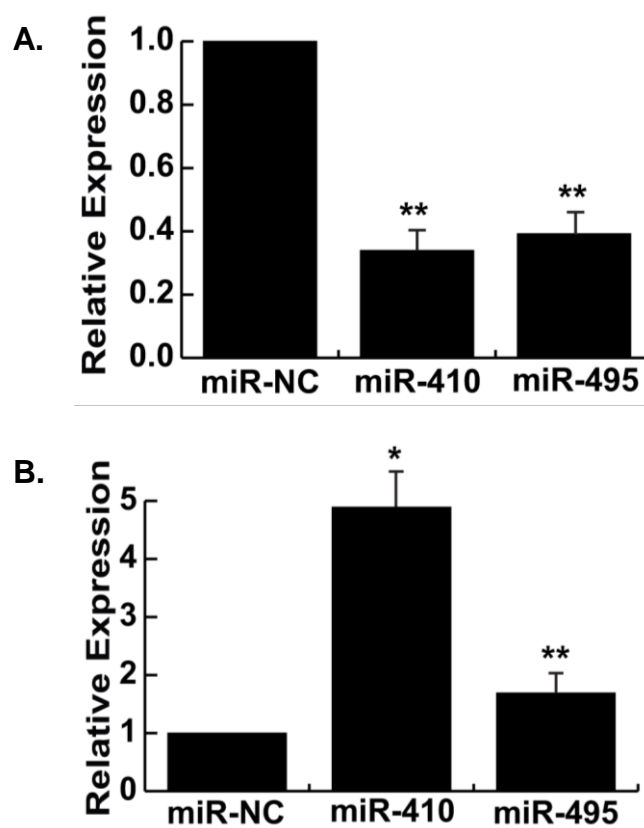
Figure 3.21 Overexpression of miRNA-410 or miRNA-495 results in decreased *Cdkn1c/p57/Kip2* **expression and increased** *Vegfa* **expression in NRVMs.** A) Quantitative RT-PCR of *Cdkn1c/p57/Kip2* expression levels when overexpressing miR-410 or miR-495 results in 2.5-fold reduction in *Cdkn1c/p57/Kip2*. B) Quantitative RT-PCR of *Vegfa* expression levels when overexpressing miRNA-410 or miRNA-495 results in 2.0-fold or greater increase in *Vegfa*. Gene expression values in miR-NC NRVMs were normalized to one. Relative expression represents the fold change in gene expression in miR-410 NRVMs and miR-495 NRVMs compared to miR-NC NRVMs. Error bars represent S.E.M. n≥3. *, $p<0.05$; **, $p<0.01$.
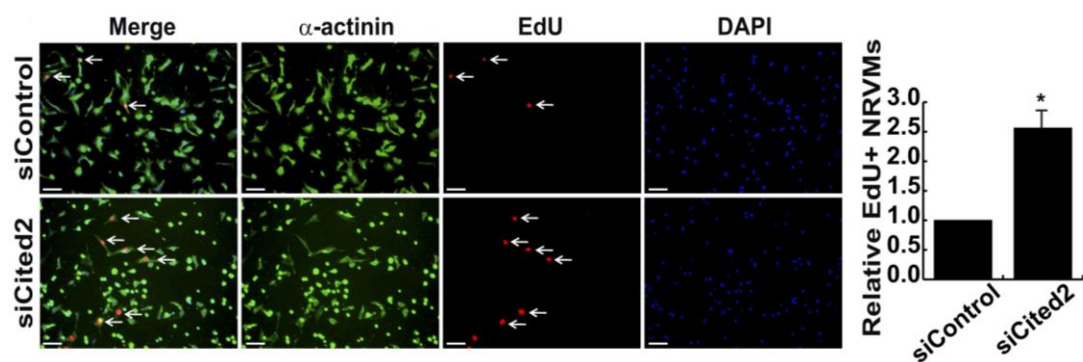
Figure 3.22 Cited2 knockdown results in increased cardiomyocyte proliferation. Representative images of EdU assay. siControl (top), siCited2 (bottom). α-actinin staining in green, EdU staining in red, DAPI staining in blue. Quantification of EdU$^+$ NRVMs. Relative fold change of EdU$^+$ NRVMs in siCited2 compared to siControl. Arrows indicate EdU$^+$ NRVMs. For each knockdown, a total of 1400 cardiomyocytes were counted. Scale bars are 20 μm. Error bars represent S.E.M. n≥3. *, $p<0.05$; **, $p<0.01$.
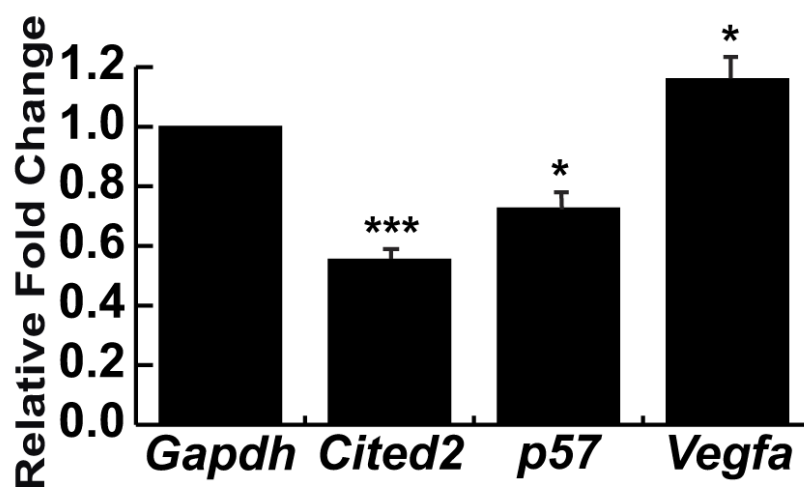
Figure 3.23 Knockdown of Cited2 results in decreased *p57* expression and increased *Vegfa* expression in NRVMs. Quantitative RT-PCR of *Cited2*, *p57*, and *Vegfa* expression levels when knocking down *Cited2* via siRNA. Gene expression values in siControl NRVMs were normalized to one. Relative fold change represents the fold change in expression in siCited2 NRVMs compared to siControl NRVMs. Error bars represent S.E.M. n≥3. *, $p<0.05$; ***, $p<0.001$.
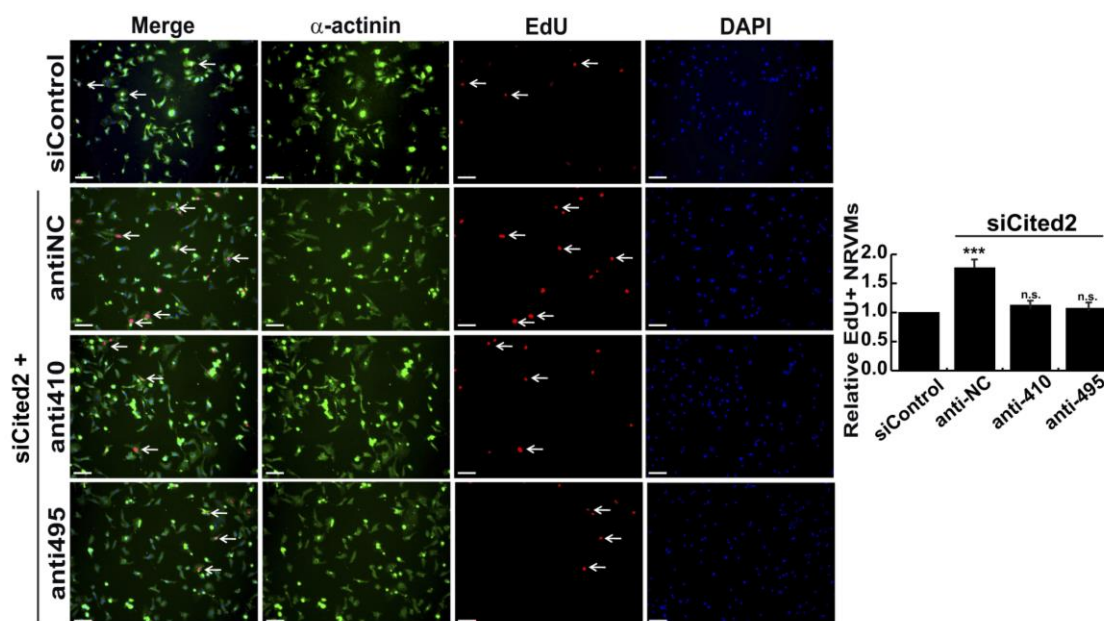
Figure 3.24 Cotransfecting siCited2 and antimiRNA-410 or antimiRNA-495 returns proliferation to normal levels. Co-silencing *Cited2*, miR-410, and miR-495 prevent cardiomyocyte proliferation. Representative images of EdU incorporation assay. siControl (top), siCited2+antimiR-NC, siCited2+antimiR-410, siCited2+antimiR-495 (bottom). α-actinin staining in green, EdU staining in red, DAPI staining in blue. Relative fold change of EdU+ NRVMs shows combinatorial knockdown of *Cited2* and miR-410 and miR-495 results in normal cardiomyocyte proliferation. Arrows indicate EdU[+] NRVMs. For each knockdown, a total of 1000 cardiomyocytes were counted. Scale bars are 20 μm. Error bars represent S.E.M. n≥3. n.s., not significant; ***, *p*<0.001.
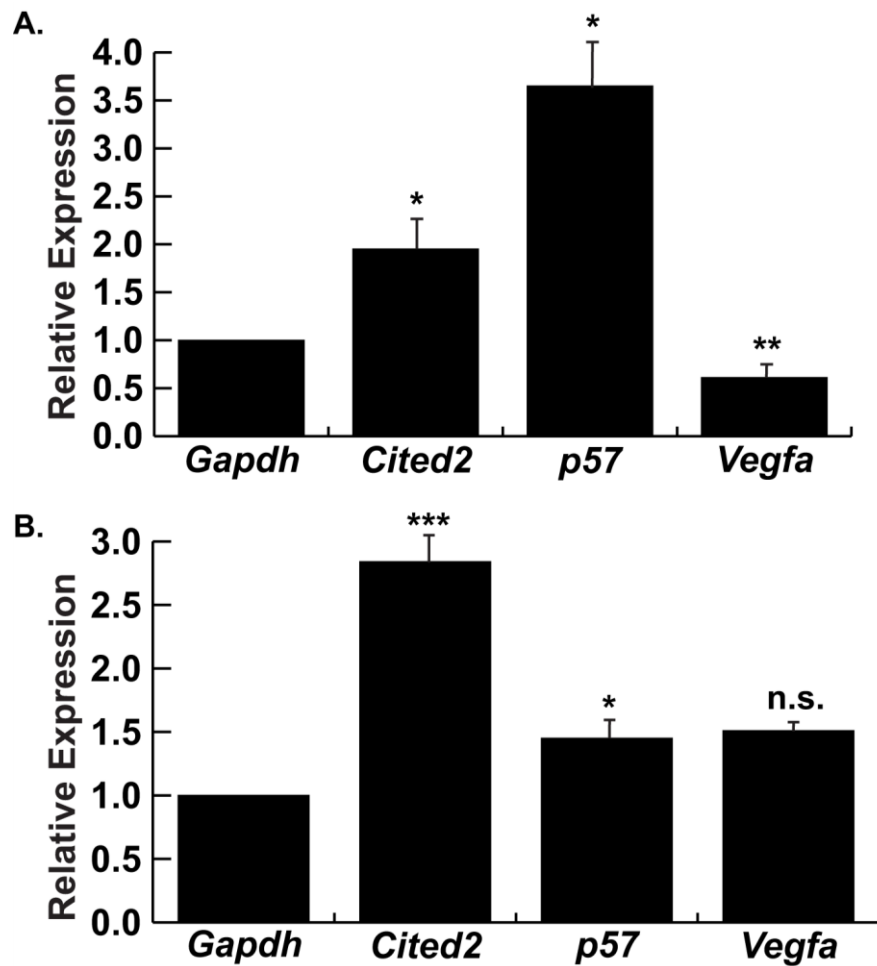
Figure 3.25 Dysregulated Cited2, p57, and Vegfa expression in MEF2A-deficient cardiomyocytes. A) Quantitative RT-PCR of *Cited2, p57,* and *Vegfa* expression levels in MEF2A-deficient NRVMs. B) Quantitative RT-PCR of *Cited2, p57,* and *Vegfa* expression levels in perinatal MEF2A knockout cardiac muscle. Error bars represent S.E.M. n≥3. n.s., not significant; *, $p<0.05$; **, $p<0.01$; ***, $p<0.001$.

Target	Known Role(s)
CITED2	Mutations result in cardiac septal defects; left-right patterning defects
NR3C1	Linked to coronary heart disease and heart failure
ERRFI1	Upregulated in cell growth; Overexpression inhibits cellular proliferation
PPP1CB	Regulates cell growth; Linked to human carcinogenesis
SMAD7	Regulates hepatocyte proliferation
RERE	Cell survival; enhances apoptosis
STAT3	Activation leads to cellular transformation
GAD1	Linked to Stiff Person Syndrome; Progressive muscle stiffness
ADM	Linked to malignant hypertension
DPYSL2	Knockdown results in decreased proliferation

Table 3.1 Top 10 Predicted Targets of miRNA-410 and miRNA-495. The top 10 predicted targets of both miR-410 and miR-495 and their known roles in cardiac muscle and/or proliferation.

CHAPTER FOUR – *GTL2-DIO3* NONCODING RNAS ARE DYNAMICALLY REGULATED IN DIVERSE CARDIOMYOPATHIES AND THEIR INHIBITION ATTENUATES PATHOLOGICAL HYPERTROPHY

4.1   Introduction

Cardiovascular disease is the leading cause of death and morbidity in the developed world (Mozaffarian et al. 2015). Elucidating the underlying gene regulatory mechanisms that lead to heart failure could uncover new ways to develop novel therapeutics for cardiovascular disease. Recently, miRNAs have been shown to play roles in cardiac hypertrophy and heart failure. Accumulating evidence suggests that manipulating miRNA expression is an effective therapeutic approach in the treatment of cardiovascular disease (van Rooij and Olson 2007, Thum et al. 2008, Small and Olson 2011, Neppl and Wang 2014).

The *Gtl2-Dio3* noncoding RNA locus (described in detail in Chapter 1.5) generates more than 50 miRNAs and one or more long noncoding RNAs (lncRNAs) including *Gtl2*, which resides at the 5'-end of the putative, single (~200 kilobases) polycistronic transcript (da Rocha et al. 2008). Expression of the *Gtl2-Dio3* locus has been shown to correlate with pluripotency in embryonic and induced pluripotent stem cells, and its dysregulation is associated with a number of human diseases (Liu et al. 2010, Benetatos et al. 2013). Moreover, the *Gtl2* lncRNA has recently emerged as a key epigenetic factor in pluripotency by modulating the activity of Polycomb Repressive Complex 2 (PRC2) (Zhao et al. 2010, Kaneko et al. 2014). The regulation of PRC2 activity in *cis* by *Gtl2* is required to maintain

proper and coordinated expression of the entire *Gtl2-Dio3* noncoding RNA locus in ES cells (Das et al. 2015).

Because of the ability of miR-410 and miR-495 to promote proliferation of post-mitotic cardiomyocytes (described in Chapter 3) and the potential of harnessing this activity to promote cardiac regeneration, I was interested in examining their regulation in heart disease. Additionally, given that MEF2 is a key mediator of pathological remodeling of the heart, I was interested in determining whether misexpression of its noncoding RNA targets is capable of modulating the response to stress signaling in cardiomyocytes. Therefore, in this chapter, I examined expression of multiple noncoding RNAs throughout the *Gtl2-Dio3* locus including the lncRNA *Gtl2*, miR-410, miR-495, and miR-433.

In this chapter, I performed a comprehensive expression analysis of a subset of *Gtl2-Dio3* miRNAs and the *Gtl2* lncRNA in a mouse model of myocardial infarction (MI) as well as a model of pathological hypertrophy induced by administration of the hypertensive agonist angiotensin II (Ang II). Moreover, I examined cardiac expression of *Gtl2-Dio3* noncoding RNAs in cardiomyopathies that result from genetic defects including dystrophic cardiomyopathies, such as the *mdx* mouse model of Duchenne Muscular Dystrophy (DMD) and the *DyW* mouse model of laminin-α2 deficient congenital muscular dystrophy type 1A (MDC1A), as well as the adult MEF2A knockout mouse and the MEF2A/*mdx* mouse. Although the aforementioned cardiac disease models have distinct etiologies, the miRNAs and *Gtl2* lncRNA were upregulated in all cardiomyopathies. However, the *Gtl2* lncRNA and miRNAs displayed dramatic differences in their temporal regulation in the progression of MI and in MEF2A knockout hearts. Finally, I show for the

first time that knockdown of the *Gtl2-Dio3* miRNAs in cardiomyocytes subjected to stress signaling *in vitro* attenuates the maladaptive increase in cell size, indicating that the *Gtl2-Dio3* noncoding RNAs are essential mediators of pathological signaling in the heart.

4.2   *Gtl2-Dio3* Noncoding RNAs are Dynamically Regulated in Cardiac Injury and Hypertrophy Mouse Models

As explained in Chapter 3, two miRNAs in the *Gtl2-Dio3* locus, miR-410 and miR-495, are abundantly expressed in neonatal mouse hearts and their overexpression potently stimulates proliferation of neonatal cardiomyocytes *in vitro* (Clark and Naya 2015). By contrast, I found that these miRNAs were expressed at significantly lower levels in the adult heart, consistent with the permanent cell cycle withdrawal of adult cardiomyocytes. Because mature cardiomyocytes are unable to proliferate in the adult heart in response to damage or disease, I was interested in determining whether expression of the *Gtl2-Dio3* noncoding RNAs is regulated in pathological conditions by examining expression of *Gtl2-Dio3* noncoding RNAs in adult cardiomyopathies.

Initially, I examined expression of *Gtl2-Dio3* noncoding RNAs in a heart injury model by surgically inducing myocardial infarction (MI) in mice (Shibata et al. 2007). I examined temporal expression of the *Gtl2* lncRNA and the *Gtl2-Dio3*-encoded miRNAs miR-410, miR-495, and miR-433 in the progression of this cardiac injury at 1-, 3-, and 7-days post-infarction. Moreover, I compared their spatial expression differences in remote uninjured or spared myocardium (RM) and infarcted area (IA) regions of the heart. As shown in Figure 4.1, one day after infarction there was a significant increase in the *Gtl2* lncRNA in both the RM and IA compared to sham-operated control hearts. I also noted a

lesser but significant upregulation of the miRNAs in the RM which was not observed in the IA (Figure 4.1). By 3 days post-injury, however, expression of these miRNAs was significantly upregulated in both the remote and infarcted areas of the heart, but to a significantly greater extent in the IA relative to the RM (Figure 4.2). On the other hand, at 3 days post-infarction, expression of the *Gtl2* lncRNA was significantly reduced in the RM but expression in the IA remained relatively unchanged. By 7 days post-infarct, expression of the *Gtl2-Dio3* miRNAs in the RM remained significantly upregulated compared to sham and at levels comparable to those seen at day 3 (Figure 4.3). Notably, expression of the miRNAs in the IA was now 10-30-fold higher relative to the RM levels (Figure 4.3). In striking contrast, by 7 days post-infarction, expression of the *Gtl2* lncRNA was downregulated to control levels (Figure 4.3). To my knowledge, these results reveal for the first time an uncoupling of the regulation of the *Gtl2* lncRNA from the downstream miRNAs in the injured heart.

To determine whether the *Gtl2-Dio3* noncoding RNAs are regulated in response to pathological cardiac hypertrophy, I also examined the expression of these transcripts 3-, 7-, and 14-days after administration of Ang II, a potent cardiotoxic hormone that promotes extensive myocardial hypertrophy and fibrosis (Kim and Iwao 2000). Similar to the temporal expression differences observed in MI, the *Gtl2* lncRNA was significantly upregulated in the early stages of Ang II-mediated hypertrophy at day 3, whereas two out of the three miRNAs were unaffected (Figure 4.4). However, after 7 days of chronic Ang II treatment, the lncRNA and miRNAs were significantly upregulated relative to sham controls and to day 3 levels. The *Gtl2* lncRNA and miRNAs remained significantly

upregulated at 14 days post-angiotensin II treatment (Figure 4.4). Interestingly, the lncRNA showed a significant reduction in expression on day 14 compared to its levels on day 7 (Figure 4.4). These data indicate that the *Gtl2-Dio3* noncoding RNAs are also dynamically regulated in response to pathological hypertrophy.

4.3   *Gtl2-Dio3* Noncoding RNAs are Upregulated in Cardiomyopathies from Genetic Defects

To determine whether the *Gtl2-Dio3* noncoding RNAs are regulated in cardiomyopathies stemming from genetic structural mutations, I examined their expression in hearts from dystrophin- and laminin $\alpha 2$ (merosin)-deficient muscular dystrophy mice. Dystrophin-deficient *mdx* mice are the most commonly used mouse model of Duchenne Muscular Dystrophy (DMD) (Partridge 2013). While the major phenotype of DMD is skeletal muscle wasting, these patients often suffer from cardiomyopathy and often die due to cardiac complications (Duan 2006, Finsterer and Cripe 2014, McGreevy et al. 2015, van Westering et al. 2015). *Mdx* mice exhibit an aging-related cardiomyopathy but have been shown to display intolerance to cardiac stress between 1 and 3 months of age (Stuckey et al. 2012). I examined the expression of the *Gtl2-Dio3* noncoding RNAs at 10 weeks and found them to be uniformly and significantly upregulated in the heart (Figure 4.5). I next examined *Gtl2-Dio3* noncoding RNA expression in laminin-α2 (merosin)-deficient *DyW* mice, a model of Congenital Muscular Dystrophy (MDC1A). While *mdx* mice are capable of successful regeneration, laminin-α2-deficient mice have limited or no regenerative capacity (Kuang et al. 1999). Although cardiac failure in this muscular dystrophy is less common, moderate cardiac abnormalities have been reported (Spyrou et al. 1998, Carboni

et al. 2011). Similar to *mdx* hearts, expression of the *Gtl2-Dio3* noncoding RNAs in 7 week old laminin-α2-deficient hearts was significantly upregulated (Figure 4.6). Together, these data indicate that the *Gtl2-Dio3* noncoding RNAs are upregulated in cardiomyopathies arising from structural mutations.

Lastly, I examined the expression of the *Gtl2-Dio3* noncoding RNAs in the adult MEF2A knockout heart. In Chapter 3, I showed that the *Gtl2-Dio3* miRNAs are downregulated in perinatal MEF2A mutant hearts (Clark and Naya 2015). However, it is unknown whether this locus is dependent on this transcription factor in the adult heart. Moreover, a subset of MEF2A knockout mice survives and displays adult onset cardiomyopathy characterized by mitochondrial and conduction abnormalities (Naya et al. 2002). Interestingly, these adult mutant hearts also show elevated MEF2 activity, likely due to the stress-induced activation of MEF2D, the other adult MEF2 isoform known to be required in pathological cardiac remodeling (Kim et al. 2008). In contrast to the downregulated expression of the *Gtl2-Dio3* miRNAs in perinatal mutant hearts, these miRNAs were significantly upregulated in adult MEF2A knockout hearts (Figure 4.7). Unexpectedly, whereas the miRNAs were upregulated, there was a significant downregulation in *Gtl2* lncRNA expression (Figure 4.7). This differential effect on the *Gtl2-Dio3* locus in adult MEF2A mutant hearts is reminiscent of the uncoupled regulation observed between the lncRNA and miRNAs in the MI model described in Figure 4.3. Furthermore, I generated a MEF2A/*mdx* double mutant mouse and examined the expression of the *Gtl2-Dio3* miRNAs. Interestingly, I found the double mutant resulted in an additive effect on the expression of the *Gtl2-Dio3* miRNAs in the heart (Figure 4.8).

Together, these results support the notion that the *Gtl2-Dio3* miRNAs are upregulated in response to genetic defects that result in cardiomyopathy.

4.4 *Gtl2-Dio3* Noncoding RNAs are Regulated by MEF2 in Cardiac Stress Signaling

To determine whether the upregulation of the *Gtl2-Dio3* noncoding RNAs in diseased hearts occurred in cardiomyocytes, I examined their expression in isolated cardiomyocytes subjected to stress stimuli. NRVMs were treated with Ang II or phenylephrine (PE), another hormonal cardiac stressor that promotes pathological cardiac hypertrophy. Both Ang II and PE induced cardiac hypertrophy, demonstrated by increased cardiomyocyte (CM) area (Figure 4.9) and *Nppa*, induced atrial natriuretic factor (ANF), and *Nppb*, brain natriuretic peptide (BNP), expression (Figure 4.10). Similar to my *in vivo* data, I found that the *Gtl2-Dio3* lncRNA and miRNAs were significantly upregulated in response to both hypertrophic conditions (Figure 4.11).

The above results prompted me to investigate the molecular pathway leading to the induction of the *Gtl2-Dio3* noncoding RNAs in stressed cardiomyocytes. For these studies, I examined the response of the *Gtl2-Dio3* promoter to the above hypertrophic stimuli using a luciferase reporter assay. As shown in Figure 4.12, activity of the *Gtl2* proximal promoter in PE- and Ang II-treated NRVMs was significantly increased in the presence of these stimuli. Given that *Gtl2-Dio3* is a direct MEF2 target gene and that MEF2 is a key mediator of cardiac stress signaling, I next examined the activity of a mutant *Gtl2* promoter harboring a mutation in the MEF2 site. Mutation of the MEF2 site significantly attenuated

the response of the *Gtl2* promoter to both stimuli, demonstrating the requirement of MEF2 in this response (Figure 4.12).

4.5 Knockdown of *Gtl2-Dio3* microRNAs Reduces Hypertrophic Growth in Cardiomyocytes

In order to determine the requirement of *Gtl2-Dio3* miRNAs in cardiomyocyte hypertrophy, their expression was inhibited in NRVMs treated with PE since this hormone induced the most robust effect. I first confirmed that addition of miRNA-specific antimiRs significantly decreased expression of miR-410, miR-495, and miR-433, respectively (Figure 4.13A-C). Knockdown of these miRNAs individually in PE-treated NRVMs resulted in significantly decreased cardiomyocyte area (Figure 4.14). Furthermore, expression of the hypertrophic marker genes *Nppa* (ANF) and *Nppb* (BNP) was significantly reduced (Figure 4.15). Together, these results indicate that inhibition of miR-410, miR-495, and miR-433 individually is sufficient to attenuate the response of cardiomyocytes to stress signals, indicating a role for these noncoding RNAs in pathological cardiac remodeling.

4.6 Discussion

In this chapter, I demonstrate that the *Gtl2-Dio3* noncoding RNA locus is dynamically regulated in cardiomyopathies with diverse etiologies and function as pro-hypertrophic molecules in cardiomyocyte stress signaling. Expression analysis of the *Gtl2* lncRNA and the miRNAs (miR-410, miR-433, and miR-495) in acute MI and chronic Ang II administration revealed marked differences in their spatio-temporal regulation in response to these cardiac stressors. Furthermore, hypertrophic agonists potently activated

the *Gtl2-Dio3* proximal promoter and induced expression of both the lncRNA and miRNAs in isolated cardiomyocytes. Consistent with their upregulation, inhibition of the miRNAs blunted cardiomyocyte hypertrophy. These data demonstrate the complex regulation of the *Gtl2-Dio3* locus in cardiac diseases and how differential expression of its noncoding RNAs may be associated with distinct pathophysiological gene regulatory mechanisms.

In this Chapter, I examined the spatio-temporal regulation of the *Gtl2-Dio3* lncRNA and miRNAs in the progression of myocardial infarction and Ang II-induced hypertrophy. While other studies have reported the dysregulation of *Gtl2-Dio3* miRNAs in cardiomyopathy models including myocardial infarction (Ikeda et al. 2007, Thum et al. 2007, Yang et al. 2012, Janssen et al. 2013), these studies did not analyze expression of these transcripts in disease progression. Moreover, comparative expression of both classes of noncoding RNAs (lncRNAs and miRNAs) in discrete regions of the injured heart, e.g. the remote myocardium and infarct area, whose pathological microenvironments are radically different, was not performed.

The upregulation of these miRNAs in *mdx* and *DyW* hearts warrants further investigation. Currently, only treatments to alleviate symptoms of muscular dystrophy are available. Previously, the *Gtl2-Dio3* miRNAs were reported to be upregulated in serum of the DMD *mdx* mouse model, the golden retriever dog model, as well as in humans (Jeanson-Leh et al. 2014). I show here that these miRNAs are upregulated in the cardiac muscle of these mice. Examining the expression of these miRNAs in older *mdx* and *DyW* mice as well as investigating the pathways they may be regulating may provide insight into other therapeutic treatment options for these diseases.

My detailed analyses revealed different expression profiles of the *Gtl2-Dio3* noncoding RNAs in a subset of the cardiac disease models. These differences were most evident in the MI model, which revealed contrasting spatio-temporal expression patterns of the *Gtl2* lncRNA and miRNAs in the early and late stages of this cardiac injury. These differences may reflect the pathophysiology unique to this cardiomyopathy such that the distinct functional classes of noncoding RNAs processed from this locus are utilized for different aspects of genome reprogramming in cardiomyocytes that help drive pathological gene expression patterns. Indeed, the *Gtl2* lncRNA has an epigenetic function and is required for recruitment of PRC2 to positively regulate the locus in *cis* in embryonic stem cells by preventing DNA methylation in an upstream distal enhancer (Das et al. 2015). To my knowledge, the miRNAs processed from the *Gtl2-Dio3* locus regulate expression of target mRNAs and have not been shown to modulate chromatin structure.

There is growing appreciation for the complex regulation of this maternally expressed, imprinted locus. Prior studies by us and others demonstrated coordinate dysregulated expression of the noncoding RNAs throughout the locus in mouse embryos and in cardiac and skeletal muscle (Zhou et al. 2010, Snyder et al. 2013, Das et al. 2015). In addition, our studies show that coordinate regulation is dependent on activation of the *Gtl2* proximal promoter by MEF2 (Snyder et al. 2013, Clark and Naya 2015). Contrary to these findings, some reports have described enhancers neighboring discrete miRNA clusters within the 200kb *Gtl2-Dio3* mega locus. One of these enhancers is located upstream of the miRNA cluster harboring miR-433, and the other is upstream of the cluster containing both miR-410 and miR-495 (Song and Wang 2008, Fiore et al. 2009, Hagan et

al. 2009). Adding to the complexity of *Gtl2-Dio3* regulation are reports indicating either no significant change in expression or downregulation of some of its miRNAs, such as miR-495 in ischemic and dilated cardiomyopathies (Ikeda et al. 2007, Thum et al. 2007). Apart from possible technical differences in the analysis methods or severity of disease, these data suggest that differential expression of *Gtl2-Dio3* noncoding RNAs depends on the specific cardiac pathology. Our data support the notion that the *Gtl2-Dio3* noncoding RNAs, in addition to their coordinate regulation by the *Gtl2* promoter, can be subject to alternative and separable regulation through the utilization of the various enhancers embedded in the locus or perhaps at the level of post-transcriptional processing in a cardiac disease-specific manner.

Although overexpression of the *Gtl2-Dio3* miRNAs is sufficient to promote proliferation of neonatal cardiomyocytes *in vitro* (Clark and Naya 2015), their upregulation in cardiac disease does not stimulate proliferation. One obvious explanation relates to potential differences between *in vitro* and *in vivo* environments. Alternatively, their levels, though elevated, may be insufficient to induce cardiomyocyte proliferation. Finally, counter-regulatory mechanisms in cardiac disease may activate pathways that prevent these noncoding RNAs from inducing proliferation.

In conclusion, I demonstrate that the *Gtl2-Dio3* noncoding RNAs are upregulated in multiple models of cardiac disease but display different spatio-temporal expression patterns. I also show that a subset of these miRNAs function as pro-hypertrophic molecules such that their inhibition in stressed cardiomyocytes attenuates the hypertrophic growth response. In the future, it will be of interest to examine the expression profile of the *Gtl2-*

Dio3 locus in additional cardiomyopathies to determine whether each disease is associated with a unique expression signature of this locus. Additionally, determining the pathways regulated by the *Gtl2-Dio3* noncoding RNAs in cardiomyopathies will lead to a broader understanding of the shared pathways in cardiac disease. Understanding the roles of the *Gtl2* lncRNA and miRNAs from this dynamically regulated mega-locus in cardiomyopathies poses to be a challenging but potentially fruitful endeavor that may facilitate the development of strategies to target this locus in a disease-specific manner.
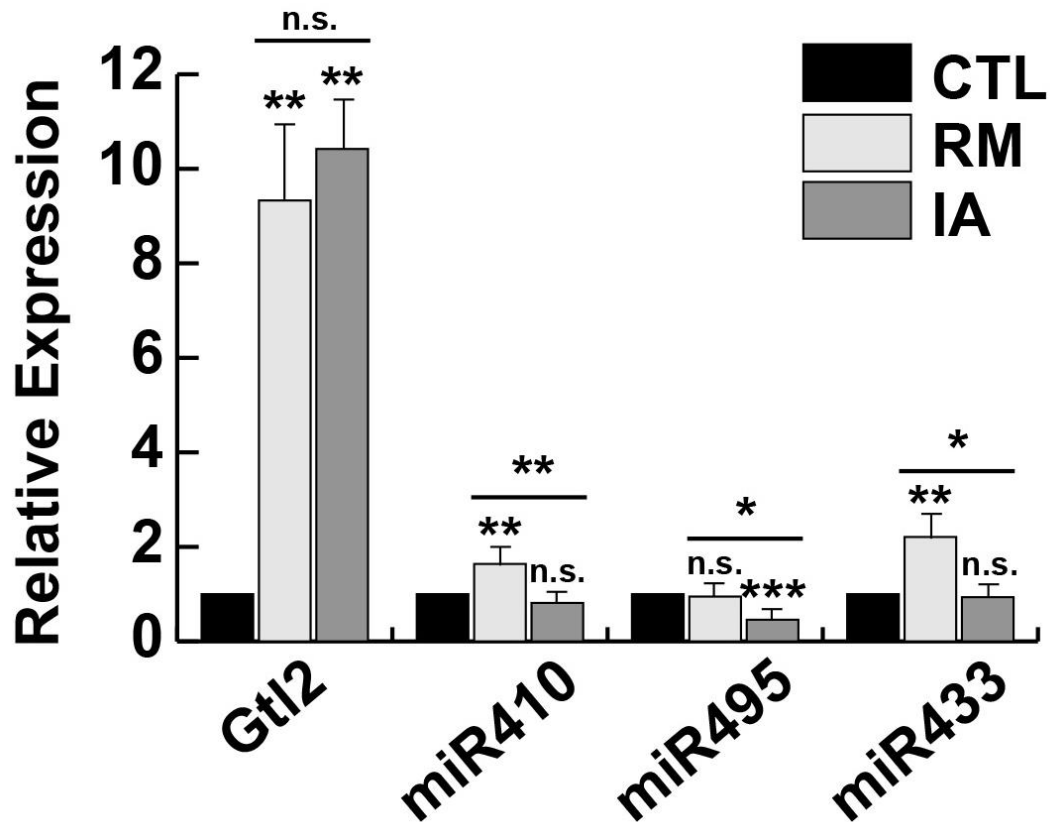
Figure 4.1 *Gtl2-Dio3* noncoding RNA expression 1 day after myocardial infarction.
Quantitative RT-PCR of *Gtl2* lncRNA, miR-410, miR-495, and miR-433 expression 1 day
post-myocardial infarct. Expression is relative to GAPDH and 5S rRNA internal controls.
Gene expression values in CTL tissue were normalized to one. Relative expression
represents the fold change in gene expression in RM and IA tissue compared to CTL tissue.
Uninjured ventricle (CTL); Remote/uninjured ventricle (RM); Infarcted/injured ventricle
(IA). Error bars represent S.E.M. n≥3. n.s., not significant; *, $p<0.05$, **, $p<0.01$; ***,
$p<0.001$.
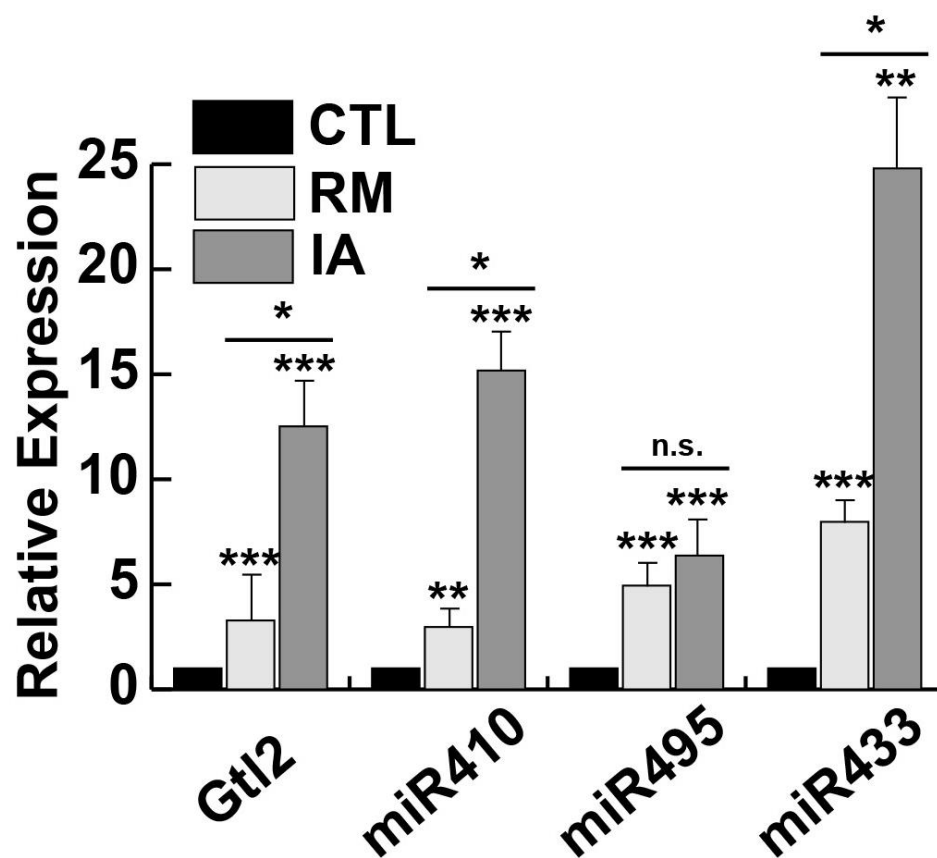
Figure 4.2 *Gtl2-Dio3* noncoding RNA expression 3 days after myocardial infarction.

Quantitative RT-PCR of *Gtl2* lncRNA, miR-410, miR-495, and miR-433 expression 3 days post-myocardial infarct. Expression is relative to GAPDH and 5S rRNA internal controls. Gene expression values in CTL tissue were normalized to one. Relative expression represents the fold change in gene expression in RM and IA tissue compared to CTL tissue. Uninjured ventricle (CTL); Remote/uninjured ventricle (RM); Infarcted/injured ventricle (IA). Error bars represent S.E.M. $n \geq 3$. n.s., not significant; *, $p<0.05$, **, $p<0.01$; ***, $p<0.001$.
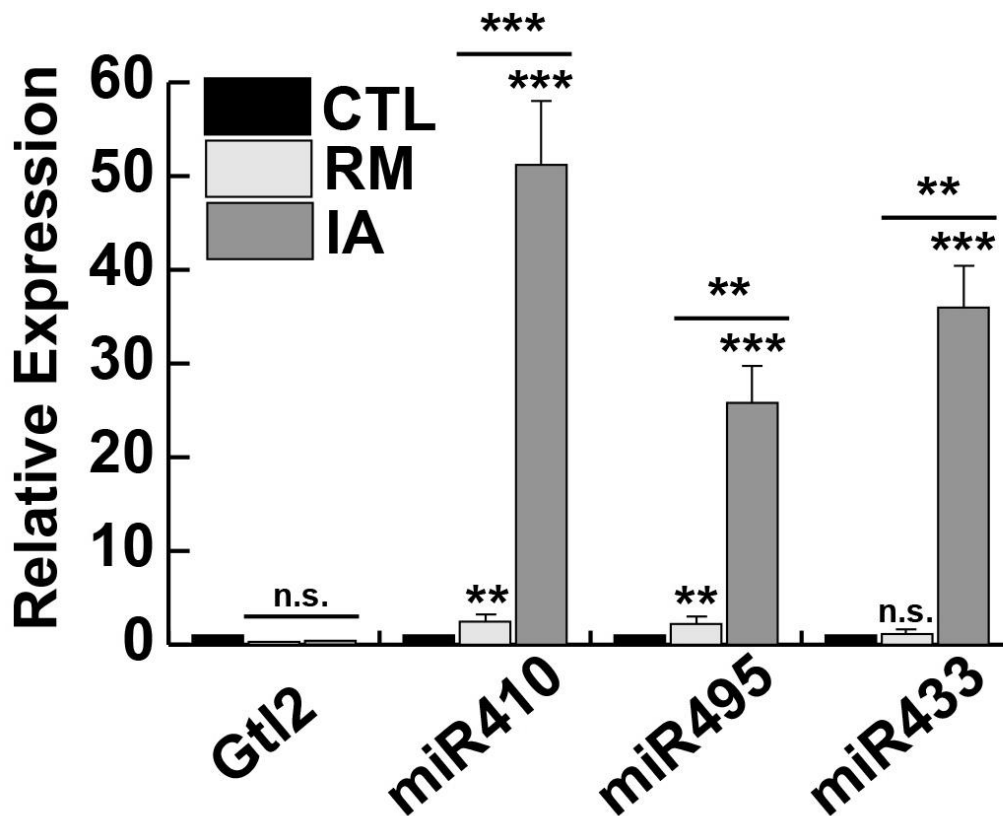
Figure 4.3 *Gtl2-Dio3* noncoding RNA expression 7 days after myocardial infarction. Quantitative RT-PCR of *Gtl2* lncRNA, miR-410, miR-495, and miR-433 expression 7 days post-myocardial infarct. Expression is relative to GAPDH and 5S rRNA internal controls. Gene expression values in CTL tissue were normalized to one. Relative expression represents the fold change in gene expression in RM and IA tissue compared to CTL tissue. Uninjured ventricle (CTL); Remote/uninjured ventricle (RM); Infarcted/injured ventricle (IA). Error bars represent S.E.M. n≥3. n.s., not significant; *, $p<0.05$, **, $p<0.01$; ***, $p<0.001$.
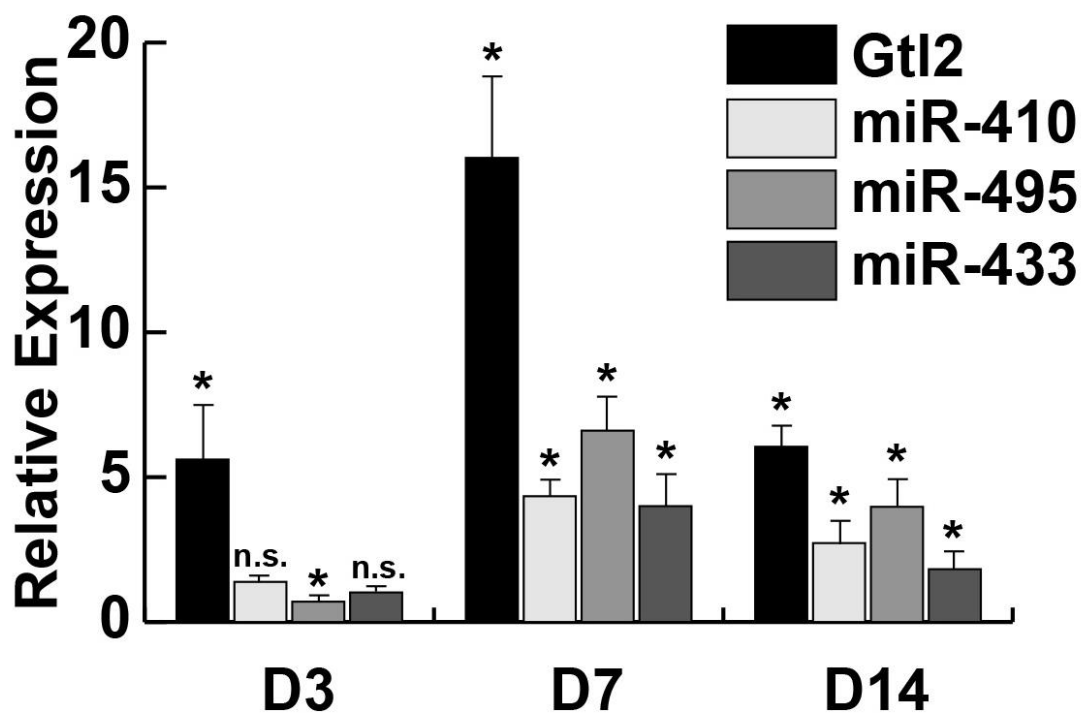
Figure 4.4 *Gtl2-Dio3* noncoding RNA expression is upregulated in Angiotensin II-treated cardiac muscle. Quantitative RT-PCR of *Gtl2* lncRNA, miR-410, miR-495, and miR-433 expression 3-, 7-, and 14-days post-Angiotensin II treatment compared to uninjured control. Expression is relative to GAPDH and 5S rRNA internal controls. Gene expression values in CTL tissue were normalized to one. Relative expression represents the fold change in gene expression in Angiotensin II-administered tissue compared to CTL tissue. Error bars represent S.E.M. $n \geq 3$. n.s., not significant; *, $p < 0.05$.
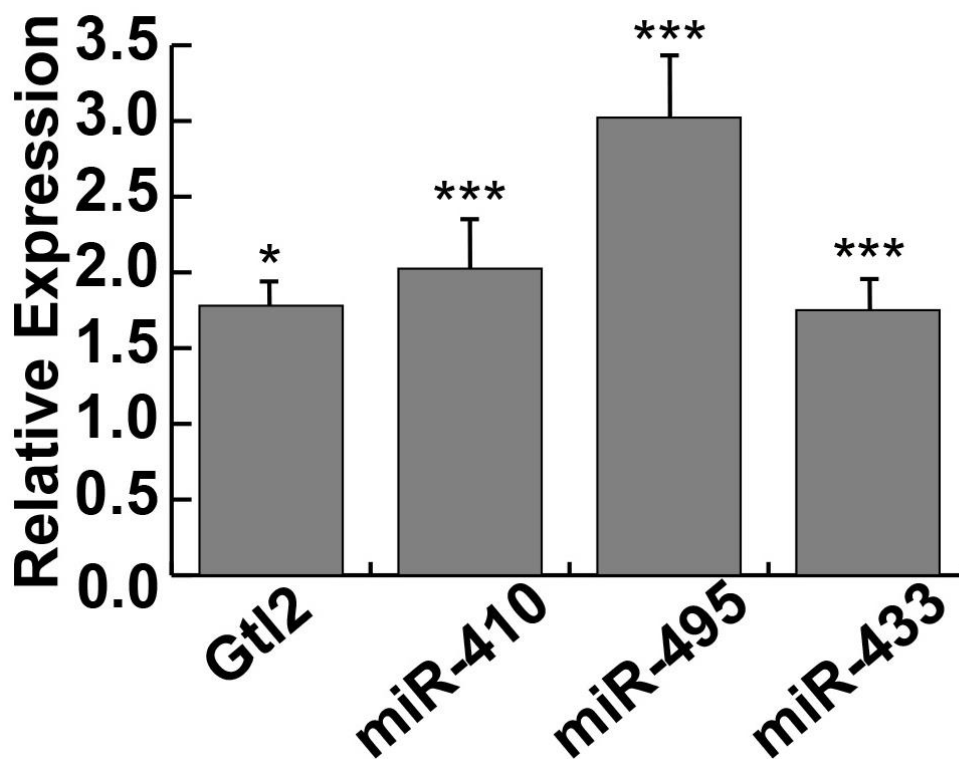
Figure 4.5 *Gtl2-Dio3* noncoding RNA expression is upregulated in *mdx* cardiac muscle. Quantitative RT-PCR of *Gtl2* lncRNA, miR-410, miR-495, and miR-433 expression in the 10 week *mdx* hearts compared to wildtype hearts. Expression is relative to GAPDH and 5S rRNA internal controls. Gene expression values in wildtype tissue were normalized to one. Relative expression represents the fold change in gene expression in *mdx* tissue compared to wildtype tissue. Error bars represent S.E.M. n≥3. *, $p<0.05$; **, $p<0.01$; ***, $p<0.001$.
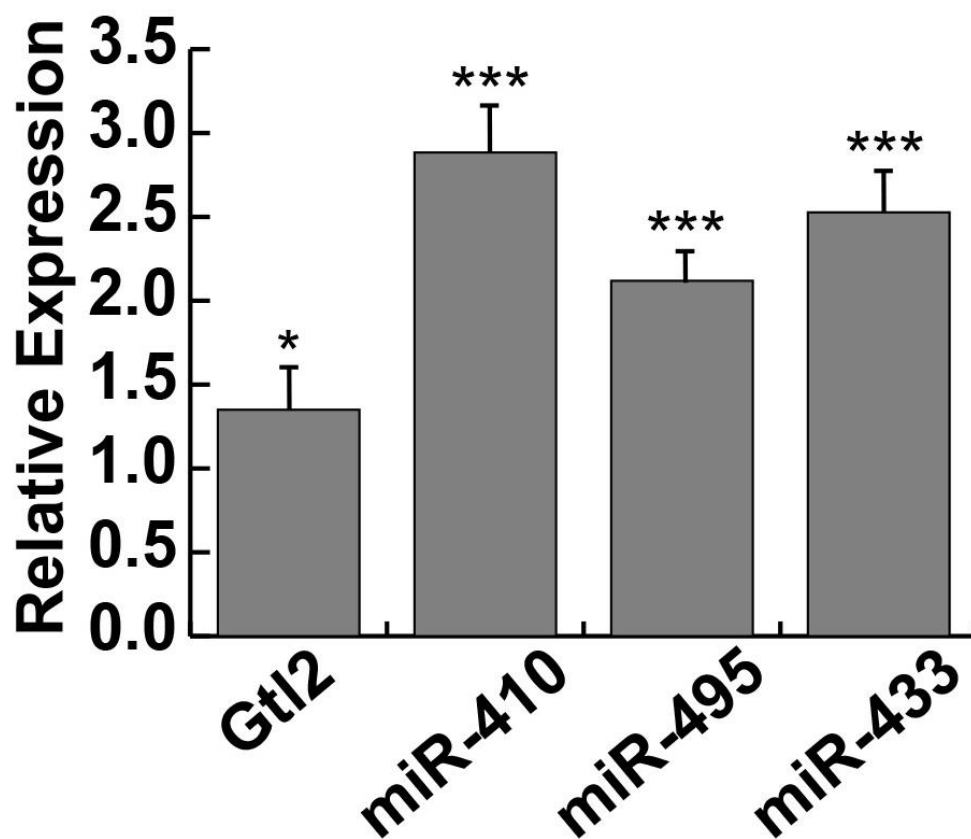
Figure 4.6 ***Gtl2-Dio3* noncoding RNA expression is upregulated in *DyW* cardiac muscle.** Quantitative RT-PCR of *Gtl2* lncRNA, miR-410, miR-495, and miR-433 expression in the 7 week *DyW* hearts compared to wildtype hearts. Expression is relative to GAPDH and 5S rRNA internal controls. Gene expression values in wildtype tissue were normalized to one. Relative expression represents the fold change in gene expression in *DyW* tissue compared to wildtype tissue. Error bars represent S.E.M. n$\geq$3. *, $p<0.05$; ***, $p<0.001$.
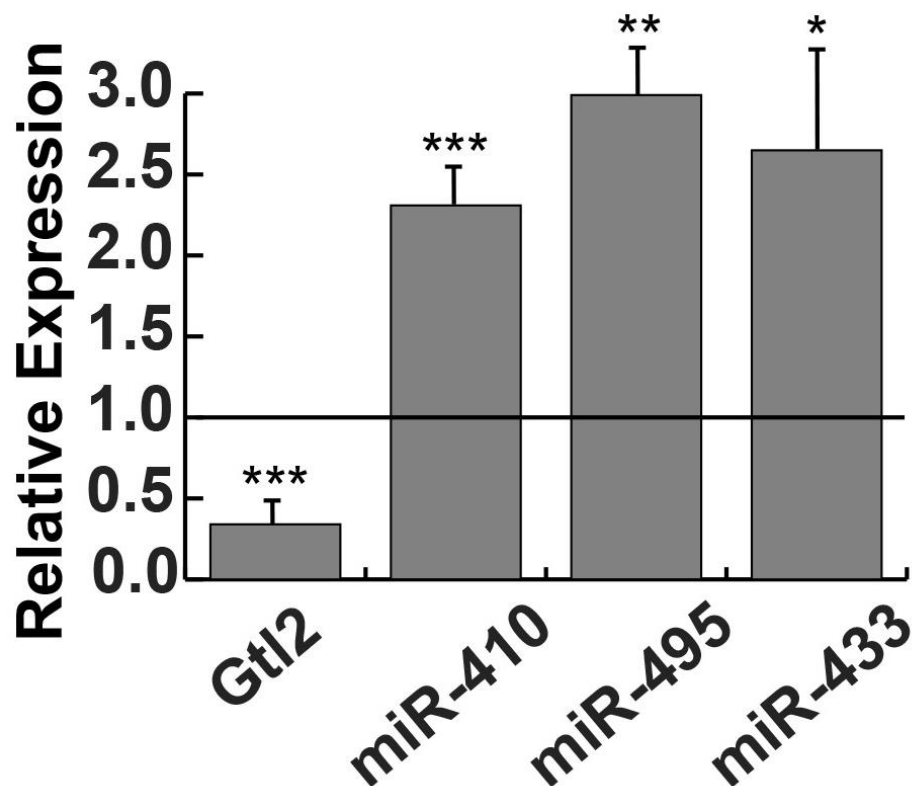
Figure 4.7 *Gtl2-Dio3* **microRNA expression is upregulated in adult MEF2A knockout cardiac muscle.** Quantitative RT-PCR of *Gtl2* lncRNA, miR-410, miR-495, and miR-433 expression in adult MEF2A KO hearts compared to wildtype control. Expression is relative to GAPDH and 5S rRNA internal controls. Gene expression values in wildtype tissue were normalized to one. Relative expression represents the fold change in gene expression in MEF2A KO tissue compared to wildtype tissue. Error bars represent S.E.M. $n \geq 3$. *, $p<0.05$; **, $p<0.01$; ***, $p<0.001$.
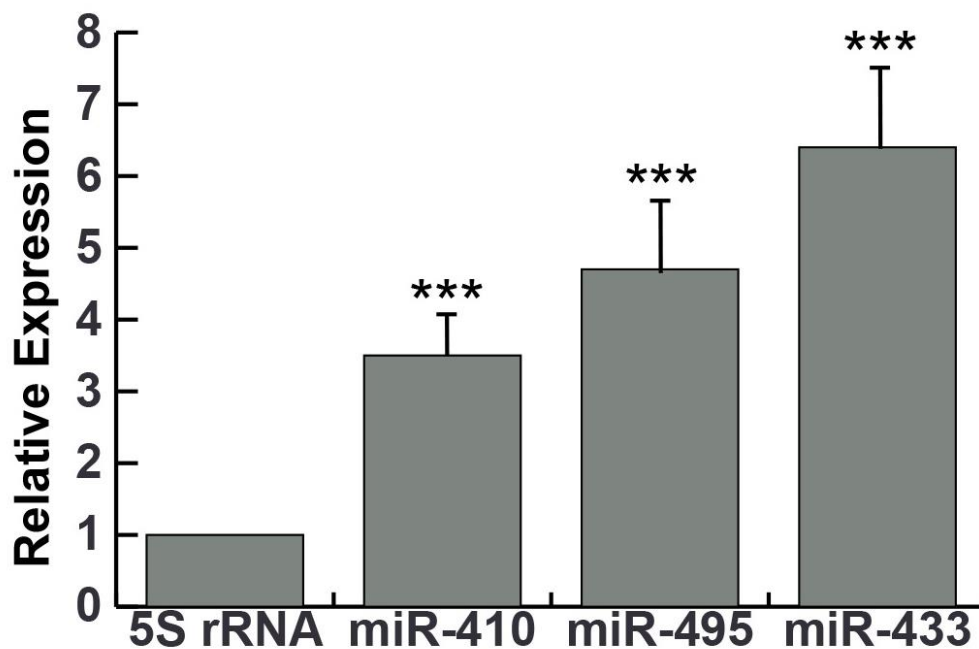
Figure 4.8 *Gtl2-Dio3* **microRNA expression is upregulated in adult MEF2A/***mdx* **double mutant cardiac muscle.** Quantitative RT-PCR miR-410, miR-495, and miR-433 expression in adult MEF2A/*mdx* KO hearts compared to wildtype control. Expression is relative to 5S rRNA internal controls. Gene expression values in wildtype tissue were normalized to one. Relative expression represents the fold change in gene expression in MEF2A/*mdx* KO tissue compared to wildtype tissue. Error bars represent S.E.M. n≥3. ***, *p*<0.001.

A.
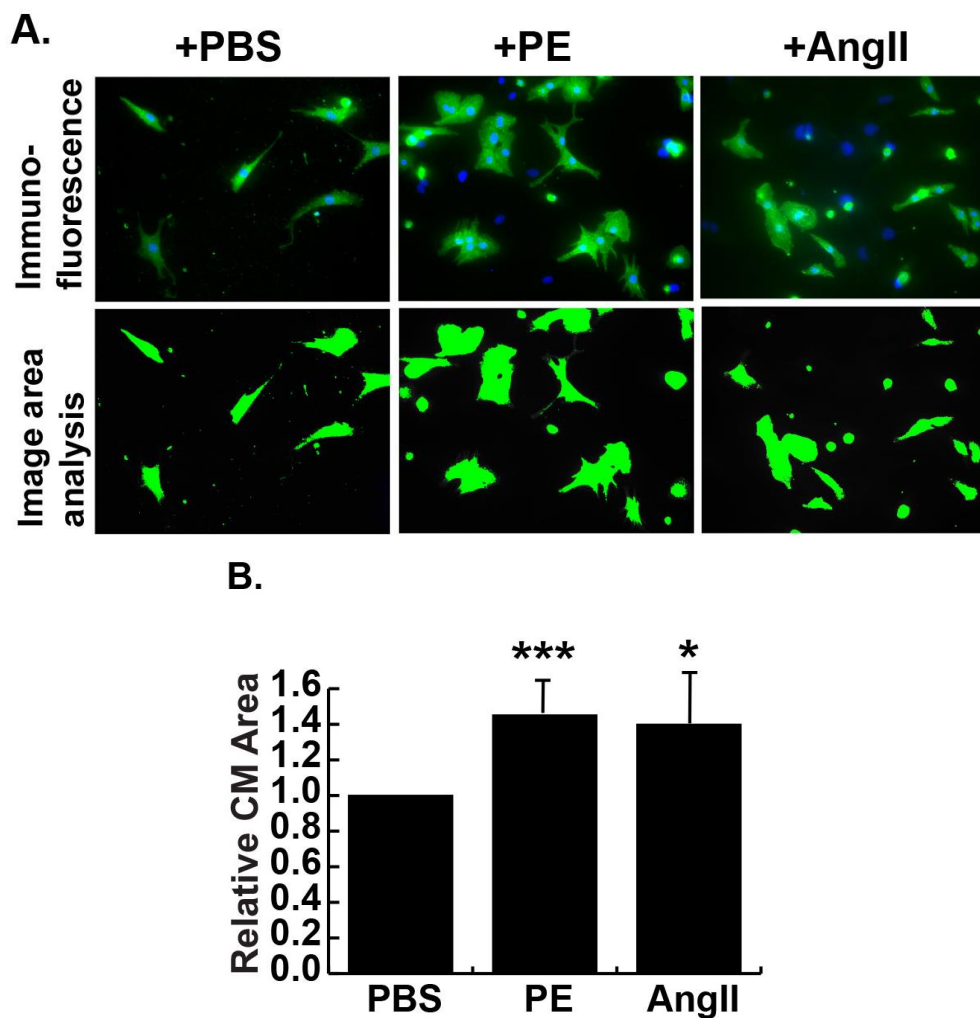
Figure 4.9 Phenylephrine and Angiotensin II induce cardiomyocyte hypertrophy *in vitro*. A) Representative images of PBS, PE, and Ang II-treated NRVMs. Top, immunofluorescent images. α-actinin in green. DAPI in blue. Bottom, cardiomyocyte area analysis. B) Quantification of relative cardiomyocyte (CM) area in PBS-, PE-, and Ang II-treated NRVMs. Computer generated area analysis for each cardiomyocyte was quantified for 100 cardiomyocytes. Average cardiomyocyte area relative to PBS control is shown for PE- and Ang II-treated NRVMs. Error bars represent S.E.M. n≥3. *, $p<0.05$; ***, $p<0.001$.
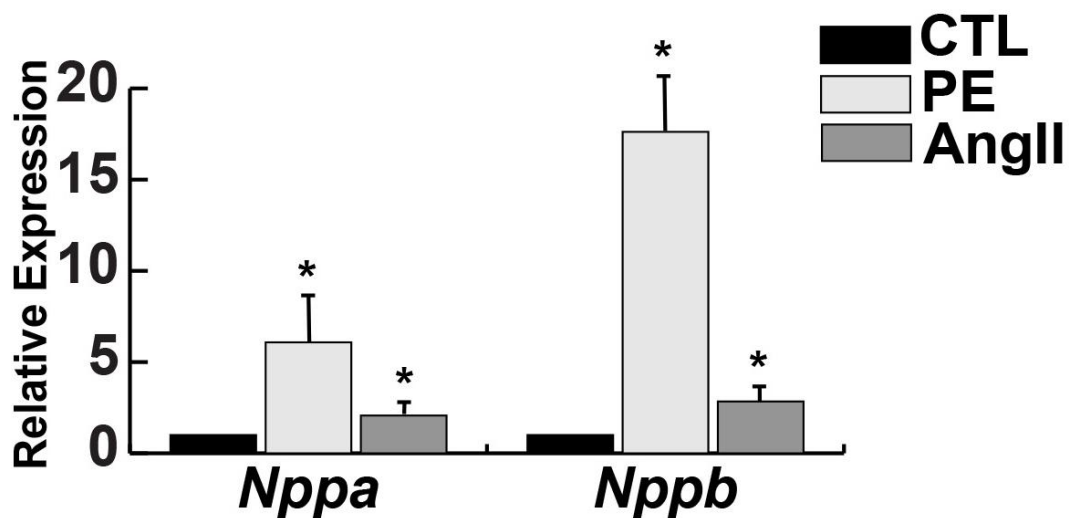
Figure 4.10 Phenylephrine and Angiotensin II induce hypertrophic marker genes *in vitro*. Quantitative RT-PCR of cardiac hypertrophy marker genes ANF (*Nppa*) and BNP (*Nppb*) in PE- and Ang II-treated NRVMs compared to PBS-treated control NRVMs (CTL). Expression is relative to GAPDH internal control. Gene expression values in CTL NRVMs were normalized to one. Relative expression represents the fold change in gene expression in PE- and Ang II-treated NRVMs compared to CTL NRVMs. Error bars represent S.E.M. n≥3. *, $p<0.05$.
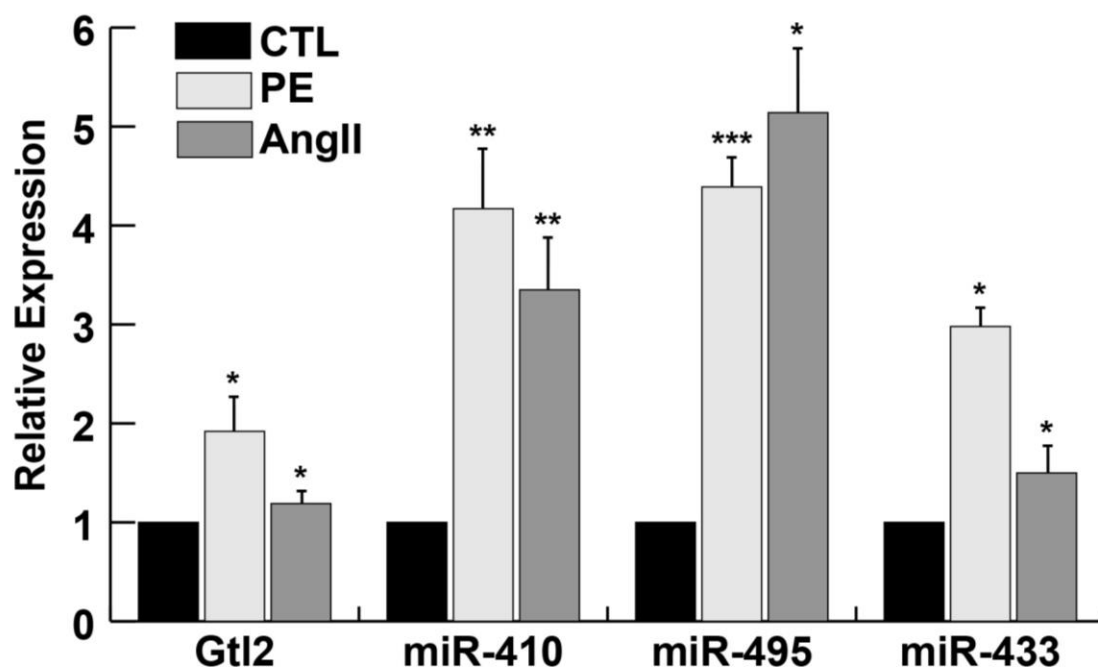
Figure 4.11 *Gtl2-Dio3* **noncoding RNAs are upregulated in cardiomyocyte hypertrophy** *in vitro*. Quantitative RT-PCR of *Gtl2* lncRNA, miR-410, miR-495, and miR-433 expression in PE- and Ang II-treated NRVMs. Expression is relative to GAPDH and 5S rRNA internal controls. Expression values in CTL NRVMs were normalized to one. Relative expression represents the fold change in gene expression in PE- and Ang II-treated NRVMs compared to CTL NRVMs. Error bars represent S.E.M. n≥3. *, $p<0.05$; **, $p<0.01$; ***, $p<0.001$.
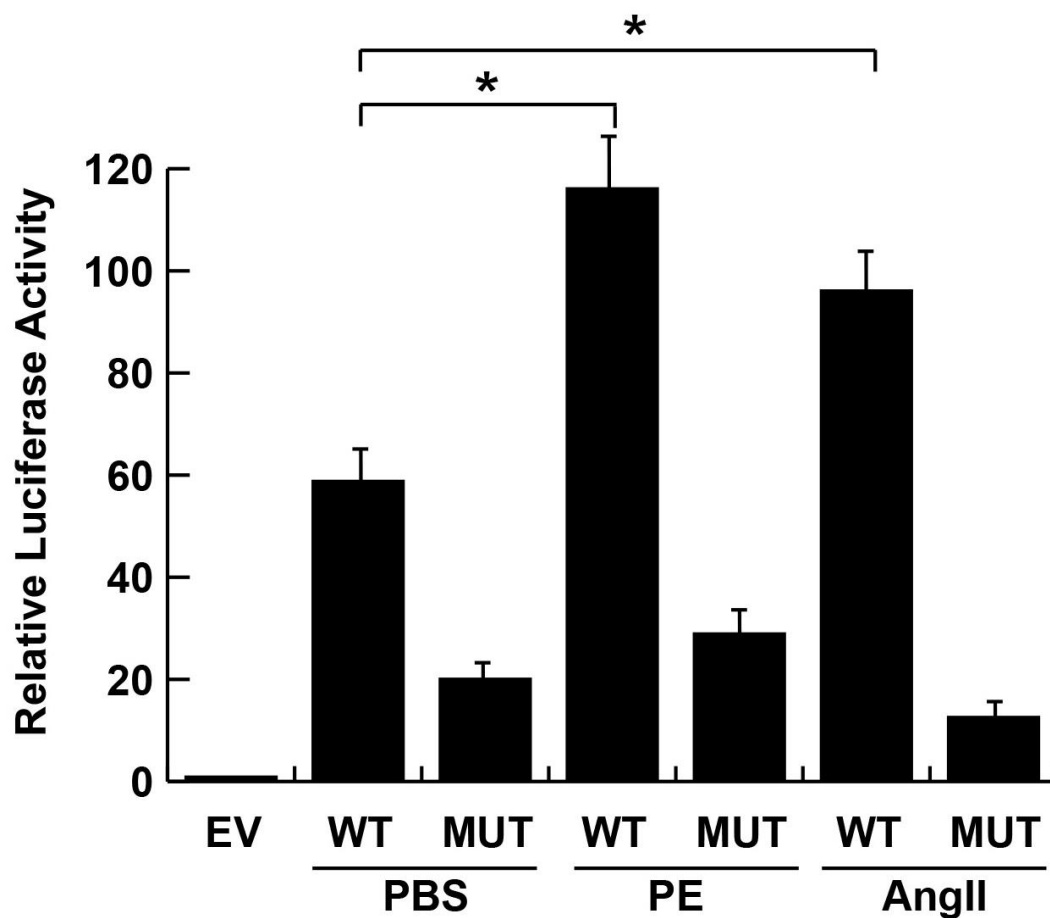
Figure 4.12 *Gtl2* **promoter activity is increased in cardiomyocyte hypertrophy** *in vitro***.**

Luciferase analysis of the *Gtl2* promoter containing a wild type MEF2 site (WT) and a mutant MEF2 site (MUT) in PBS-, PE-, and Ang II-treated NRVMs compared to empty vector (EV) control. Error bars represent S.E.M. n≥3. *, *p*<0.05.
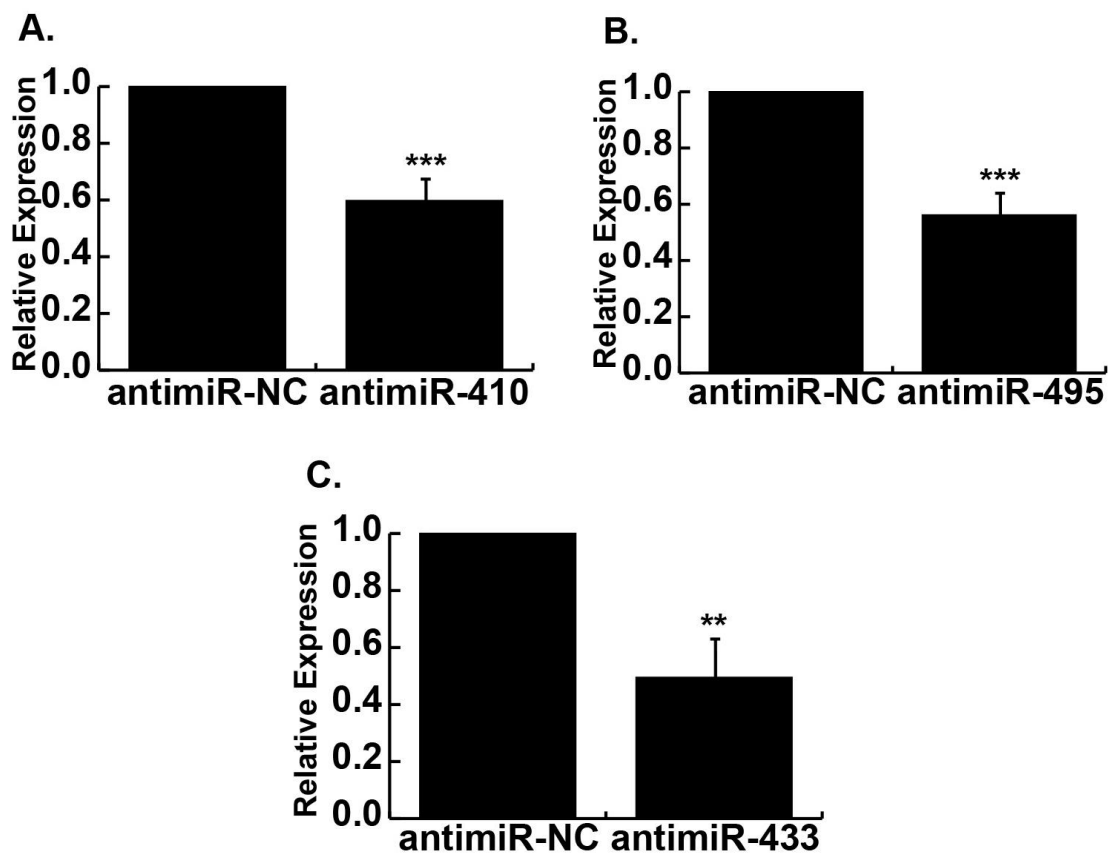
Figure 4.13 AntimiRs robustly knockdown expression of miRNA-410, -495, and -433, respectively. A) Quantitative RT-PCR of miR-410 upon addition of antimiR-NC (control) and antimiR-410. B) Quantitative RT-PCR of miR-495 upon addition of antimiR-NC (control) and antimiR-495. C) Quantitative RT-PCR of miR-433 upon addition of antimiR-NC (control) and antimiR-433. Error bars represent S.E.M. n≥3. **, $p<0.01$; ***, $p<0.001$.
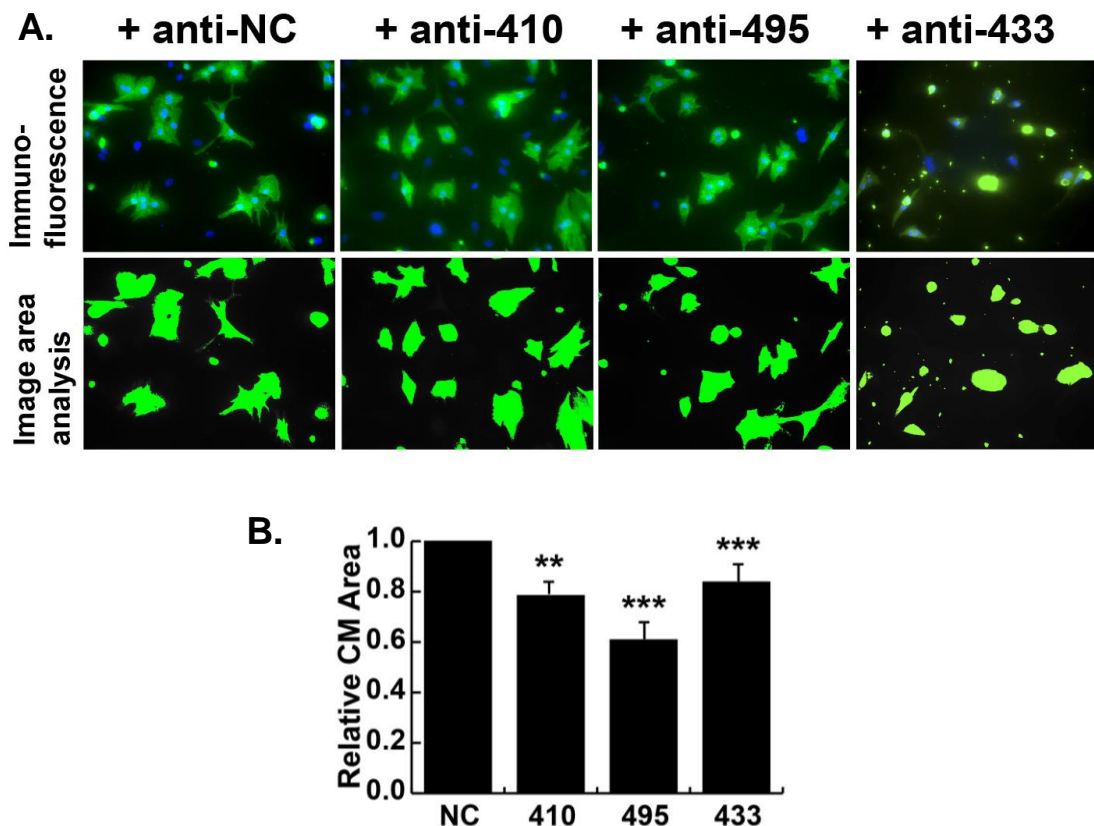
Figure 4.14 Knockdown of *Gtl2-Dio3* miRNAs reduces hypertrophic growth in cardiomyocytes *in vitro*. A) Representative images of PE-treated NRVMs upon the addition of antimiR-NC, antimiR-410, antimiR-495, or antimiR-433. Top, immunofluorescent images. α-actinin in green. DAPI in blue. Bottom, cardiomyocyte area analysis. B) Quantification of relative cardiomyocyte (CM) area in PE-treated NRVMs upon the addition of antimiR-NC, antimiR-410, antimiR-495, or antimiR-433. Computer generated area analysis for each cardiomyocyte was quantified for 100 cardiomyocytes. Average cardiomyocyte area relative to miR-NC control is shown for antimiR-410, -495, and -433-treated NRVMs Error bars represent S.E.M. n≥3. **, $p<0.01$; ***, $p<0.001$.
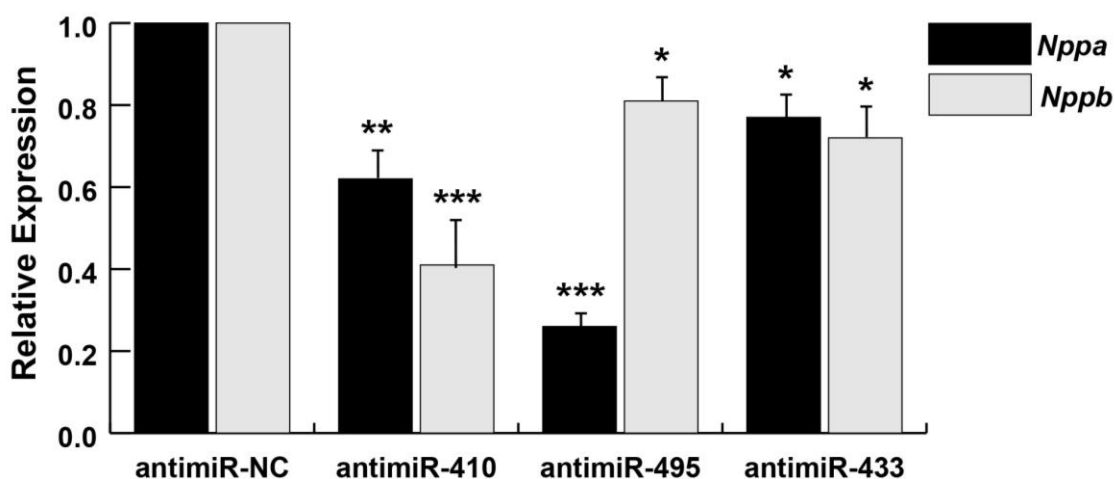
Figure 4.15 Knocking down *Gtl2-Dio3* miRNAs results in decreased expression of cardiac hypertrophy markers. Quantitative RT-PCR for markers of hypertrophy ANF (*Nppa*) and BNP (*Nppb*) in PE-treated NRVMs transfected with antimiR-410, antimiR-495, or antimiR-433 compared to antimiR-NC control. Gene expression values in antimiR-NC NRVMs were normalized to one. Relative expression represents the fold change in gene expression in antimiR-410, -495, and -433 NRVMs compared to antimiR-NC NRVMs. *Nppa*, ANF. *Nppb*, BNP. Expression is relative to GAPDH internal control. Error bars represent S.E.M. n≥3. *, $p<0.05$; **, $p<0.01$; ***, $p<0.001$.

CHAPTER FIVE – DISCUSSION

5.1   Conclusions

Mature cardiomyocytes are post-mitotic, fully differentiated cells with a limited capacity to repair or replace cells from aging or injury. Improving cardiac function post-injury proves difficult because the underlying molecular mechanisms that lead to neonatal cardiomyocyte cell cycle exit are not well understood. In this dissertation, I investigated the expression and role of the MEF2-regulated *Gtl2-Dio3* miRNAs in cardiac muscle and disease.

MEF2 is an important transcription factor for skeletal and cardiac muscle differentiation. We recently showed that MEF2A, one of four mammalian MEF2 isoforms, regulates the *Gtl2-Dio3* miRNA mega-cluster in skeletal muscle and that a subset of these miRNAs target Sfrp2 to regulate WNT signaling in skeletal muscle regeneration (Snyder et al. 2013). Furthermore, in this dissertation I showed that MEF2A also regulates this miRNA cluster in cardiac muscle and elucidated a mechanism for these miRNAs in cardiomyocyte proliferation (Figure 5.1). In Chapter 3, I showed that the *Gtl2-Dio3* miRNAs are expressed at higher levels in the perinatal heart compared to adult, indicating they may play a role in cardiac maturation shortly after birth. I demonstrated that the *Gtl2-Dio3* miRNAs miR-410 and miR-495 promote neonatal cardiomyocyte proliferation. These miRNAs induce proliferation, in part by targeting the transcriptional co-activator Cited2. Furthermore, inhibition of Cited2 also stimulates neonatal cardiomyocyte proliferation. Proliferation induced by overexpressing miR-410 and miR-495 or knockdown of Cited2 was associated with reduced expression of the cell cycle inhibitor

p57 and increased expression of the pro-proliferative factor *Vegfa*. This chapter identified a novel miRNA-transcriptional co-activator pathway that induces cardiomyocyte proliferation.

Recently, there has been considerable focus on knocking down miRNAs to alter the cell cycle in cardiac cells. Interestingly, overexpressing miR-21 immediately following myocardial infarction decreased myocardial infarct size (Dong et al. 2009). Furthermore, knocking down miR-21 in cardiac fibroblasts resulted in reduced fibrosis (Thum et al. 2008). Knocking down members of the miR-15 family resulted in increased mitotic cardiomyocytes, indicating a potential role for this miR family in cardiac regeneration (Porrello et al. 2011, van Rooij et al. 2012, Porrello et al. 2013). Based on the above results, these miRNAs may be deemed potential therapeutic targets for cardiac injury. In the present study, I demonstrated that the *Gtl2-Dio3* miRNAs may be prime therapeutic candidates for agonist drugs and that their overexpression may be beneficial for cardiomyocyte proliferation.

In Chapter 4, I examined expression of the *Gtl2-Dio3* noncoding RNAs in different models of cardiomyopathy. I found miR-410, miR-495, and miR-433 to be upregulated in mouse models of myocardial infarction and pathological hypertrophy induced by chronic administration of angiotensin II. Moreover, I found expression of the *Gtl2-Dio3* miRNAs was upregulated in dystrophic cardiomyopathies such as the *mdx* and *DyW* mouse models. Lastly, I found these miRNAs to be upregulated in the adult MEF2A knockout heart, which display adult onset cardiomyopathy. The fact that these miRNAs are upregulated in diverse cardiomyopathy models indicates there may be a common pathway that is initiated upon

cardiac injury. Furthermore, I examined the expression of the *Gtl2* lncRNA in these cardiomyopathies. Interestingly, I observed that the *Gtl2* lncRNA and miRNAs were differentially regulated from each other both in the MI model and the MEF2A knockout heart. This is the first time the *Gtl2-Dio3* locus has been shown to be dynamically regulated in the heart in the context of injury. Further investigations are needed to determine the complex regulation of the *Gtl2-Dio3* noncoding RNA locus.

Moreover, I showed that these *Gtl2-Dio3* miRNAs are upregulated in response to hypertrophic stimuli *in vitro* and that their induction is dependent on MEF2 activating the proximal promoter. Additionally, silencing miR-410, miR-495, and miR-433 using anti-miRs resulted in a decreased hypertrophic response in neonatal cardiomyocytes *in vitro*. Currently there are a number of therapeutic options to help relieve symptoms of heart disease but there is still no cure. Patients are often prescribed drug therapy and exercise in order to slow the progression of heart disease. These drug therapies include angiotensin-converting enzyme (ACE) inhibitors, drugs that prevent the formation of angiotensin II, β-blockers, which slow heart rate, as well as others including therapies that alter calcium handling, target β-adrenergic signaling, and inhibit histone deacetylases (HDACs) (Tham et al. 2015).

The first miRNA-targeted drug is currently being used in clinical trials for hepatitis C. miR-122 has been shown to protect the hepatitis C virus from degradation. Miravirsen is a locked nucleic acid-modified antisense oligonucleotide that inhibits miR-122. Administration of miravirsen to patients with hepatitis C results in viral suppression (Janssen et al. 2013). This clinical trial gives hope to the potential for miRNA-based

therapies for cardiovascular disease. Understanding the molecular changes in the heart post-injury will allow for new therapeutic options for patients with cardiac disease. Determining the targets of the *Gtl2-Dio3* lncRNA and miRNAs in the context of cardiac injury may provide novel viable therapeutic targets to reduce cardiac injury and improve cardiac function post-injury.

5.2   Future Perspectives

5.2.1   Determine the Cardiac Requirement for *Gtl2-Dio3* miRNAs

In Chapter 3, I demonstrated that the *Gtl2-Dio3* miRNAs are expressed in both the postnatal and adult heart and that they promote cardiomyocyte proliferation in neonatal cardiomyocytes. Since these miRNAs are capable of inducing cardiomyocyte proliferation after birth, it is possible that they may be required for embryonic cardiomyocyte proliferation. However, we do not have information regarding the temporal expression of these miRNAs in cardiac development.

Therefore, it is worth determining when these miRNAs are first expressed in the developing heart. To do this, expression analyses should be performed at embryonic time points. In order to look at the spatial expression pattern in the heart, *in situ* hybridization for these miRNAs should also be performed to determine if they are expressed throughout the heart or if they are expressed in distinct regions of the developing heart. To identify areas of high *Gtl2* activity in the developing embryo, we have generated a *Gtl2*-lacZ reporter construct. 0.4kb of the proximal promoter of *Gtl2* harboring the MEF2 site was cloned upstream of the hsp68 lacZ reporter. This transgene can be directly injected into embryos and embryos can be collected at different time points and X-gal staining can be

performed for β-galactosidase to see when the *Gtl2* promoter is active. Preliminarily, the Black Lab (UCSF) injected the *Gtl2*-LacZ construct and observed activation of this reporter in the heart and somites at E11.5 (Figure 5.2). While these preliminary results are consistent with our data, this experiment needs to be repeated and it will be interesting to determine exactly when the *Gtl2* locus is first active in these areas.

Once we know when the *Gtl2-Dio3* miRNAs are expressed in the developing heart, we can determine whether they are required for cardiac proliferation by knocking out the locus. Because the *Gtl2-Dio3* noncoding region spans over 200 kilobases, it proves difficult to knock down. Additionally, because the *Gtl2-Dio3* locus contains multiple noncoding RNAs, knocking out a portion may not be effective to knock down all the miRNAs. Based on the knowledge that the *Gtl2-Dio3* miRNA cluster is coordinately transcribed (Zhou et al. 2010), knocking out the promoter of this locus would address the role of all of the noncoding RNAs throughout the locus.

Initially, we hypothesized that designing a shRNA against the *Gtl2* region would be sufficient to knock down the entire locus, since all the miRNAs are thought to be transcribed together. However, upon generating an adenoviral vector containing sh*Gtl2*, our results varied *in vitro* (Clark and Kontor, data not shown). The requirement of this locus in the heart could also be determined by conditionally knocking out the promoter of this locus in a cardiac-specific manner using the αMHC promoter *in vivo*.

Furthermore, determining the requirement of the *Gtl2* lncRNA remains to be determined. Knocking down the lncRNA may also disrupt the expression of the *Gtl2-Dio3* miRNAs. lncRNAs can be knocked down using GapmeRs, a technique similar to siRNA

(Stein et al. 2010). Moreover, the role of the *Gtl2* lncRNA has yet to be investigated. Investigating the function of the *Gtl2* lncRNA is another current project in our lab and will contribute to a greater understanding of the *Gtl2-Dio3* locus in the heart.

Based on my data from Chapter 4, the *Gtl2-Dio3* noncoding RNAs may not be coordinately regulated and instead may display dynamic regulation in different contexts. Knockdown of individual miRNAs or multiple miRNAs may be sufficient to determine their requirement in the heart. Knockdown of individual miRNAs from the *Gtl2-Dio3* cluster *in vitro*, specifically miR-410 and miR-495, did not show an overt phenotype. However, combinatorial knockout of both miR-410 and miR-495 may show an overt phenotype and may indicate the requirement of these miRNAs for cardiac proliferation.

Lastly, the potential role of the *Gtl2-Dio3* noncoding RNAs in cardiomyocyte differentiation should be determined. Because these noncoding RNAs are expressed in pluripotent stem cells (Zhao et al. 2010, Kaneko et al. 2014), they may be required to specify a cell lineage. As shown in Chapter 3, overexpression of miR-495 was able to partially rescue the MEF2A-deficient phenotype and led to an increase in sarcomeric gene expression and a decrease in apoptosis. To determine the role of this locus in cardiomyocyte differentiation, it should be knocked down in embryonic stem (ES) cells. We can then induce cardiomyocyte differentiation and examine any changes in cardiogenic populations *in vitro*. Together, these data will indicate whether the *Gtl2-Dio3* noncoding RNA locus is required for cardiomyocyte differentiation and proliferation.

5.2.2 Induce Adult Cardiomyocyte Proliferation by Overexpressing *Gtl2-Dio3* miRNAs

In Chapter 3, I demonstrated that overexpressing miR-410 and miR-495 in neonatal cardiomyocytes induced proliferation. In order for this data to be relevant to human disease, it would be worthwhile to overexpress these miRNAs in older cardiomyocytes to see if proliferation is still able to be induced. Recently, one study demonstrated a slight increase in proliferation of adult rat cardiomyocytes *in vitro* upon overexpression of miR-495 (Pandey and Ahmed 2015). However, this data was only shown in a table and no additional characterization was performed.

In order to demonstrate that overexpression of miR-410 and miR-495 promotes cardiomyocyte proliferation in adult cardiomyocytes, miRNA mimics should be transfected into cardiomyocytes harvested from 7 day old rats as well as 8 week old rats. Based on the knowledge that the neonatal heart exits the cell cycle within one week (Porrello et al. 2011), it would be interesting to see whether there was a difference in the ability to promote proliferation at these two time points. BrdU, EdU, Aurora B kinase, and/or phospho histone H3 immunostaining should be performed to verify an increase in cardiomyocyte proliferation.

Furthermore, these miRNAs should be overexpressed in neonatal and adult hearts *in vivo*. Adenoviral associated vectors (AAVs), specifically AAV9 for cardiac expression, would need to be generated for these miRNAs to be directly injected into hearts of neonatal and adult mice. I have already generated adenoviral vectors containing miR-410, miR-495, and miR-433 (data not shown). These would have to be cloned into the appropriate AAV

plasmid and purified according to the proper protocols but this could easily be accomplished using our current knowledge of adenoviral viruses and use of the reagents required.

Lastly, a transgenic mouse overexpressing miR-410 and/or miR-495 in the heart could be generated to provide even more information. To do this, the αMHC promoter should be used because it is expressed specifically in cardiomyocytes throughout development and postnatally. Together, these studies would indicate whether these *Gtl2-Dio3* miRNAs are capable of promoting cardiomyocyte proliferation in adult hearts.

5.2.3   Determine the Role of the *Gtl2-Dio3* miRNAs in Cardiac Injury

It is intriguing that the *Gtl2-Dio3* miRNAs are upregulated in multiple models of cardiomyopathy as shown in Chapter 4. This is interesting because based on the data from Chapter 3, we would expect that overexpression of these miRNAs would have a positive effect, such as increased proliferation, on injured hearts. The misexpression of these miRNAs in injured hearts could mean a few different things. First, they could be upregulated in response to the cardiac stress of injury like many other fetal gene programs. Because we know these miRNAs are highly expressed in the neonatal heart, they may also be required for embryonic development. Information from Section 5.2.1 could verify that these miRNAs are part of a fetal gene program required for cardiomyocyte proliferation and development. If this is the case, the fact that they are upregulated post-injury in the adult heart indicates that they are upregulated in response to the injury but that their ability to induce proliferation is somehow blocked, perhaps by counter-regulatory mechanisms such as an increase in cell cycle inhibitor expression. Determining other molecular

pathways regulated by these miRNAs may uncover other therapeutic options for treating cardiac disease.

Second, the *Gtl2-Dio3* miRNAs may be regulating different downstream pathways in response to injury compared to their effect on proliferation in neonatal cardiomyocytes. To help identify the possible molecular pathways involved, a microarray or RNA sequencing (RNA-seq) should be performed to identify dysregulated genes when knocking down these miRNAs *in vitro* and inducing hypertrophy, as in Chapter 4. Because knockdown of these miRNAs resulted in a reduced hypertrophic response, candidate genes that are upregulated on the microarray may indicate new hypertrophic signaling pathways that can be altered to reduce hypertrophy. These candidate genes should be verified using qRT-PCR and their pathways should be confirmed using techniques such as target prediction algorithms and pMIR-REPORT luciferase reporter assays to confirm direct targeting by these miRNAs, as described in Chapter 3.

Finally, the information gathered from this *in vitro* analysis can be applied to an *in vivo* cardiac injury model. It would be interesting to determine whether knockdown of these *Gtl2-Dio3* miRNAs post-injury is able to reduce infarct size after myocardial infarction. To test this, miRNAs can be injected immediately after LAD coronary artery ligation in the myocardial infarction mouse model. The infarct can then be analyzed by histological and functional analyses. The size of the infarct should be quantified using histological methods as well as Mason's trichrome staining, which indicates accumulation of fibrosis. Furthermore, electrocardiogram analysis of cardiac function should be performed to determine if function improves by knocking down these miRNAs.

Together, these studies will tell us whether the *Gtl2-Dio3* miRNAs are required for embryonic cardiomyocyte proliferation and development and whether these miRNAs regulate different pathways in the adult heart and in response to cardiac stress and injury. Elucidating the molecular mechanisms that the *Gtl2-Dio3* miRNAs regulate may provide important insight into new therapeutic targets to improve cardiac function post-injury.
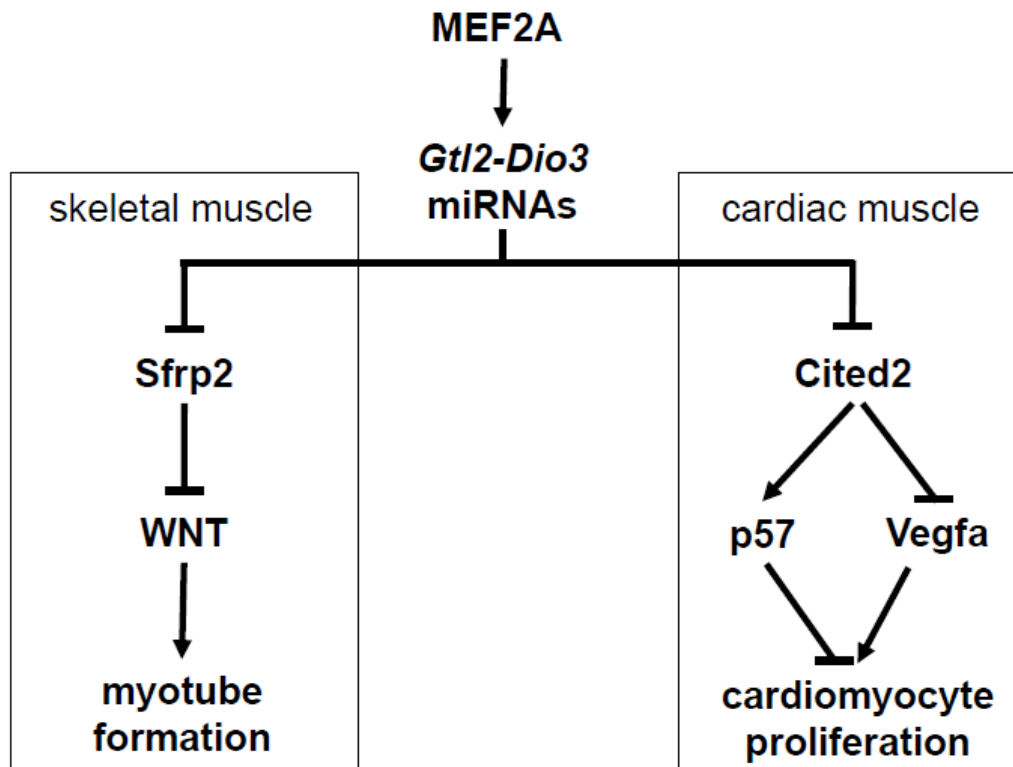
Figure 5.1 Model for MEF2A-regulated *Gtl2-Dio3* miRNAs in skeletal and cardiac muscle. MEF2A regulates the *Gtl2-Dio3* miRNAs in skeletal and cardiac muscle. In skeletal muscle, a subset of the *Gtl2-Dio3* miRNAs target Sfrp2, a WNT inhibitor, to modulate WNT signaling in skeletal muscle regeneration. In cardiac muscle, a subset of the *Gtl2-Dio3* miRNAs target Cited2, a transcriptional co-activator, leading to an increase in cardiomyocyte proliferation.
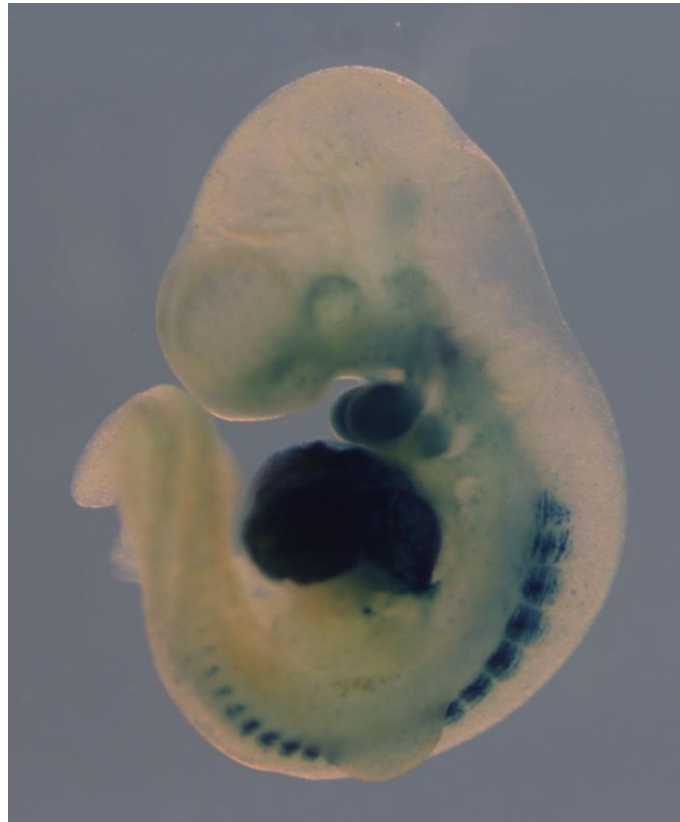
Figure 5.2 *Gtl2-LacZ* enhancer activity at E11.5. Preliminary data indicating Gtl2 activity in the somites and heart.

LIST OF JOURNAL ABBREVIATIONS

Am Heart J	American Heart Journal
Am J Human Genet	American Journal of Human Genetics
Am J Pathol	American Journal of Pathology
Am J Physiol Lung Cell Mol Physiol	American Journal of Physiology Lung Cellular and Molecular Physiology
Anat Embryol	Anatomy and Embryology
Annu Rev Cell Dev Biol	Annual Review of Cell and Developmental Biology
Arch Toxicol	Archives of Toxicology
Biochem Biophys Res Commun	Biochemical and Biophysical Research Communications
Biochim Biophys Acta	Biochimica et Biophysica Acta
BMC Genomics	BioMed Central Genomics
Br J Cancer	British Journal of Cancer
Brain Res	Brain Research
Cardiol	Cardiology
Cardiovasc Pathol	Cardiovascular Pathology
Cardiovasc Regen Med	Cardiovascular Regenerative Medicine
Cardiovasc Res	Cardiovascular Research
Cell Death Diff	Cell Death and Differentiation
Cell Growth Diff	Cell Growth and Differentiation
Cell Mol Life Sci	Cellular and Molecular Life Sciences

Cell Rep	Cell Reports
Circ Heart Fail	Circulation: Heart Failure
Circ Res	Circulation Research
Clin Chem	Clinical Chemistry
Clin Sci (Lond)	Clinical Sciences (London, England)
Curr Biol	Current Biology
Curr Hypertens Rep	Current Hypertension Reports
Curr Opin Nephrol Hypertens	Current Opinion in Nephrology and Hypertension
Dev Biol	Developmental Biology
Dis Model Mech	Disease Models & Mechanisms
EMBO J	EMBO Journal
Eur Heart J	European Heart Journal
Exp Cell Res	Experimental Cell Research
FEBS J	Federation of European Biochemical Societies Journal
FEBS Lett	Federation of European Biochemical Societies Letters
Front Endocrinol	Frontiers in Endocrinology
Gene Ther	Gene Therapy
Genes Dev	Genes and Development
Genes Dis	Genes and Diseases
Genome Biol	Genome Biology

Genome Res	Genome Research
Gynecol Oncol	Gynecologic Oncology
Heart Lung Circ	Heart, Lung & Circulation
Histol Histopathol	Histology and Histopathology
Hum Mol Genet	Human Molecular Genetics
Hum Metat	Human Mutation
Hypertens Res	Hypertension Research
Indian J Med Res	Indian Journal of Medical Research
Int J Biochem Cell Biol	International Journal of Biochemistry and Cell Biology
Int J Mol Sci	International Journal of Molecular Sciences
Int J Oncol	International Journal of Oncology
J Biochem	Journal of Biochemistry
J Biol Chem	Journal of Biological Chemistry
J Biomed Sci	Journal of Biomedical Science
J Cardiovasc Magn Reson	Journal of Cardiovascular Magnetic Resonance
J Cell Sci	Journal of Cell Science
J Clin Endocrinol Metab	Journal of Clinical Endocrinology and Metabolism
J Clin Invest	Journal of Clinical Investigation
J Control Release	Journal of Controlled Release
J Exp Med	Journal of Experimental Medicine
J Exp Zool	Journal of Experimental Zoology

J Mol Biol	Journal of Molecular Biology
J Mol Cell Cardiol	Journal of Molecular and Cellular Cardiology
J Mol Hist	Journal of Molecular Histology
J Surg Res	Journal of Surgical Research
J Thorac Dis	Journal of Thoracic Disease
Lab Invest	Laboratory Investigation
Mamm Genome	Mammalian Genome
Mech Dev	Mechanisms of Development
Mol Biol Evol	Molecular Biology and Evolution
Mol Cancer	Molecular Cancer
Mol Cancer Res	Molecular Cancer Research
Mol Cell	Molecular Cell
Mol Cell Biochem	Molecular and Cellular Biochemistry
Mol Cell Biol	Molecular and Cellular Biology
Nat Genet	Nature Genetics
Nat Med	Nature Medicine
Nat Rev Cardiol	Nature Reviews: Cardiology
Nat Rev Drug Discov	Nature Reviews: Drug Discovery
Nat Rev Genet	Nature Reviews: Genetics
Nat Rev Mol Cell Biol	Nature Reviews: Molecular Cell Biology
N Engl J Med	New England Journal of Medicine
Nucleic Acids Res	Nucleic Acids Research

Pharmacol Rev	Pharmacological Reviews
Physiol Genomics	Physiological Genomics
Physiol Rev	Physiological Reviews
PLoS One	Public Library of Science One
Proc Nat Acad Sci U.S.A.	Proceedings of the National Academy of Sciences of the United States of America
Recent Prog Horm Res	Recent Progress in Hormone Research
Sci China Life Sci	Science China Life Sciences
Sci Transl Med	Science Translational Medicine
Semin Cell Dev Biol	Seminars in Cell and Developmental Biology
Thromb Res	Thrombosis Research
Tohoku J Exp Med	Tohoku Journal of Experimental Medicine
Transl Res	Translational Research
Trends Biochem Sci	Trends in Biochemical Sciences
Trends Genet	Trends in Genetics
Tumour Biol	Tumour Biology
World J Surg Oncol	World Journal of Surgical Oncology
Zhonghua Er Ke Za Zhi	Chinese Journal of Pediatrics

REFERENCES

Advani, A. (2014). "Vascular endothelial growth factor and the kidney: something of the marvellous." <u>Curr Opin Nephrol Hypertens</u> **23**(1): 87-92.

Ahuja, P., P. Sdek and W. R. MacLellan (2007). "Cardiac myocyte cell cycle control in development, disease, and regeneration." <u>Physiol Rev</u> **87**(2): 521-544.

Andersen, D. C., J. Laborda, V. Baladron, M. Kassem, S. P. Sheikh and C. H. Jensen (2013). "Dual role of delta-like 1 homolog (DLK1) in skeletal muscle development and adult muscle regeneration." <u>Development</u> **140**(18): 3743-3753.

Araki, S., Y. Izumiya, S. Hanatani, T. Rokutanda, H. Usuku, Y. Akasaki, T. Takeo, N. Nakagata, K. Walsh and H. Ogawa (2012). "Akt1-mediated skeletal muscle growth attenuates cardiac dysfunction and remodeling after experimental myocardial infarction." <u>Circ Heart Fail</u> **5**(1): 116-125.

Avrahami, D., C. Li, M. Yu, Y. Jiao, J. Zhang, A. Naji, S. Ziaie, B. Glaser and K. H. Kaestner (2014). "Targeting the cell cycle inhibitor p57Kip2 promotes adult human beta cell replication." <u>J Clin Invest</u> **124**(2): 670-674.

Awada, H. K., N. R. Johnson and Y. Wang (2015). "Sequential delivery of angiogenic growth factors improves revascularization and heart function after myocardial infarction." <u>J Control Release</u> **207**: 7-17.

Bamforth, S. D., J. Braganca, J. J. Eloranta, J. N. Murdoch, F. I. Marques, K. R. Kranc, H. Farza, D. J. Henderson, H. C. Hurst and S. Bhattacharya (2001). "Cardiac malformations, adrenal agenesis, neural crest defects and exencephaly in mice lacking Cited2, a new Tfap2 co-activator." <u>Nat Genet</u> **29**(4): 469-474.

Bamforth, S. D., J. Braganca, C. R. Farthing, J. E. Schneider, C. Broadbent, A. C. Michell, K. Clarke, S. Neubauer, D. Norris, N. A. Brown, R. H. Anderson and S. Bhattacharya (2004). "Cited2 controls left-right patterning and heart development through a Nodal-Pitx2c pathway." <u>Nat Genet</u> **36**(11): 1189-1196.

Bandres, E., E. Cubedo, X. Agirre, R. Malumbres, R. Zarate, N. Ramirez, A. Abajo, A. Navarro, I. Moreno, M. Monzo and J. Garcia-Foncillas (2006). "Identification by Real-time PCR of 13 mature microRNAs differentially expressed in colorectal cancer and non-tumoral tissues." <u>Mol Cancer</u> **5**: 29.

Bartel, D. P. (2009). "MicroRNAs: target recognition and regulatory functions." <u>Cell</u> **136**(2): 215-233.

Benetatos, L., E. Hatzimichael, E. Londin, G. Vartholomatos, P. Loher, I. Rigoutsos and E. Briasoulis (2013). "The microRNAs within the DLK1-DIO3 genomic region: involvement in disease pathogenesis." Cell Mol Life Sci **70**(5): 795-814.

Bergmann, O., R. D. Bhardwaj, S. Bernard, S. Zdunek, F. Barnabe-Heider, S. Walsh, J. Zupicich, K. Alkass, B. A. Buchholz, H. Druid, S. Jovinge and J. Frisen (2009). "Evidence for cardiomyocyte renewal in humans." Science **324**(5923): 98-102.

Bergmann, O., S. Zdunek, J. Frisen, S. Bernard, H. Druid and S. Jovinge (2012). "Cardiomyocyte renewal in humans." Circ Res **110**(1): e17-18; author reply e19-21.

Bernardo, B. C., F. J. Charchar, R. C. Lin and J. R. McMullen (2012). "A microRNA guide for clinicians and basic scientists: background and experimental techniques." Heart Lung Circ **21**(3): 131-142.

Bernstein, E., S. Y. Kim, M. A. Carmell, E. P. Murchison, H. Alcorn, M. Z. Li, A. A. Mills, S. J. Elledge, K. V. Anderson and G. J. Hannon (2003). "Dicer is essential for mouse development." Nat Genet **35**(3): 215-217.

Betel, D., A. Koppal, P. Agius, C. Sander and C. Leslie (2010). "Comprehensive modeling of microRNA targets predicts functional non-conserved and non-canonical sites." Genome Biol **11**(8): R90.

Black, B. L. (2007). "Transcriptional pathways in second heart field development." Semin Cell Dev Biol **18**(1): 67-76.

Black, B. L. and E. N. Olson (1998). "Transcriptional control of muscle development by myocyte enhancer factor-2 (MEF2) proteins." Annu Rev Cell Dev Biol **14**: 167-196.

Braganca, J., J. J. Eloranta, S. D. Bamforth, J. C. Ibbitt, H. C. Hurst and S. Bhattacharya (2003). "Physical and functional interactions among AP-2 transcription factors, p300/CREB-binding protein, and CITED2." J Biol Chem **278**(18): 16021-16029.

Braun, T. and M. Gautel (2011). "Transcriptional mechanisms regulating skeletal muscle differentiation, growth and homeostasis." Nat Rev Mol Cell Biol **12**(6): 349-361.

Breitbart, R. E., C. S. Liang, L. B. Smoot, D. A. Laheru, V. Mahdavi and B. Nadal-Ginard (1993). "A fourth human MEF2 transcription factor, hMEF2D, is an early marker of the myogenic lineage." Development **118**(4): 1095-1106.

Brewer, S., X. Jiang, S. Donaldson, T. Williams and H. M. Sucov (2002). "Requirement for AP-2alpha in cardiac outflow tract morphogenesis." Mech Dev **110**(1-2): 139-149.

Brooks, G., R. A. Poolman and J. M. Li (1998). "Arresting developments in the cardiac myocyte cell cycle: role of cyclin-dependent kinase inhibitors." <u>Cardiovasc Res</u> **39**(2): 301-311.

Brown, K. R., K. M. England, K. L. Goss, J. M. Snyder and M. J. Acarregui (2001). "VEGF induces airway epithelial cell proliferation in human fetal lung in vitro." <u>Am J Physiol Lung Cell Mol Physiol</u> **281**(4): L1001-1010.

Bruneau, B. G. (2008). "The developmental genetics of congenital heart disease." <u>Nature</u> **451**(7181): 943-948.

Buckingham, M., S. Meilhac and S. Zaffran (2005). "Building the mammalian heart from two sources of myocardial cells." <u>Nat Rev Genet</u> **6**(11): 826-835.

Callis, T. E., K. Pandya, H. Y. Seok, R. H. Tang, M. Tatsuguchi, Z. P. Huang, J. F. Chen, Z. Deng, B. Gunn, J. Shumate, M. S. Willis, C. H. Selzman and D. Z. Wang (2009). "MicroRNA-208a is a regulator of cardiac hypertrophy and conduction in mice." <u>J Clin Invest</u> **119**(9): 2772-2786.

Cao, X., J. Wang, Z. Wang, J. Du, X. Yuan, W. Huang, J. Meng, H. Gu, Y. Nie, B. Ji, S. Hu and Z. Zheng (2013). "MicroRNA profiling during rat ventricular maturation: A role for miR-29a in regulating cardiomyocyte cell cycle re-entry." <u>FEBS Lett</u> **587**(10): 1548-1555.

Carboni, N., G. Marrosu, M. Porcu, A. Mateddu, E. Solla, E. Cocco, M. A. Maioli, V. Oppo, R. Piras and M. G. Marrosu (2011). "Dilated cardiomyopathy with conduction defects in a patient with partial merosin deficiency due to mutations in the laminin-alpha2-chain gene: a chance association or a novel phenotype?" <u>Muscle Nerve</u> **44**(5): 826-828.

Cavaille, J., H. Seitz, M. Paulsen, A. C. Ferguson-Smith and J. P. Bachellerie (2002). "Identification of tandemly-repeated C/D snoRNA genes at the imprinted human 14q32 domain reminiscent of those at the Prader-Willi/Angelman syndrome region." <u>Hum Mol Genet</u> **11**(13): 1527-1538.

Chambers, A. E., S. Kotecha, N. Towers and T. J. Mohun (1992). "Muscle-specific expression of SRF-related genes in the early embryo of Xenopus laevis." <u>EMBO J</u> **11**(13): 4981-4991.

Charlier, C., K. Segers, D. Wagenaar, L. Karim, S. Berghmans, O. Jaillon, T. Shay, J. Weissenbach, N. Cockett, G. Gyapay and M. Georges (2001). "Human-ovine comparative sequencing of a 250-kb imprinted domain encompassing the callipyge (clpg) locus and identification of six imprinted transcripts: DLK1, DAT, GTL2, PEG11, antiPEG11, and MEG8." <u>Genome Res</u> **11**(5): 850-862.

Chen, C., D. A. Ridzon, A. J. Broomer, Z. Zhou, D. H. Lee, J. T. Nguyen, M. Barbisin, N. L. Xu, V. R. Mahuvakar, M. R. Andersen, K. Q. Lao, K. J. Livak and K. J. Guegler (2005). "Real-time quantification of microRNAs by stem-loop RT-PCR." Nucleic Acids Res **33**(20): e179.

Chen, J., Z. P. Huang, H. Y. Seok, J. Ding, M. Kataoka, Z. Zhang, X. Hu, G. Wang, Z. Lin, S. Wang, W. T. Pu, R. Liao and D. Z. Wang (2013). "mir-17-92 cluster is required for and sufficient to induce cardiomyocyte proliferation in postnatal and adult hearts." Circ Res **112**(12): 1557-1566.

Chen, J. F., T. E. Callis and D. Z. Wang (2009). "microRNAs and muscle disorders." J Cell Sci **122**(Pt 1): 13-20.

Chen, J. F., E. M. Mandel, J. M. Thomson, Q. Wu, T. E. Callis, S. M. Hammond, F. L. Conlon and D. Z. Wang (2006). "The role of microRNA-1 and microRNA-133 in skeletal muscle proliferation and differentiation." Nat Genet **38**(2): 228-233.

Chen, J. F., E. P. Murchison, R. Tang, T. E. Callis, M. Tatsuguchi, Z. Deng, M. Rojas, S. M. Hammond, M. D. Schneider, C. H. Selzman, G. Meissner, C. Patterson, G. J. Hannon and D. Z. Wang (2008). "Targeted deletion of Dicer in the heart leads to dilated cardiomyopathy and heart failure." Proc Natl Acad Sci U S A **105**(6): 2111-2116.

Chen, L., J. Zhang, Y. Feng, R. Li, X. Sun, W. Du, X. Piao, H. Wang, D. Yang, Y. Sun, X. Li, T. Jiang, C. Kang, Y. Li and C. Jiang (2012). "MiR-410 regulates MET to influence the proliferation and invasion of glioma." Int J Biochem Cell Biol **44**(11): 1711-1717.

Chen, S. M., H. C. Chen, S. J. Chen, C. Y. Huang, P. Y. Chen, T. W. Wu, L. Y. Feng, H. C. Tsai, T. N. Lui, C. Hsueh and K. C. Wei (2013). "MicroRNA-495 inhibits proliferation of glioblastoma multiforme cells by downregulating cyclin-dependent kinase 6." World J Surg Oncol **11**: 87.

Chu, H., X. Chen, H. Wang, Y. Du, Y. Wang, W. Zang, P. Li, J. Li, J. Chang, G. Zhao and G. Zhang (2014). "MiR-495 regulates proliferation and migration in NSCLC by targeting MTA3." Tumour Biol **35**(4): 3487-3494.

Clark, A. L. and F. J. Naya (2015). "MicroRNAs in the Myocyte Enhancer Factor 2 (MEF2)-regulated Gtl2-Dio3 Noncoding RNA Locus Promote Cardiomyocyte Proliferation by Targeting the Transcriptional Coactivator Cited2." J Biol Chem **290**(38): 23162-23172.

da Rocha, S. T., C. A. Edwards, M. Ito, T. Ogata and A. C. Ferguson-Smith (2008). "Genomic imprinting at the mammalian Dlk1-Dio3 domain." Trends Genet **24**(6): 306-316.

Das, P. P., D. A. Hendrix, E. Apostolou, A. H. Buchner, M. C. Canver, S. Beyaz, D. Ljuboja, R. Kuintzle, W. Kim, R. Karnik, Z. Shao, H. Xie, J. Xu, A. De Los Angeles, Y. Zhang, J. Choe, D. L. Jun, X. Shen, R. I. Gregory, G. Q. Daley, A. Meissner, M. Kellis, K. Hochedlinger, J. Kim and S. H. Orkin (2015). "PRC2 Is Required to Maintain Expression of the Maternal Gtl2-Rian-Mirg Locus by Preventing De Novo DNA Methylation in Mouse Embryonic Stem Cells." Cell Rep **12**(9): 1456-1470.

Delli Carpini, J., A. K. Karam and L. Montgomery (2010). "Vascular endothelial growth factor and its relationship to the prognosis and treatment of breast, ovarian, and cervical cancer." Angiogenesis **13**(1): 43-58.

Dichoso, D., T. Brodigan, K. Y. Chwoe, J. S. Lee, R. Llacer, M. Park, A. K. Corsi, S. A. Kostas, A. Fire, J. Ahnn and M. Krause (2000). "The MADS-Box factor CeMEF2 is not essential for Caenorhabditis elegans myogenesis and development." Dev Biol **223**(2): 431-440.

Dodou, E. and R. Treisman (1997). "The Saccharomyces cerevisiae MADS-box transcription factor Rlm1 is a target for the Mpk1 mitogen-activated protein kinase pathway." Mol Cell Biol **17**(4): 1848-1859.

Dong, S., Y. Cheng, J. Yang, J. Li, X. Liu, X. Wang, D. Wang, T. J. Krall, E. S. Delphin and C. Zhang (2009). "MicroRNA expression signature and the role of microRNA-21 in the early phase of acute myocardial infarction." J Biol Chem **284**(43): 29514-29525.

Doppler, S. A., M. A. Deutsch, R. Lange and M. Krane (2013). "Cardiac regeneration: current therapies-future concepts." J Thorac Dis **5**(5): 683-697.

Du, J., Y. Chen, Q. Li, X. Han, C. Cheng, Z. Wang, D. Danielpour, S. L. Dunwoodie, K. D. Bunting and Y. C. Yang (2012). "HIF-1alpha deletion partially rescues defects of hematopoietic stem cell quiescence caused by Cited2 deficiency." Blood **119**(12): 2789-2798.

Du, J. and Y. C. Yang (2012). "HIF-1 and its antagonist Cited2: regulators of HSC quiescence." Cell Cycle **11**(13): 2413-2414.

Duan, D. (2006). "Challenges and opportunities in dystrophin-deficient cardiomyopathy gene therapy." Hum Mol Genet **15 Spec No 2**: R253-261.

Dunwoodie, S. L., T. A. Rodriguez and R. S. Beddington (1998). "Msg1 and Mrg1, founding members of a gene family, show distinct patterns of gene expression during mouse embryogenesis." Mech Dev **72**(1-2): 27-40.

Edelhoff, S., C. E. Grubin, A. E. Karlsen, D. A. Alder, D. Foster, C. M. Disteche and A. Lernmark (1993). "Mapping of glutamic acid decarboxylase (GAD) genes." Genomics **17**(1): 93-97.

Estrella, N. L., C. A. Desjardins, S. E. Nocco, A. L. Clark, Y. Maksimenko and F. J. Naya (2015). "MEF2 transcription factors regulate distinct gene programs in mammalian skeletal muscle differentiation." J Biol Chem **290**(2): 1256-1268.

Estrella, N. L. and F. J. Naya (2014). "Transcriptional networks regulating the costamere, sarcomere, and other cytoskeletal structures in striated muscle." Cell Mol Life Sci **71**(9): 1641-1656.

Eulalio, A., M. Mano, M. Dal Ferro, L. Zentilin, G. Sinagra, S. Zacchigna and M. Giacca (2012). "Functional screening identifies miRNAs inducing cardiac regeneration." Nature **492**(7429): 376-381.

Ewen, E. P., C. M. Snyder, M. Wilson, D. Desjardins and F. J. Naya (2011). "The Mef2A transcription factor coordinately regulates a costamere gene program in cardiac muscle." J Biol Chem **286**(34): 29644-29653.

Feng, T., J. Dzieran, X. Gu, S. Marhenke, A. Vogel, K. Machida, T. S. Weiss, P. Ruemmele, O. Kollmar, P. Hoffmann, F. Grasser, H. Allgayer, J. Fabian, H. L. Weng, A. Teufel, T. Maass, C. Meyer, U. Lehmann, C. Zhu, P. R. Mertens, C. F. Gao, S. Dooley and N. M. Meindl-Beinker (2015). "Smad7 regulates compensatory hepatocyte proliferation in damaged mouse liver and positively relates to better clinical outcome in human hepatocellular carcinoma." Clin Sci (Lond) **128**(11): 761-774.

Ferrarini, M., N. Arsic, F. A. Recchia, L. Zentilin, S. Zacchigna, X. Xu, A. Linke, M. Giacca and T. H. Hintze (2006). "Adeno-associated virus-mediated transduction of VEGF165 improves cardiac tissue viability and functional recovery after permanent coronary occlusion in conscious dogs." Circ Res **98**(7): 954-961.

Finsterer, J. and L. Cripe (2014). "Treatment of dystrophin cardiomyopathies." Nat Rev Cardiol **11**(3): 168-179.

Fiore, R., S. Khudayberdiev, M. Christensen, G. Siegel, S. W. Flavell, T. K. Kim, M. E. Greenberg and G. Schratt (2009). "Mef2-mediated transcription of the miR379-410 cluster regulates activity-dependent dendritogenesis by fine-tuning Pumilio2 protein levels." EMBO J **28**(6): 697-710.

Fiorentino, L., C. Pertica, M. Fiorini, C. Talora, M. Crescenzi, L. Castellani, S. Alema, P. Benedetti and O. Segatto (2000). "Inhibition of ErbB-2 mitogenic and transforming activity by RALT, a mitogen-induced signal transducer which binds to the ErbB-2 kinase domain." Mol Cell Biol **20**(20): 7735-7750.

Flink, I. L. (2002). "Cell cycle reentry of ventricular and atrial cardiomyocytes and cells within the epicardium following amputation of the ventricular apex in the axolotl, Amblystoma mexicanum: confocal microscopic immunofluorescent image analysis of bromodeoxyuridine-labeled nuclei." Anat Embryol (Berl) **205**(3): 235-244.

Gilbert, S. F. (2006). <u>Developmental Biology</u>, Sinauer Associates Inc.

Glazov, E. A., S. McWilliam, W. C. Barris and B. P. Dalrymple (2008). "Origin, evolution, and biological role of miRNA cluster in DLK-DIO3 genomic region in placental mammals." <u>Mol Biol Evol</u> **25**(5): 939-948.

Gossett, L. A., D. J. Kelvin, E. A. Sternberg and E. N. Olson (1989). "A new myocyte-specific enhancer-binding factor that recognizes a conserved element associated with multiple muscle-specific genes." <u>Mol Cell Biol</u> **9**(11): 5022-5033.

Gray, M. O., C. S. Long, J. E. Kalinyak, H. T. Li and J. S. Karliner (1998). "Angiotensin II stimulates cardiac myocyte hypertrophy via paracrine release of TGF-beta 1 and endothelin-1 from fibroblasts." <u>Cardiovasc Res</u> **40**(2): 352-363.

Gunthorpe, D., K. E. Beatty and M. V. Taylor (1999). "Different levels, but not different isoforms, of the Drosophila transcription factor DMEF2 affect distinct aspects of muscle differentiation." <u>Dev Biol</u> **215**(1): 130-145.

Guo, J., J. Cai, L. Yu, H. Tang, C. Chen and Z. Wang (2011). "EZH2 regulates expression of p57 and contributes to progression of ovarian cancer in vitro and in vivo." <u>Cancer Sci</u> **102**(3): 530-539.

Hagan, J. P., B. L. O'Neill, C. L. Stewart, S. V. Kozlov and C. M. Croce (2009). "At least ten genes define the imprinted Dlk1-Dio3 cluster on mouse chromosome 12qF1." <u>PLoS One</u> **4**(2): e4352.

Han, Z., H. He, F. Zhang, Z. Huang, Z. Liu, H. Jiang and Q. Wu (2012). "Spatiotemporal expression pattern of Mirg, an imprinted non-coding gene, during mouse embryogenesis." <u>J Mol Histol</u> **43**(1): 1-8.

Harvey, R. P. (2002). "Patterning the vertebrate heart." <u>Nat Rev Genet</u> **3**(7): 544-556.

Hashimoto, Y., Y. Akiyama and Y. Yuasa (2013). "Multiple-to-multiple relationships between microRNAs and target genes in gastric cancer." <u>PLoS One</u> **8**(5): e62589.

He, L. and G. J. Hannon (2004). "MicroRNAs: small RNAs with a big role in gene regulation." <u>Nat Rev Genet</u> **5**(7): 522-531.

Hierlihy, A. M., P. Seale, C. G. Lobe, M. A. Rudnicki and L. A. Megeney (2002). "The post-natal heart contains a myocardial stem cell population." <u>FEBS Lett</u> **530**(1-3): 239-243.

Hwang-Verslues, W. W., P. H. Chang, P. C. Wei, C. Y. Yang, C. K. Huang, W. H. Kuo, J. Y. Shew, K. J. Chang, E. Y. Lee and W. H. Lee (2011). "miR-495 is upregulated by E12/E47 in breast cancer stem cells, and promotes oncogenesis and hypoxia resistance via downregulation of E-cadherin and REDD1." Oncogene **30**(21): 2463-2474.

Iida, K., K. Hidaka, M. Takeuchi, M. Nakayama, C. Yutani, T. Mukai and T. Morisaki (1999). "Expression of MEF2 genes during human cardiac development." Tohoku J Exp Med **187**(1): 15-23.

Ikeda, S., S. W. Kong, J. Lu, E. Bisping, H. Zhang, P. D. Allen, T. R. Golub, B. Pieske and W. T. Pu (2007). "Altered microRNA expression in human heart disease." Physiol Genomics **31**(3): 367-373.

Iyer, N. V., L. E. Kotch, F. Agani, S. W. Leung, E. Laughner, R. H. Wenger, M. Gassmann, J. D. Gearhart, A. M. Lawler, A. Y. Yu and G. L. Semenza (1998). "Cellular and developmental control of O2 homeostasis by hypoxia-inducible factor 1 alpha." Genes Dev **12**(2): 149-162.

Janssen, H. L., H. W. Reesink, E. J. Lawitz, S. Zeuzem, M. Rodriguez-Torres, K. Patel, A. J. van der Meer, A. K. Patick, A. Chen, Y. Zhou, R. Persson, B. D. King, S. Kauppinen, A. A. Levin and M. R. Hodges (2013). "Treatment of HCV infection by targeting microRNA." N Engl J Med **368**(18): 1685-1694.

Janssen, R., M. Zuidwijk, A. Muller, J. Mulders, C. B. Oudejans and W. S. Simonides (2013). "Cardiac expression of deiodinase type 3 (Dio3) following myocardial infarction is associated with the induction of a pluripotency microRNA signature from the Dlk1-Dio3 genomic region." Endocrinology **154**(6): 1973-1978.

Jeanson-Leh, L., J. Lameth, S. Krimi, J. Buisset, F. Amor, C. Le Guiner, I. Barthelemy, L. Servais, S. Blot, T. Voit and D. Israeli (2014). "Serum profiling identifies novel muscle miRNA and cardiomyopathy-related miRNA biomarkers in Golden Retriever muscular dystrophy dogs and Duchenne muscular dystrophy patients." Am J Pathol **184**(11): 2885-2898.

Jonckheere, N., V. Fauquette, L. Stechly, N. Saint-Laurent, S. Aubert, C. Susini, G. Huet, N. Porchet, I. Van Seuningen and P. Pigny (2009). "Tumour growth and resistance to gemcitabine of pancreatic cancer cells are decreased by AP-2alpha overexpression." Br J Cancer **101**(4): 637-644.

Jopling, C., E. Sleep, M. Raya, M. Marti, A. Raya and J. C. Izpisua Belmonte (2010). "Zebrafish heart regeneration occurs by cardiomyocyte dedifferentiation and proliferation." Nature **464**(7288): 606-609.

Jopling, C., G. Sune, A. Faucherre, C. Fabregat and J. C. Izpisua Belmonte (2012). "Hypoxia induces myocardial regeneration in zebrafish." Circulation **126**(25): 3017-3027.

Kampen, K. R., A. Ter Elst and E. S. de Bont (2013). "Vascular endothelial growth factor signaling in acute myeloid leukemia." Cell Mol Life Sci **70**(8): 1307-1317.

Kaneko, S., R. Bonasio, R. Saldana-Meyer, T. Yoshida, J. Son, K. Nishino, A. Umezawa and D. Reinberg (2014). "Interactions between JARID2 and noncoding RNAs regulate PRC2 recruitment to chromatin." Mol Cell **53**(2): 290-300.

Kikuchi, K., J. E. Holdway, A. A. Werdich, R. M. Anderson, Y. Fang, G. F. Egnaczyk, T. Evans, C. A. Macrae, D. Y. Stainier and K. D. Poss (2010). "Primary contribution to zebrafish heart regeneration by gata4(+) cardiomyocytes." Nature **464**(7288): 601-605.

Kim, S. and H. Iwao (2000). "Molecular and cellular mechanisms of angiotensin II-mediated cardiovascular and renal diseases." Pharmacol Rev **52**(1): 11-34.

Kim, Y., D. Phan, E. van Rooij, D. Z. Wang, J. McAnally, X. Qi, J. A. Richardson, J. A. Hill, R. Bassel-Duby and E. N. Olson (2008). "The MEF2D transcription factor mediates stress-dependent cardiac remodeling in mice." J Clin Invest **118**(1): 124-132.

Kircher, M., C. Bock and M. Paulsen (2008). "Structural conservation versus functional divergence of maternally expressed microRNAs in the Dlk1/Gtl2 imprinting region." BMC Genomics **9**: 346.

Kobayashi, Y., T. Nakayama, N. Sato, Y. Izumi, S. Kokubun and M. Soma (2005). "Haplotype-based case-control study revealing an association between the adrenomedullin gene and proteinuria in subjects with essential hypertension." Hypertens Res **28**(3): 229-236.

Kuang, W., H. Xu, J. T. Vilquin and E. Engvall (1999). "Activation of the lama2 gene in muscle regeneration: abortive regeneration in laminin alpha2-deficiency." Lab Invest **79**(12): 1601-1613.

Laborda, J. (2000). "The role of the epidermal growth factor-like protein dlk in cell differentiation." Histol Histopathol **15**(1): 119-129.

Lee, Y., C. Ahn, J. Han, H. Choi, J. Kim, J. Yim, J. Lee, P. Provost, O. Radmark, S. Kim and V. N. Kim (2003). "The nuclear RNase III Drosha initiates microRNA processing." Nature **425**(6956): 415-419.

Lee, Y., K. Jeon, J. T. Lee, S. Kim and V. N. Kim (2002). "MicroRNA maturation: stepwise processing and subcellular localization." EMBO J **21**(17): 4663-4670.

Li, F., X. Wang, J. M. Capasso and A. M. Gerdes (1996). "Rapid transition of cardiac myocytes from hyperplasia to hypertrophy during postnatal development." J Mol Cell Cardiol **28**(8): 1737-1746.

Li, Q., H. Pan, L. Guan, D. Su and X. Ma (2012). "CITED2 mutation links congenital heart defects to dysregulation of the cardiac gene VEGF and PITX2C expression." Biochem Biophys Res Commun **423**(4): 895-899.

Li, Q., D. L. Ramirez-Bergeron, S. L. Dunwoodie and Y. C. Yang (2012). "Cited2 gene controls pluripotency and cardiomyocyte differentiation of murine embryonic stem cells through Oct4 gene." J Biol Chem **287**(34): 29088-29100.

Li, Z., J. Lu, M. Sun, S. Mi, H. Zhang, R. T. Luo, P. Chen, Y. Wang, M. Yan, Z. Qian, M. B. Neilly, J. Jin, Y. Zhang, S. K. Bohlander, D. E. Zhang, R. A. Larson, M. M. Le Beau, M. J. Thirman, T. R. Golub, J. D. Rowley and J. Chen (2008). "Distinct microRNA expression profiles in acute myeloid leukemia with common translocations." Proc Natl Acad Sci U S A **105**(40): 15535-15540.

Lilly, B., S. Galewsky, A. B. Firulli, R. A. Schulz and E. N. Olson (1994). "D-MEF2: a MADS box transcription factor expressed in differentiating mesoderm and muscle cell lineages during Drosophila embryogenesis." Proc Natl Acad Sci U S A **91**(12): 5662-5666.

Lilly, B., B. Zhao, G. Ranganayakulu, B. M. Paterson, R. A. Schulz and E. N. Olson (1995). "Requirement of MADS domain transcription factor D-MEF2 for muscle formation in Drosophila." Science **267**(5198): 688-693.

Lin, Q., J. Lu, H. Yanagisawa, R. Webb, G. E. Lyons, J. A. Richardson and E. N. Olson (1998). "Requirement of the MADS-box transcription factor MEF2C for vascular development." Development **125**(22): 4565-4574.

Lin, Q., J. Schwarz, C. Bucana and E. N. Olson (1997). "Control of mouse cardiac morphogenesis and myogenesis by transcription factor MEF2C." Science **276**(5317): 1404-1407.

Lin, S. P., P. Coan, S. T. da Rocha, H. Seitz, J. Cavaille, P. W. Teng, S. Takada and A. C. Ferguson-Smith (2007). "Differential regulation of imprinting in the murine embryo and placenta by the Dlk1-Dio3 imprinting control region." Development **134**(2): 417-426.

Lin, S. P., N. Youngson, S. Takada, H. Seitz, W. Reik, M. Paulsen, J. Cavaille and A. C. Ferguson-Smith (2003). "Asymmetric regulation of imprinting on the maternal and paternal chromosomes at the Dlk1-Gtl2 imprinted cluster on mouse chromosome 12." Nat Genet **35**(1): 97-102.

Lingaiah, K., D. M. Sosalagere, S. R. Mysore, B. Krishnamurthy, D. Narayanappa and R. B. Nallur (2011). "Mutations of TFAP2B in congenital heart disease patients in Mysore, South India." Indian J Med Res **134**(5): 621-626.

Liu, D., X. L. Zhang, C. H. Yan, Y. Li, X. X. Tian, N. Zhu, J. J. Rong, C. F. Peng and Y. L. Han (2015). "MicroRNA-495 regulates the proliferation and apoptosis of human umbilical vein endothelial cells by targeting chemokine CCL2." Thromb Res **135**(1): 146-154.

Liu, L., G. Z. Luo, W. Yang, X. Zhao, Q. Zheng, Z. Lv, W. Li, H. J. Wu, L. Wang, X. J. Wang and Q. Zhou (2010). "Activation of the imprinted Dlk1-Dio3 region correlates with pluripotency levels of mouse stem cells." J Biol Chem **285**(25): 19483-19490.

Liu, N., A. H. Williams, Y. Kim, J. McAnally, S. Bezprozvannaya, L. B. Sutherland, J. A. Richardson, R. Bassel-Duby and E. N. Olson (2007). "An intragenic MEF2-dependent enhancer directs muscle-specific expression of microRNAs 1 and 133." Proc Natl Acad Sci U S A **104**(52): 20844-20849.

Liu, Y., F. Wang, Y. Wu, S. Tan, Q. Wen, J. Wang, X. Zhu, X. Wang, C. Li, X. Ma and H. Pan (2014). "Variations of CITED2 are associated with congenital heart disease (CHD) in Chinese population." PLoS One **9**(5): e98157.

MacDonald, S. T., S. D. Bamforth, J. Braganca, C. M. Chen, C. Broadbent, J. E. Schneider, R. J. Schwartz and S. Bhattacharya (2013). "A cell-autonomous role of Cited2 in controlling myocardial and coronary vascular development." Eur Heart J **34**(32): 2557-2565.

Mahmoud, A. I., F. Kocabas, S. A. Muralidhar, W. Kimura, A. S. Koura, S. Thet, E. R. Porrello and H. A. Sadek (2013). "Meis1 regulates postnatal cardiomyocyte cell cycle arrest." Nature **497**(7448): 249-253.

Mani, A., J. Radhakrishnan, A. Farhi, K. S. Carew, C. A. Warnes, C. Nelson-Williams, R. W. Day, B. Pober, M. W. State and R. P. Lifton (2005). "Syndromic patent ductus arteriosus: evidence for haploinsufficient TFAP2B mutations and identification of a linked sleep disorder." Proc Natl Acad Sci U S A **102**(8): 2975-2979.

Martin, J. F., J. M. Miano, C. M. Hustad, N. G. Copeland, N. A. Jenkins and E. N. Olson (1994). "A Mef2 gene that generates a muscle-specific isoform via alternative mRNA splicing." Mol Cell Biol **14**(3): 1647-1656.

Martin, J. F., J. J. Schwarz and E. N. Olson (1993). "Myocyte enhancer factor (MEF) 2C: a tissue-restricted member of the MEF-2 family of transcription factors." Proc Natl Acad Sci U S A **90**(11): 5282-5286.

McGreevy, J. W., C. H. Hakim, M. A. McIntosh and D. Duan (2015). "Animal models of Duchenne muscular dystrophy: from basic mechanisms to gene therapy." <u>Dis Model Mech</u> **8**(3): 195-213.

McKinsey, T. A., C. L. Zhang and E. N. Olson (2002). "MEF2: a calcium-dependent regulator of cell division, differentiation and death." <u>Trends Biochem Sci</u> **27**(1): 40-47.

Miyoshi, N., H. Wagatsuma, S. Wakana, T. Shiroishi, M. Nomura, K. Aisaka, T. Kohda, M. A. Surani, T. Kaneko-Ishino and F. Ishino (2000). "Identification of an imprinted gene, Meg3/Gtl2 and its human homologue MEG3, first mapped on mouse distal chromosome 12 and human chromosome 14q." <u>Genes Cells</u> **5**(3): 211-220.

Mok, G. F. and D. Sweetman (2011). "Many routes to the same destination: lessons from skeletal muscle development." <u>Reproduction</u> **141**(3): 301-312.

Molkentin, J. D., B. L. Black, J. F. Martin and E. N. Olson (1996). "Mutational analysis of the DNA binding, dimerization, and transcriptional activation domains of MEF2C." <u>Mol Cell Biol</u> **16**(6): 2627-2636.

Mollova, M., K. Bersell, S. Walsh, J. Savla, L. T. Das, S. Y. Park, L. E. Silberstein, C. G. Dos Remedios, D. Graham, S. Colan and B. Kuhn (2013). "Cardiomyocyte proliferation contributes to heart growth in young humans." <u>Proc Natl Acad Sci U S A</u> **110**(4): 1446-1451.

Mozaffarian, D., E. J. Benjamin, A. S. Go, D. K. Arnett, M. J. Blaha, M. Cushman, S. de Ferranti, J. P. Despres, H. J. Fullerton, V. J. Howard, M. D. Huffman, S. E. Judd, B. M. Kissela, D. T. Lackland, J. H. Lichtman, L. D. Lisabeth, S. Liu, R. H. Mackey, D. B. Matchar, D. K. McGuire, E. R. Mohler, 3rd, C. S. Moy, P. Muntner, M. E. Mussolino, K. Nasir, R. W. Neumar, G. Nichol, L. Palaniappan, D. K. Pandey, M. J. Reeves, C. J. Rodriguez, P. D. Sorlie, J. Stein, A. Towfighi, T. N. Turan, S. S. Virani, J. Z. Willey, D. Woo, R. W. Yeh, M. B. Turner, C. American Heart Association Statistics and S. Stroke Statistics (2015). "Heart disease and stroke statistics--2015 update: a report from the American Heart Association." <u>Circulation</u> **131**(4): e29-322.

Murry, C. E., R. W. Wiseman, S. M. Schwartz and S. D. Hauschka (1996). "Skeletal myoblast transplantation for repair of myocardial necrosis." <u>J Clin Invest</u> **98**(11): 2512-2523.

Naya, F. J., B. L. Black, H. Wu, R. Bassel-Duby, J. A. Richardson, J. A. Hill and E. N. Olson (2002). "Mitochondrial deficiency and cardiac sudden death in mice lacking the MEF2A transcription factor." <u>Nat Med</u> **8**(11): 1303-1309.

Naya, F. J., C. Wu, J. A. Richardson, P. Overbeek and E. N. Olson (1999). "Transcriptional activity of MEF2 during mouse embryogenesis monitored with a MEF2-dependent transgene." <u>Development</u> **126**(10): 2045-2052.

Neppl, R. L. and D. Z. Wang (2014). "The myriad essential roles of microRNAs in cardiovascular homeostasis and disease." Genes Dis **1**(1): 18-39.

Oberpriller, J. O. and J. C. Oberpriller (1974). "Response of the adult newt ventricle to injury." J Exp Zool **187**(2): 249-253.

Ornatsky, O. I. and J. C. McDermott (1996). "MEF2 protein expression, DNA binding specificity and complex composition, and transcriptional activity in muscle and non-muscle cells." J Biol Chem **271**(40): 24927-24933.

Otte, C., S. Wust, S. Zhao, L. Pawlikowska, P. Y. Kwok and M. A. Whooley (2010). "Glucocorticoid receptor gene, low-grade inflammation, and heart failure: the Heart and Soul study." J Clin Endocrinol Metab **95**(6): 2885-2891.

Pandey, R. and R. P. Ahmed (2015). "MicroRNAs Inducing Proliferation of Quiescent Adult Cardiomyocytes." Cardiovasc Regen Med **2**(1).

Parente, V., S. Balasso, G. Pompilio, L. Verduci, G. I. Colombo, G. Milano, U. Guerrini, L. Squadroni, F. Cotelli, O. Pozzoli and M. C. Capogrossi (2013). "Hypoxia/reoxygenation cardiac injury and regeneration in zebrafish adult heart." PLoS One **8**(1): e53748.

Partridge, T. A. (2013). "The mdx mouse model as a surrogate for Duchenne muscular dystrophy." FEBS J **280**(17): 4177-4186.

Pasumarthi, K. B., H. Nakajima, H. O. Nakajima, M. H. Soonpaa and L. J. Field (2005). "Targeted expression of cyclin D2 results in cardiomyocyte DNA synthesis and infarct regression in transgenic mice." Circ Res **96**(1): 110-118.

Pateras, I. S., K. Apostolopoulou, K. Niforou, A. Kotsinas and V. G. Gorgoulis (2009). "p57KIP2: "Kip"ing the cell under control." Mol Cancer Res **7**(12): 1902-1919.

Pfister, O., G. Della Verde, R. Liao and G. M. Kuster (2014). "Regenerative therapy for cardiovascular disease." Transl Res **163**(4): 307-320.

Pierpont, M. E., C. T. Basson, D. W. Benson, Jr., B. D. Gelb, T. M. Giglia, E. Goldmuntz, G. McGee, C. A. Sable, D. Srivastava, C. L. Webb and C. o. C. D. i. t. Y. American Heart Association Congenital Cardiac Defects Committee (2007). "Genetic basis for congenital heart defects: current knowledge: a scientific statement from the American Heart Association Congenital Cardiac Defects Committee, Council on Cardiovascular Disease in the Young: endorsed by the American Academy of Pediatrics." Circulation **115**(23): 3015-3038.

Pollock, R. and R. Treisman (1991). "Human SRF-related proteins: DNA-binding properties and potential regulatory targets." Genes Dev **5**(12A): 2327-2341.

Porrello, E. R., B. A. Johnson, A. B. Aurora, E. Simpson, Y. J. Nam, S. J. Matkovich, G. W. Dorn, 2nd, E. van Rooij and E. N. Olson (2011). "MiR-15 family regulates postnatal mitotic arrest of cardiomyocytes." <u>Circ Res</u> **109**(6): 670-679.

Porrello, E. R., A. I. Mahmoud, E. Simpson, J. A. Hill, J. A. Richardson, E. N. Olson and H. A. Sadek (2011). "Transient regenerative potential of the neonatal mouse heart." <u>Science</u> **331**(6020): 1078-1080.

Porrello, E. R., A. I. Mahmoud, E. Simpson, B. A. Johnson, D. Grinsfelder, D. Canseco, P. P. Mammen, B. A. Rothermel, E. N. Olson and H. A. Sadek (2013). "Regulation of neonatal and adult mammalian heart regeneration by the miR-15 family." <u>Proc Natl Acad Sci U S A</u> **110**(1): 187-192.

Poss, K. D. (2007). "Getting to the heart of regeneration in zebrafish." <u>Semin Cell Dev Biol</u> **18**(1): 36-45.

Potthoff, M. J. and E. N. Olson (2007). "MEF2: a central regulator of diverse developmental programs." <u>Development</u> **134**(23): 4131-4140.

Pyle, W. G. and R. J. Solaro (2004). "At the crossroads of myocardial signaling: the role of Z-discs in intracellular signaling and cardiac function." <u>Circ Res</u> **94**(3): 296-305.

Sanganalmath, S. K. and R. Bolli (2013). "Cell therapy for heart failure: a comprehensive overview of experimental and clinical studies, current challenges, and future directions." <u>Circ Res</u> **113**(6): 810-834.

Santelli, E. and T. J. Richmond (2000). "Crystal structure of MEF2A core bound to DNA at 1.5 A resolution." <u>J Mol Biol</u> **297**(2): 437-449.

Schmidt, J. V., P. G. Matteson, B. K. Jones, X. J. Guan and S. M. Tilghman (2000). "The Dlk1 and Gtl2 genes are linked and reciprocally imprinted." <u>Genes Dev</u> **14**(16): 1997-2002.

Seitz, H., H. Royo, M. L. Bortolin, S. P. Lin, A. C. Ferguson-Smith and J. Cavaille (2004). "A large imprinted microRNA gene cluster at the mouse Dlk1-Gtl2 domain." <u>Genome Res</u> **14**(9): 1741-1748.

Seitz, H., N. Youngson, S. P. Lin, S. Dalbert, M. Paulsen, J. P. Bachellerie, A. C. Ferguson-Smith and J. Cavaille (2003). "Imprinted microRNA genes transcribed antisense to a reciprocally imprinted retrotransposon-like gene." <u>Nat Genet</u> **34**(3): 261-262.

Shibata, R., Y. Izumiya, K. Sato, K. Papanicolaou, S. Kihara, W. S. Colucci, F. Sam, N. Ouchi and K. Walsh (2007). "Adiponectin protects against the development of systolic dysfunction following myocardial infarction." <u>J Mol Cell Cardiol</u> **42**(6): 1065-1074.

Shibata, R., N. Ouchi, M. Ito, S. Kihara, I. Shiojima, D. R. Pimentel, M. Kumada, K. Sato, S. Schiekofer, K. Ohashi, T. Funahashi, W. S. Colucci and K. Walsh (2004). "Adiponectin-mediated modulation of hypertrophic signals in the heart." Nat Med **10**(12): 1384-1389.

Shibuya, M. (2013). "Vascular endothelial growth factor and its receptor system: physiological functions in angiogenesis and pathological roles in various diseases." J Biochem **153**(1): 13-19.

Shih, K. K., L. X. Qin, E. J. Tanner, Q. Zhou, M. Bisogna, F. Dao, N. Olvera, A. Viale, R. R. Barakat and D. A. Levine (2011). "A microRNA survival signature (MiSS) for advanced ovarian cancer." Gynecol Oncol **121**(3): 444-450.

Skalsky, R. L. and B. R. Cullen (2011). "Reduced expression of brain-enriched microRNAs in glioblastomas permits targeted regulation of a cell death gene." PLoS One **6**(9): e24248.

Small, E. M. and E. N. Olson (2011). "Pervasive roles of microRNAs in cardiovascular biology." Nature **469**(7330): 336-342.

Snyder, C. M., A. L. Rice, N. L. Estrella, A. Held, S. C. Kandarian and F. J. Naya (2013). "MEF2A regulates the Gtl2-Dio3 microRNA mega-cluster to modulate WNT signaling in skeletal muscle regeneration." Development **140**(1): 31-42.

Sondell, M., G. Lundborg and M. Kanje (1999). "Vascular endothelial growth factor stimulates Schwann cell invasion and neovascularization of acellular nerve grafts." Brain Res **846**(2): 219-228.

Song, G. and L. Wang (2008). "MiR-433 and miR-127 arise from independent overlapping primary transcripts encoded by the miR-433-127 locus." PLoS One **3**(10): e3574.

Sperling, S., C. H. Grimm, I. Dunkel, S. Mebus, H. P. Sperling, A. Ebner, R. Galli, H. Lehrach, C. Fusch, F. Berger and S. Hammer (2005). "Identification and functional analysis of CITED2 mutations in patients with congenital heart defects." Hum Mutat **26**(6): 575-582.

Spyrou, N., J. Philpot, R. Foale, P. G. Camici and F. Muntoni (1998). "Evidence of left ventricular dysfunction in children with merosin-deficient congenital muscular dystrophy." Am Heart J **136**(3): 474-476.

Stein, C. A., J. B. Hansen, J. Lai, S. Wu, A. Voskresenskiy, A. Hog, J. Worm, M. Hedtjarn, N. Souleimanian, P. Miller, H. S. Soifer, D. Castanotto, L. Benimetskaya, H. Orum and T. Koch (2010). "Efficient gene silencing by delivery of locked nucleic acid antisense oligonucleotides, unassisted by transfection reagents." Nucleic Acids Res **38**(1): e3.

Stuckey, D. J., C. A. Carr, P. Camelliti, D. J. Tyler, K. E. Davies and K. Clarke (2012). "In vivo MRI characterization of progressive cardiac dysfunction in the mdx mouse model of muscular dystrophy." PLoS One **7**(1): e28569.

Takada, S., M. Tevendale, J. Baker, P. Georgiades, E. Campbell, T. Freeman, M. H. Johnson, M. Paulsen and A. C. Ferguson-Smith (2000). "Delta-like and Gtl2 are reciprocally expressed, differentially methylated linked imprinted genes on mouse chromosome 12." Current Biology **10**(18): 1135-1138.

Takahashi, N., A. Okamoto, R. Kobayashi, M. Shirai, Y. Obata, H. Ogawa, Y. Sotomaru and T. Kono (2009). "Deletion of Gtl2, imprinted non-coding RNA, with its differentially methylated region induces lethal parent-origin-dependent defects in mice." Hum Mol Genet **18**(10): 1879-1888.

Takakura, S., T. Kohno, R. Manda, A. Okamoto, T. Tanaka and J. Yokota (2001). "Genetic alterations and expression of the protein phosphatase 1 genes in human cancers." Int J Oncol **18**(4): 817-824.

Tang, H., X. Liu, Z. Wang, X. She, X. Zeng, M. Deng, Q. Liao, X. Guo, R. Wang, X. Li, F. Zeng, M. Wu and G. Li (2011). "Interaction of hsa-miR-381 and glioma suppressor LRRC4 is involved in glioma growth." Brain Res **1390**: 21-32.

Tao, Z., B. Chen, X. Tan, Y. Zhao, L. Wang, T. Zhu, K. Cao, Z. Yang, Y. W. Kan and H. Su (2011). "Coexpression of VEGF and angiopoietin-1 promotes angiogenesis and cardiomyocyte proliferation reduces apoptosis in porcine myocardial infarction (MI) heart." Proc Natl Acad Sci U S A **108**(5): 2064-2069.

Taylor, D. A., B. Z. Atkins, P. Hungspreugs, T. R. Jones, M. C. Reedy, K. A. Hutcheson, D. D. Glower and W. E. Kraus (1998). "Regenerating functional myocardium: improved performance after skeletal myoblast transplantation." Nat Med **4**(8): 929-933.

Tham, Y. K., B. C. Bernardo, J. Y. Ooi, K. L. Weeks and J. R. McMullen (2015). "Pathophysiology of cardiac hypertrophy and heart failure: signaling pathways and novel therapeutic targets." Arch Toxicol **89**(9): 1401-1438.

Thum, T., D. Catalucci and J. Bauersachs (2008). "MicroRNAs: novel regulators in cardiac development and disease." Cardiovasc Res **79**(4): 562-570.

Thum, T., P. Galuppo, C. Wolf, J. Fiedler, S. Kneitz, L. W. van Laake, P. A. Doevendans, C. L. Mummery, J. Borlak, A. Haverich, C. Gross, S. Engelhardt, G. Ertl and J. Bauersachs (2007). "MicroRNAs in the human heart: a clue to fetal gene reprogramming in heart failure." Circulation **116**(3): 258-267.

Thum, T., C. Gross, J. Fiedler, T. Fischer, S. Kissler, M. Bussen, P. Galuppo, S. Just, W. Rottbauer, S. Frantz, M. Castoldi, J. Soutschek, V. Koteliansky, A. Rosenwald, M. A. Basson, J. D. Licht, J. T. Pena, S. H. Rouhanifard, M. U. Muckenthaler, T. Tuschl, G. R. Martin, J. Bauersachs and S. Engelhardt (2008). "MicroRNA-21 contributes to myocardial disease by stimulating MAP kinase signalling in fibroblasts." Nature **456**(7224): 980-984.

Tian, Y., Y. Liu, T. Wang, N. Zhou, J. Kong, L. Chen, M. Snitow, M. Morley, D. Li, N. Petrenko, S. Zhou, M. Lu, E. Gao, W. J. Koch, K. M. Stewart and E. E. Morrisey (2015). "A microRNA-Hippo pathway that promotes cardiomyocyte proliferation and cardiac regeneration in mice." Sci Transl Med **7**(279): 279ra238.

Tierling, S., S. Dalbert, S. Schoppenhorst, C. E. Tsai, S. Oliger, A. C. Ferguson-Smith, M. Paulsen and J. Walter (2006). "High-resolution map and imprinting analysis of the Gtl2-Dnchc1 domain on mouse chromosome 12." Genomics **87**(2): 225-235.

Tsai, C. E., S. P. Lin, M. Ito, N. Takagi, S. Takada and A. C. Ferguson-Smith (2002). "Genomic imprinting contributes to thyroid hormone metabolism in the mouse embryo." Curr Biol **12**(14): 1221-1226.

Tsai, Y. T., Y. H. Su, S. S. Fang, T. N. Huang, Y. Qiu, Y. S. Jou, H. M. Shih, H. J. Kung and R. H. Chen (2000). "Etk, a Btk family tyrosine kinase, mediates cellular transformation by linking Src to STAT3 activation." Mol Cell Biol **20**(6): 2043-2054.

van Rooij, E. (2011). "The art of microRNA research." Circ Res **108**(2): 219-234.

van Rooij, E. and E. N. Olson (2007). "MicroRNAs: powerful new regulators of heart disease and provocative therapeutic targets." J Clin Invest **117**(9): 2369-2376.

van Rooij, E. and E. N. Olson (2012). "MicroRNA therapeutics for cardiovascular disease: opportunities and obstacles." Nat Rev Drug Discov **11**(11): 860-872.

van Rooij, E., A. L. Purcell and A. A. Levin (2012). "Developing microRNA therapeutics." Circ Res **110**(3): 496-507.

van Rooij, E., L. B. Sutherland, N. Liu, A. H. Williams, J. McAnally, R. D. Gerard, J. A. Richardson and E. N. Olson (2006). "A signature pattern of stress-responsive microRNAs that can evoke cardiac hypertrophy and heart failure." Proc Natl Acad Sci U S A **103**(48): 18255-18260.

van Rooij, E., L. B. Sutherland, X. Qi, J. A. Richardson, J. Hill and E. N. Olson (2007). "Control of stress-dependent cardiac growth and gene expression by a microRNA." Science **316**(5824): 575-579.

van Weerd, J. H., K. Koshiba-Takeuchi, C. Kwon and J. K. Takeuchi (2011). "Epigenetic factors and cardiac development." Cardiovasc Res **91**(2): 203-211.

van Westering, T. L., C. A. Betts and M. J. Wood (2015). "Current understanding of molecular pathology and treatment of cardiomyopathy in duchenne muscular dystrophy." Molecules **20**(5): 8823-8855.

Vera Janavel, G., A. Crottogini, P. Cabeza Meckert, L. Cuniberti, A. Mele, M. Papouchado, N. Fernandez, A. Bercovich, M. Criscuolo, C. Melo and R. Laguens (2006). "Plasmid-mediated VEGF gene transfer induces cardiomyogenesis and reduces myocardial infarct size in sheep." Gene Ther **13**(15): 1133-1142.

Vong, L. H., M. J. Ragusa and J. J. Schwarz (2005). "Generation of conditional Mef2cloxP/loxP mice for temporal- and tissue-specific analyses." Genesis **43**(1): 43-48.

Waddell, J. N., P. Zhang, Y. Wen, S. K. Gupta, A. Yevtodiyenko, J. V. Schmidt, C. A. Bidwell, A. Kumar and S. Kuang (2010). "Dlk1 is necessary for proper skeletal muscle development and regeneration." PLoS One **5**(11): e15055.

Waerner, T., P. Gardellin, K. Pfizenmaier, A. Weith and N. Kraut (2001). "Human RERE is localized to nuclear promyelocytic leukemia oncogenic domains and enhances apoptosis." Cell Growth Differ **12**(4): 201-210.

Walsh, S., A. Ponten, B. K. Fleischmann and S. Jovinge (2010). "Cardiomyocyte cell cycle control and growth estimation in vivo--an analysis based on cardiomyocyte nuclei." Cardiovasc Res **86**(3): 365-373.

Wang, Y., J. Fu, M. Jiang, X. Zhang, L. Cheng, X. Xu, Z. Fan, J. Zhang, Q. Ye and H. Song (2014). "MiR-410 is overexpressed in liver and colorectal tumors and enhances tumor cell growth by silencing FHL1 via a direct/indirect mechanism." PLoS One **9**(10): e108708.

Weninger, W. J., K. Lopes Floro, M. B. Bennett, S. L. Withington, J. I. Preis, J. P. Barbera, T. J. Mohun and S. L. Dunwoodie (2005). "Cited2 is required both for heart morphogenesis and establishment of the left-right axis in mouse development." Development **132**(6): 1337-1348.

Wick, M., C. Burger, M. Funk and R. Muller (1995). "Identification of a novel mitogen-inducible gene (mig-6): regulation during G1 progression and differentiation." Exp Cell Res **219**(2): 527-535.

Woo, Y. J., C. M. Panlilio, R. K. Cheng, G. P. Liao, P. Atluri, V. M. Hsu, J. E. Cohen and H. W. Chaudhry (2006). "Therapeutic delivery of cyclin A2 induces myocardial regeneration and enhances cardiac function in ischemic heart failure." <u>Circulation</u> **114**(1 Suppl): I206-213.

Wu, Y., R. Dey, A. Han, N. Jayathilaka, M. Philips, J. Ye and L. Chen (2010). "Structure of the MADS-box/MEF2 domain of MEF2A bound to DNA and its implication for myocardin recruitment." <u>J Mol Biol</u> **397**(2): 520-533.

Xin, M., Y. Kim, L. B. Sutherland, M. Murakami, X. Qi, J. McAnally, E. R. Porrello, A. I. Mahmoud, W. Tan, J. M. Shelton, J. A. Richardson, H. A. Sadek, R. Bassel-Duby and E. N. Olson (2013). "Hippo pathway effector Yap promotes cardiac regeneration." <u>Proc Natl Acad Sci U S A</u> **110**(34): 13839-13844.

Xin, M., E. N. Olson and R. Bassel-Duby (2013). "Mending broken hearts: cardiac development as a basis for adult heart regeneration and repair." <u>Nat Rev Mol Cell Biol</u> **14**(8): 529-541.

Xiong, F., Q. Li, C. Zhang, Y. Chen, P. Li, X. Wei, Q. Li, W. Zhou, L. Li, X. Shang and X. Xu (2013). "Analyses of GATA4, NKX2.5, and TFAP2B genes in subjects from southern China with sporadic congenital heart disease." <u>Cardiovasc Pathol</u> **22**(2): 141-145.

Xu, M., X. Wu, Y. Li, X. Yang, J. Hu, M. Zheng and J. Tian (2014). "CITED2 mutation and methylation in children with congenital heart disease." <u>J Biomed Sci</u> **21**: 7.

Yang, K. C., Y. C. Ku, M. Lovett and J. M. Nerbonne (2012). "Combined deep microRNA and mRNA sequencing identifies protective transcriptomal signature of enhanced PI3Kalpha signaling in cardiac hypertrophy." <u>J Mol Cell Cardiol</u> **53**(1): 101-112.

Yang, T., H. Gu, X. Chen, S. Fu, C. Wang, H. Xu, Q. Feng and Y. Ni (2014). "Cardiac hypertrophy and dysfunction induced by overexpression of miR-214 in vivo." <u>J Surg Res</u> **192**(2): 317-325.

Yang, X., R. K. Karuturi, F. Sun, M. Aau, K. Yu, R. Shao, L. D. Miller, P. B. Tan and Q. Yu (2009). "CDKN1C (p57) is a direct target of EZH2 and suppressed by multiple epigenetic mechanisms in breast cancer cells." <u>PLoS One</u> **4**(4): e5011.

Yang, X. F., X. Y. Wu, M. Li, Y. G. Li, J. T. Dai, Y. H. Bai and J. Tian (2010). "[Mutation analysis of Cited2 in patients with congenital heart disease]." <u>Zhonghua Er Ke Za Zhi</u> **48**(4): 293-296.

Yevtodiyenko, A., M. S. Carr, N. Patel and J. V. Schmidt (2002). "Analysis of candidate imprinted genes linked to Dlk1-Gtl2 using a congenic mouse line." Mamm Genome **13**(11): 633-638.

Yin, Z., J. Haynie, X. Yang, B. Han, S. Kiatchoosakun, J. Restivo, S. Yuan, N. R. Prabhakar, K. Herrup, R. A. Conlon, B. D. Hoit, M. Watanabe and Y. C. Yang (2002). "The essential role of Cited2, a negative regulator for HIF-1alpha, in heart development and neurulation." Proc Natl Acad Sci U S A **99**(16): 10488-10493.

Yokoyama, S. and H. Asahara (2011). "The myogenic transcriptional network." Cell Mol Life Sci **68**(11): 1843-1849.

Yoshida, T., T. Hanada, T. Tokuhisa, K. Kosai, M. Sata, M. Kohara and A. Yoshimura (2002). "Activation of STAT3 by the hepatitis C virus core protein leads to cellular transformation." J Exp Med **196**(5): 641-653.

Yu, Y. T. (1996). "Distinct domains of myocyte enhancer binding factor-2A determining nuclear localization and cell type-specific transcriptional activity." J Biol Chem **271**(40): 24675-24683.

Yu, Y. T., R. E. Breitbart, L. B. Smoot, Y. Lee, V. Mahdavi and B. Nadal-Ginard (1992). "Human myocyte-specific enhancer factor 2 comprises a group of tissue-restricted MADS box transcription factors." Genes Dev **6**(9): 1783-1798.

Zacchigna, S. and M. Giacca (2014). "Extra- and intracellular factors regulating cardiomyocyte proliferation in postnatal life." Cardiovasc Res **102**(2): 312-320.

Zhang, C., C. Wang, X. Chen, C. Yang, K. Li, J. Wang, J. Dai, Z. Hu, X. Zhou, L. Chen, Y. Zhang, Y. Li, H. Qiu, J. Xing, Z. Liang, B. Ren, C. Yang, K. Zen and C. Y. Zhang (2010). "Expression profile of microRNAs in serum: a fingerprint for esophageal squamous cell carcinoma." Clin Chem **56**(12): 1871-1879.

Zhao, D., P. Jia, W. Wang and G. Zhang (2015). "VEGF-mediated suppression of cell proliferation and invasion by miR-410 in osteosarcoma." Mol Cell Biochem **400**(1-2): 87-95.

Zhao, F., C. G. Weismann, M. Satoda, M. E. Pierpont, E. Sweeney, E. M. Thompson and B. D. Gelb (2001). "Novel TFAP2B mutations that cause Char syndrome provide a genotype-phenotype correlation." Am J Hum Genet **69**(4): 695-703.

Zhao, J., T. K. Ohsumi, J. T. Kung, Y. Ogawa, D. J. Grau, K. Sarma, J. J. Song, R. E. Kingston, M. Borowsky and J. T. Lee (2010). "Genome-wide identification of polycomb-associated RNAs by RIP-seq." Mol Cell **40**(6): 939-953.

Zhao, Y., J. F. Ransom, A. Li, V. Vedantham, M. von Drehle, A. N. Muth, T. Tsuchihashi, M. T. McManus, R. J. Schwartz and D. Srivastava (2007). "Dysregulation of cardiogenesis, cardiac conduction, and cell cycle in mice lacking miRNA-1-2." Cell **129**(2): 303-317.

Zhou, Y., P. Cheunsuchon, Y. Nakayama, M. W. Lawlor, Y. Zhong, K. A. Rice, L. Zhang, X. Zhang, F. E. Gordon, H. G. Lidov, R. T. Bronson and A. Klibanski (2010). "Activation of paternally expressed genes and perinatal death caused by deletion of the Gtl2 gene." Development **137**(16): 2643-2652.

Zhu, B., B. Ramachandran and T. Gulick (2005). "Alternative pre-mRNA splicing governs expression of a conserved acidic transactivation domain in myocyte enhancer factor 2 factors of striated muscle and brain." J Biol Chem **280**(31): 28749-28760.

CURRICULUM VITAE